



Validation report of the Convection
Product Processors of the NWC/GEO

Code: NWC/CDOP3/GEO/MF-PI/SCI/VR
Issue: 1.1 **Date:** 18th December 2019
File: NWC-CDOP3-GEO-MF-PI-SCI-VR-Convection_v1.1.odt
Page: 1/67

The EUMETSAT
Network of
Satellite
Application
Facilities



NWC SAF

Support to Nowcasting and
Very Short Range Forecasting

Validation report of the Convection Product Processors of the NWC/GEO

NWC/CDOP3/GEO/MF-PI/SCI/VR, Issue 1, Rev. 1

18th December 2019

Applicable to

GEO-CI v.2.1 (NWC-053)

GEO-RDT-CW v.5.1 (NWC-056)

**Prepared by METEO-FRANCE Toulouse (MFT) / Direction des Opérations – Prévision
Immédiate**

 	Validation report of the Convection Product Processors of the NWC/GEO	Code: NWC/CDOP3/GEO/MF-PI/SCI/VR Issue: 1.1 Date: 18th December 2019 File: NWC-CDOP3-GEO-MF-PI-SCI-VR-Convection_v1.1.odt Page: 2/67
---	--	--

REPORT SIGNATURE TABLE

Function	Name	Signature	Date
Prepared by	Météo-France MFT (F. Autonès and M. Claudon)	Signed, F. Autonès Signed, M. Claudon	<i>18th December 2019</i>
Reviewed by	Météo-France MFT (J.-M. Moisselin)	Signed, J.-M. Moisselin	<i>18th December 2019</i>
Authorised by	P. Ripodas NWC SAF Project Manager		<i>18th December 2019</i>

 	Validation report of the Convection Product Processors of the NWC/GEO	Code: NWC/CDOP3/GEO/MF-PI/SCI/VR Issue: 1.1 Date: 18th December 2019 File: NWC-CDOP3-GEO-MF-PI-SCI-VR-Convection_v1.1.odt Page: 3/67
---	--	--

DOCUMENT CHANGE RECORD

Version	Date	Changes
1.0	16 th October 2016	Applicable to v2016
1.0d	31 st October 2018	Applicable to v2018, version to be reviewed Main changes - CI : new validation case studies, summary of TROPOS analysis of CI v2018 - RDT-CW : validation of new discrimination scheme (GEN), previous discrimination scheme (CAL) summarized, summary of scientific report on advection scheme evaluation, lightning jump validation
1.0	21 st January 2019	Final version 1.0, applicable to v2018
1.1d	01 October 2019	version 1.1d with GOES16 data taken into account
1.1	18 th December 2019	version, reviewed GOES16 ABI data taken into account

Table of Contents

1 INTRODUCTION.....	10
1.1 SCOPE OF THE DOCUMENT.....	10
1.2 SOFTWARE VERSION IDENTIFICATION.....	10
1.3 REQUIREMENTS.....	10
1.4 DEFINITIONS, ACRONYMS AND ABBREVIATIONS.....	11
1.5 REFERENCES.....	11
1.5.1 <i>Applicable documents</i>	11
1.5.2 <i>Reference documents</i>	11
2 CONVECTION INITIATION (GEO-CI) VALIDATION.....	13
2.1 OVERVIEW.....	13
2.1.1 <i>General objectives of the validation</i>	13
2.1.2 <i>Methodology outline</i>	13
2.2 CI VERIFICATION.....	13
2.3 SPECIFICITIES OF CI VERIFICATIONS.....	16
2.4 OBJECTIVE VALIDATION.....	17
2.4.1 <i>Context</i>	17
2.4.2 <i>Data and methods</i>	17
2.4.3 <i>Results</i>	17
2.5 CASE STUDIES.....	18
2.5.1 <i>20100628 MSG Case Study</i>	18
2.5.2 <i>20180702 MSG Case Study</i>	20
2.5.3 <i>20180513 MSG Case Study</i>	23
2.5.4 <i>GOES-16 CI verification - data and method</i>	24
2.5.5 <i>20181002 GOES-16 case study</i>	27
2.5.6 <i>20181004 GOES-16 case study</i>	32
2.6 CONCLUSION AND COMPLIANCE REQUIREMENTS.....	35
3 RAPIDLY DEVELOPING THUNDERSTORM – CONVECTION WARNING (GEO-RDT-CW) VALIDATION.....	37
3.1 OVERVIEW.....	37
3.2 VALIDATION OF GEN DISCRIMINATION DIAGNOSIS.....	37
3.2.1 <i>Context</i>	37
3.2.2 <i>Data and methods</i>	37
3.2.3 <i>Results</i>	38
3.2.4 <i>Conclusion</i>	38
3.3 THE VALIDATION OF CAL DISCRIMINATION SCHEME.....	39
3.3.1 <i>Context</i>	39
3.3.2 <i>Cases study</i>	39
3.3.2.1 RDT-CW discrimination using MSG4 0°.....	39
3.3.2.1.1 <i>Inter-comparison between discrimination schemes</i>	39
3.3.2.1.2 <i>20180702 over Europe</i>	42
3.3.2.2 RDT-CW discrimination using Himawari-8.....	43
3.3.2.2.1 <i>Intercomparison between discrimination schemes</i>	43
3.3.2.2.2 <i>Case study 20180702 over East Asia</i>	45
3.3.2.3 RDT-CW discrimination using MSG3 - 9.5E° RapidScan mode.....	46
3.3.2.4 RDT-CW discrimination using MSG1 - 41.5°E.....	47
3.3.2.5 RDT-CW discrimination applied to GOES16 with 15 minutes scan rate.....	48
3.3.2.6 RDT-CW applied to GOES16 with 10 minutes scan rate.....	51
3.3.2.7 <i>Processing RDT-CW using IR10.3 (channel #15) or IR11.2 window channel (#16)</i>	53
3.4 OVERSHOOTING TOP DETECTION.....	54
3.4.1 <i>Pre selection step</i>	54
3.4.2 <i>Confirmation step</i>	55
3.4.3 <i>Subjective validation</i>	56

 	Validation report of the Convection Product Processors of the NWC/GEO	Code: NWC/CDOP3/GEO/MF-PI/SCI/VR Issue: 1.1 Date: 18th December 2019 File: NWC-CDOP3-GEO-MF-PI-SCI-VR-Convection_v1.1.odt Page: 5/67
---	--	--

<u>3.4.4 Applicability to tropical regions.....</u>	<u>58</u>
<u>3.5 LIGHTNING JUMP DIAGNOSIS.....</u>	<u>59</u>
<u>3.6 FORECAST OF CLOUD SYSTEMS.....</u>	<u>61</u>
<u>3.7 END-USERS FEEDBACKS.....</u>	<u>64</u>
<u>3.8 CONCLUSION AND COMPLIANCE REQUIREMENTS.....</u>	<u>65</u>
<u>4 CONCLUSION.....</u>	<u>67</u>

List of Tables and Figures

Table 1: List of Applicable Documents.....	11
Table 2: List of Referenced Documents.....	12
Table 3: Comparison of CI production between IR11.2µm and IR10.3µm in terms of number of CI pixels.....	33
Table 4: RDT v2011 Discrimination skill table.....	39

Figure 1: Elaboration of RDT ground truth for CI. A convex hull for accumulated contours over a given period identifies path tracks and thus areas of convective pixels..... 15

Figure 2: Elaboration of radar ground truth for CI over coverage area. Accumulated pixels with reflectivity over 30 dBZ during a given period identifies path tracks and thus areas of active pixels 16

Figure 3: Elaboration of lightning ground truth for CI over specific coverage area. Accumulated and enlarged strokes over a given period identify areas of active pixels..... 17

Figure 4: Plot of the POD FAR (figure on the left) CSI and HSS (figure on the right) of the validation of the v2018 CI 0-30' forecast product for the CI probability levels 25-50% and 75-100%. For the figure on the left the colour surfaces denotes the threshold values of POD and FAR given in PRD [AD.4]..... 19

Figure 5: 20100628 CI Case Study - 13h00Z IR image, overlayed with with CI_prob30 and [13h00Z-13h30Z] accumulated radar > 30dBZ seen as ground truth (green shading). The colour code for visualization of CI is as follow: yellow for [0-25%] probability of Convection initiation, orange for [25-50%] probability of Convection initiation, red for [50-75%] probability of Convection initiation, magenta for [75-100%] probability of Convection initiation..... 20

Figure 6: 20100628 CI Case Study. Same legend as Figure 5. Zoom allows to detect all cases : Good Detection (GD) , miss cases (MI), false alarms (FA) and double penalty when MI and FA are inside the same area..... 20

Figure 7: 20180702 CI Case Study, same legend as Figure 5 - 15h00Z 10.8 µm IR image (top left), overlayed with CI_prob30 (top right), and with [15h00Z-15h30Z] accumulated radar > 30 dBZ as ground truth (green shading bottom left). Zoom on moderate convection (bottom right)..... 21

Figure 8: 20180702 CI Case Study, same legend as Figure 5 - 15:00 Z 10.8µm IR image overlayed with CI_prob30 and [15h00Z-15h30Z] accumulated radar>30dBZ (left) , with [15h00Z-16h00Z] accumulated radar>30dBZ (right). Zoom centre France (top), over Pyrénées (bottom)..... 22

Figure 9: 20180702 CI Case Study, , same legend as Figure 5 - 15:00 Z 10.8 µm IR image overlayed with CI_prob30 and next 30 minutes accumulated radar>30dBZ. Slots 15h15Z (top left), 15h30Z (top right), 15h45Z (bottom left), 16h00Z (bottom right). Good Detection pointed with red circles, false alarm with blue circles..... 23

<i>Figure 10: 20180702 CI Case Study - Time series of pixel numbers by probability classes. X-axis ranges from 00h15Z to 23h45Z,</i>	23
<i>Figure 11: 20180513 CI Case Study - From Left to right and top to bottom, 11h00Z, 12h00Z, 15h00Z and 18h00Z, CI probabilities for next 30minutes (yellow and orange), radar ground truth (green shades)</i>	24
<i>Figure 12: 20180513 CI Case Study - Time series of pixel numbers by probability classes. X-axis ranges from 00h15Z to 23h45Z,</i>	25
<i>Figure 13: Ground Truth definition illustration</i>	26
<i>Figure 14: 2018-10-02. Ground Truths over French Guiana. Smaller objects delineate convective cells. Bigger objects delineate a spatial tolerance of 0.1° around each convective cell</i>	27
<i>Figure 15: 2018-10-04. Ground Truths over Caribbean French West Indies. Same representation of objects as in previous figure</i>	27
<i>Figure 16: Zoom on French Guiana, 2018-10-02. Top Left: Time t = 18:30:00Z. IR10.8 satellite imagery at t, CI [t+0;t+30min] forecast production (from yellow to magenta according to the class of probability to assess the forecast capacity of CI), Ground Truths at t= 0 in blue contours, at [t+5;t+30 min] in green contours. Ground Truths at [t-30;t+0min[and their evolution at t+0min and t+30min in red contours to assess the signage capacity of CI. From top to bottom and left to right: Same figures at times t = 18:45:00Z, 19:00:00Z, 19:15:00Z, 19:30:00Z</i>	29
<i>Figure 17: 2018-10-02. Repartition of CI pixels' values</i>	30
<i>Figure 18: 2018-10-02 case study. Proportion of GT paired with CI</i>	31
<i>Figure 19: Zoom on French Guiana, 2018-10-02. Same as Figure 16 with channel IR10.3µm</i>	32
<i>Figure 20: 20181002 Case Study Proportion of GT paired with CI – channel IR10.3 compared to channel IR11.2</i>	33
<i>Figure 21: Zoom on French West Indies, 2018-10-04. Top Left: Time t = 06:30:00Z. IR satellite imagery at t, CI [t+0;t+30min] forecast production (from yellow to magenta according to the class of probability), Ground Truths at t= 0 in blue contours, at [t+5;t+30 min] in green contours. Past Ground Truths and their evolution at t+0min and t+30min in red contours. From top to bottom and left to right: Same figures at times t = 06:45:00Z, 07:00:00Z, 07:15:00Z, 07:30:00Z, 07:45:00Z</i>	35
<i>Figure 22: 2018-10-04 Case Study. Proportion of GT paired with CI</i>	36
<i>Figure 23: Precocity of RDT v2011 discrimination for moderate (black) and low (red marks) ground truths</i>	39
<i>Figure 24: MSG4 case study for 12h00-15h00Z on 20180621. 15h00Z IR image (top left), 30min accumulated METEORAGE impacts around 15h00Z (top right), CAL (bottom left) and GEN (bottom right) results for 15h00Z</i>	41
<i>Figure 25: MSG4 case study for 20180621 12h00-15h00Z, zoom on South of France. IR and lightning on the left, CAL (plain blue cells) and GEN (orange dashed) on the righth. One can note a</i>	

	Validation report of the Convection Product Processors of the NWC/GEO	Code: NWC/CDOP3/GEO/MF-PI/SCI/VR Issue: 1.1 Date: 18th December 2019 File: NWC-CDOP3-GEO-MF-PI-SCI-VR-Convection_v1.1.odt Page: 8/67
---	--	--

miss near Bordeaux (top left cloud) with both CAL and GEN schemes, an early good detection more or less in the centre of image..... 41

Figure 26: MSG4 case study for 20180621 12h00-15h00Z, zoom on Central Europe. IR and lightning on the left, CAL (blue cells) and GEN (orange dashed) on the right. One can note some False Alarms with CAL on the edge of cloud systems..... 42

Figure 27: MSG4 case study for 20180621 12h00-15h00Z, large view. False Alarms suspicion in the North of the domain, more numerous with CAL (blue cells), in an area which seems out of lightning coverage area..... 42

Figure 28: MSG4 case study for 20180621 12h-15hZ. Compared time series of convective cells numbers..... 43

Figure 29: MSG4 case study for 20180702. 15h00Z IR image (top&bottom left) with METEORAGE impacts around 15h00Z, RDT-CW cells for 15h00Z with lightnings(top&bottom right)..... 44

Figure 30: MSG4 case study for 20180702. 15h00Z IR image with 1h accumulated METEORAGE impacts and RDT-CW cells..... 44

Figure 31: Himawari-8 case study for 03h00-06h00Z on 20180117. 06h00Z RGB image (top left), 1h-accumulated WWLLN impacts around 06h00Z (top right), CAL (bottom left) and GEN (bottom right) results for 06h00Z..... 45

Figure 32: Himawari-8 case study for 20180117 03h00-06h00Z. Compared time series of convective cells numbers..... 45

Figure 33: Himawari-8 case study for 20180702 03h00-06h00Z. 06Z RGB image with WWLLN flashes (left) and overlaid with RDT-CW cells (right, blue cells). Northern inner land region on top images, Southern oceanic region on bottom images,..... 46

Figure 34: Himawari-8 case study for 20180702 03h00-06h00Z. 06h00Z RGB image overlaid with 3 hours-accumulated WWLLN flashes and 3 hours-accumulated RDT-CW cells..... 47

Figure 35: MSG3-RSS and MSG4 case study for 201800207 12h00-15h00Z. 15h00Z IR image overlaid with MSG3-RSS RDT-CW cells (green) and MSG4 RDT-CW cells (magenta dashed)..... 47

Figure 36: MSG3-RSS case study for 201800207. 15:00Z IR image overlaid with 1h accumulation MSG3-RSS RDT-CW cells (black contours) and lightning data (red)..... 48

Figure 37: MSG1-41.5E case study for 20180121. Overlay of RDT-CW cell contours (black contours, blue cells) and WWLLN flash impacts (± 15 minutes, red spots). From top to bottom and left to right: 09hZ, 12hZ, 15hZ, 18hZ, 21hZ, 09-21hZ..... 49

Figure 38: GOES16 case study for 20181008 15hZ. Top: IR image overlaid with RDT-CW cell contours (red contours). Bottom: idem plus GLM flash impacts in the next hour (15hZ-16hZ)..... 50

Figure 39: GOES16 case study for 20181008 19hZ. Top: SIR image overlaid with RDT-CW cell contours (red contours). Bottom: idem plus GLM flash impacts in the next hour (19hZ-20hZ)..... 51

Figure 40: 20181008 Case study, 18h00Z to 18h45Z. GOES16 IR image overlaid with RDT-CW cell contours (red contours) and GLM flashes (yellow stars) 52

Figure 41: 20190419 Case study, 12h00Z GOES16 IR image overlayed with RDT-CW cell contours (magenta contours) and GLM flashes (yellow stars) in the 50 following minutes. Confirmed areas of false alarms in red circles, green arrow points good detection by RDT-CW with large anticipation 53

Figure 42: Same s previous figure but for 13h00Z..... 53

Figure 43: same as previous figure but for 14h00Z..... 54

Figure 44: 20190419 Case study, 19h00Z . Top: IR10.3 μ m-RDT-CW cells (empty magenta contours) overlayed with 11.2 μ m-RDT-CW cells (green dashed contours). Bottom: same with WWLLN lightning flashes over [19hZ-20hZ] period..... 55

Figure 45: 25th May 2009, slot 16h00 UTC. Zoom over Austrian-Slovenian frontier. Left: Enhanced IR10.8 image with plotted pre-selected OT. Right: HRV image with highlighted OTD from Bedka method in [RD.2.]..... 56

Figure 46: Left-above : OTD after first step plotted over NWP tropopause T°C (blue>-50,green[-50,-60],yellow-green[-60,-65],orange[-65,-67], dark orange<-67). Right above: HRV image confirming two OT (HRV not used by the algorithm). Below: the HRV OT are also found by the algorithm that takes into account (among other criterias) the gap between OT temperature and tropopause temperature..... 57

Figure 47: OTD plotted on raw IR10.8 enhanced images (left), on low resolution VIS parallax-corrected images (middle), and on raw HRV image (right)..... 57

Figure 48: As in previous figure..... 58

Figure 49: As in previous figure..... 58

Figure 50: As in previous figure..... 58

Figure 51: As in previous figure..... 59

Figure 52: 06/06/2012 12h00 UTC, south-west Africa: OTD on enhanced IR image..... 60

Figure 53: 13/06/2017 case study extreme Thunderstorm in « Haute Loire » (France) for 17:15. IR10.8 enhanced image, RDT cell, radar reflectivities and lightning strokes..... 61

Figure 54: Top: Jumps calculated for the cell described in previous figure above. Time-series of lightning rate (red), standard deviation of lightning rate in the last 12 minutes (blue), lightning rate change (brown). Jumps are plot in magenta. Hail event has been reported after the fifth jump at 17:30. Bottom: time-series of 15min flash number of successive RDT-CW cell..... 61

Figure 55: v2013 vs v2016 illustration of RDT motion vectors improvement..... 62

Figure 56: RDT-CW v2016 advection products (forecast contours in Magenta) from slot 2010-06-28T15:00:00Z (Observed contours in yellow)..... 64

Figure 57: RDT-CW v2016 advection products (green forecast contours) from previous slots valid for slot 2010-06-28T15:00:00Z (yellow observed contours)..... 65

	Validation report of the Convection Product Processors of the NWC/GEO	Code: NWC/CDOP3/GEO/MF-PI/SCI/VR Issue: 1.1 Date: 18th December 2019 File: NWC-CDOP3-GEO-MF-PI-SCI-VR-Convection_v1.1.odt Page: 10/67
---	---	---

1 INTRODUCTION

The EUMETSAT “Satellite Application Facilities” (SAF) are dedicated centres of excellence for processing satellite data, and form an integral part of the distributed EUMETSAT Application Ground Segment (<http://www.eumetsat.int>). This documentation is provided by the SAF on Support to Nowcasting and Very Short Range Forecasting, NWCSAF. The main objective of NWCSAF is to provide, further develop and maintain software packages to be used for Nowcasting applications of operational meteorological satellite data by National Meteorological Services. More information can be found at the NWCSAF webpage, <http://nwc-saf.eumetsat.int>. This document is applicable to the NWCSAF processing package for geostationary meteorological satellites, NWC/GEO.

1.1 SCOPE OF THE DOCUMENT

This document is the convection product validation report applicable to NWC/GEO software package v2018.1. The accuracies of the convection products (GEO-CI, Convection Initiation and GEO-RDT-CW, Rapidly Developing Thunderstorm Convection Warning) are discussed.

1.2 SOFTWARE VERSION IDENTIFICATION

This document describes the products obtained from the GEO-CI v2.1 (Product Id NWC-053) and from GEO-RDT-CW v5.1 (Product Id NWC-056) implemented in the release 2018.1 of the NWC/GEO software package.

1.3 REQUIREMENTS

Skill requirements had been expressed in PRD Table for RDT and CI (see [AD.4.]).

- CI:
 - Accuracy: FAR<0.6 POD>0.4 for +30’ ahead
 - Target FAR<0.5 POD>0.5 for +30’ ahead
 - Optimal: FAR<0.4 POD>0.7 for +30’ ahead
- RDT:
 - Accuracy
 - 1) early detection (before first lightning occurrence) 10%
 - 2) 30 minutes after first lightning occurrence 30%
 - 3) overall thunderstorm detection skill 50%"
 - Target
 - 1) early detection (before first lightning occurrence) 25%
 - 2) 30 minutes after first lightning occurrence 50%
 - 3) overall thunderstorm detection skill 70%"
 - Optimal
 - 1) early detection (before first lightning occurrence) 50%
 - 2) 30 minutes after first lightning occurrence 75%

	Validation report of the Convection Product Processors of the NWC/GEO	Code: NWC/CDOP3/GEO/MF-PI/SCI/VR Issue: 1.1 Date: 18th December 2019 File: NWC-CDOP3-GEO-MF-PI-SCI-VR-Convection_v1.1.odt Page: 11/67
---	---	---

- 3) overall thunderstorm detection skill 90%

1.4 DEFINITIONS, ACRONYMS AND ABBREVIATIONS

See [RD.1.] for a complete list of acronym for the NWC SAF project.

1.5 REFERENCES

1.5.1 Applicable documents

The following documents, of the exact issue shown, form part of this document to the extent specified herein. Applicable documents are those referenced in the Contract or approved by the Approval Authority. They are referenced in this document in the form [AD.X]

For dated references, subsequent amendments to, or revisions of, any of these publications do not apply. For undated references, the current edition of the document referred applies.

Current documentation can be found at the NWC SAF Helpdesk web: <http://nwc-saf.eumetsat.int>.

Ref	Title	Code	Vers	Date
[AD.1.]	Proposal for the Third Continuous Development and Operations Phase (CDOP-3) March 2017-February 2022	NWC SAF: CDOP-3 proposal	1.0	11/4/2016
[AD.2.]	Project Plan for the NWCSAF CDOP3 phase	NWC/CDOP3/SAF/AEMET/MGT/PP	1.3	12/7/2018
[AD.3.]	Configuration Management Plan for the NWCSAF	NWC/CDOP3/SAF/AEMET/MGT/CMP	1.0	21/2/2018
[AD.4.]	NWCSAF Product Requirement Document	NWC/CDOP3/SAF/AEMET/MGT/PRD	1.1	21/12/2018
[AD.5.]	System and Components Requirements Document	NWC/CDOP2/GEO/AEMET/SW/SCRD	2.2	1/4/2019
[AD.6.]	Interface Control Document for Internal and External Interfaces of the NWC/GEO	NWC/CDOP3/GEO/AEMET/SW/ICD/1	1.1	1/10/2019
[AD.7.]	Interface Control Document for the NWCLIB of the NWC/GEO	NWC/CDOP3/GEO/AEMET/SW/ICD/2	1.1	1/10/2019
[AD.8.]	Data Output Format for the NWC/GEO	NWC/CDOP3/GEO/AEMET/SW/DOF	1.1	1/10/2019
[AD.9.]	Component Design Document for the NWCLIB of the NWC/GEO	NWC/CDOP2/GEO/AEMET/SW/ACDD/NWCLIB	2.0	27/2/2017
[AD.10.]	Component Design Document for the Convection Product Processors of the NWC/GEO	NWC/CDOP2/GEO/MFT/SW/ACDD/Convection	2.1	21/1/2019
[AD.11.]	Algorithm Theoretical Basis Document for the Convection Product Processors of the NWC/GEO	NWC/CDOP2/GEO/MFT/SCI/ATBD/Convection	2.1	21/1/2019
[AD.12.]	User Manual for the tools of the NWC/GEO	NWC/CDOP3/GEO/AEMET/SW/UM/Tools	1.0	21/1/2019
[AD.13.]	NWC SAF CDOP-3 Project Plan Master Schedule	NWC/CDOP3/SAF/AEMET/MGT/PP/MasterSchedule	1.1	28/2/2018

Table 1: List of Applicable Documents

1.5.2 Reference documents

The reference documents contain useful information related to the subject of the project. These reference documents complement the applicable ones, and can be looked up to enhance the information included in this document if it is desired. They are referenced in this document in the form [RD.X]

	Validation report of the Convection Product Processors of the NWC/GEO	Code: NWC/CDOP3/GEO/MF-PI/SCI/VR Issue: 1.1 Date: 18th December 2019 File: NWC-CDOP3-GEO-MF-PI-SCI-VR-Convection_v1.1.odt Page: 12/67
---	---	---

For dated references, subsequent amendments to, or revisions of, any of these publications do not apply. For undated references, the current edition of the document referred applies

Current documentation can be found at the NWC SAF Helpdesk web: <http://nwc-saf.eumetsat.int>.

Ref	Title	Code	Vers	Date
[RD.1.]	The Nowcasting SAF glossary	NWC/CDOP2/SAF/AEMET/MGT/GLO	2.1	3/2/2017
[RD.2.]	Best Practice Document, 2013, for EUMETSAT Convection Working Group, Eds J.Mecikalski, K. Bedka and M. König »	Available on CWG Website		2013
[RD.3.]	Scientific Report on verification of RDT forecast	NWC/CDOP3/GEO/MFT/SCI/RP/01	1.2	5/9/2018
[RD.4.]	Lenk, S., Senf, F., Deneke, H., Final Report on the Associated Scientist Activity for the Validation of the Convection Initiation (CI) product of NWCSAF v2018	NWC/CDOP3/SAF/MF-PI/SCI/RP/CI_Improv_Tropos available on NWCSAF Website	1.0	November 2018
[RD.5.]	Karagiannidis, A., 2016, Final Report on Visiting Scientist Activity for the validation and improvement of the Convection Initiation (CI) product of NWC SAF v2016 and v2018, Visiting Scientist Activity followed in Nowcasting Department of Météo France, Toulouse, France Period June-December 2016 »	available on NWCSAF Website		2016
[RD.6.]	Validation report of the Convection Product Processors of the NWC/GEO	NWC/CDOP3/GEO/MF-PI/SCI/VR	1.0	15 th October 2016
[RD.7.]	Scientific Report on Extended Validation of RDT	SAF/NWC/CDOP/MFT/SCI/RP/1		7 th December 2012
[RD.8.]	Haberlie, A. M., Ashley, W., S., Pingel, T. J., 2014, The effect of urbanisation on the climatology of thunderstorm initiation, QJRMS, https://doi.org/10.1002/qj.2499			2014
[RD.9.]	Walker, J. R., W. M. MacKenzie, Jr., J. R. Mecikalski, and C. P. Jewett, 2012: An enhanced geostationary satellite-based convective initiation algorithm for 0/2-h nowcasting with object tracking. J. Appl. Meteor. Climatol., 51, 1931-1949"			2012
[RD.10.]	<u>Autonès, F., Moisselin, J.-M., 2019, Validation Report for Convection Products, available on http://nwc-saf.eumetsat.int</u>	<u>NWC/CDOP3/GEO/MFT/SCI/VR/Convection</u>	1.0	2019
[RD.11.]	https://www.vaisala.com/fr/products/data-subscriptions-and-reports/data-sets/gld360			
[RD.12.]	Brenguier, J.-L., Bouttier, F., Moisselin, J.-M., 2015, Les nouveaux services météorologiques pour l'aviation, La Météorologie 91, Novembre 2015			2015
[RD.13.]	Le Gléau, H., 2016, Algorithm Theoretical Basis Document for the Cloud Product Processors of the NWC/GEO, available on http://nwc-saf.eumetsat.int	NWC/CDOP2/GEO/MFL/SCI/ATBD/Cloud		2016
[RD.14.]	Moisselin, J.-M., 2017, Scientific report on on future verification of CI product, available on http://nwc-saf.eumetsat.int	NWC/CDOP2/GEO/MFT/SCI/RP/08		2017

Table 2: List of Referenced Documents

	Validation report of the Convection Product Processors of the NWC/GEO	Code: NWC/CDOP3/GEO/MF-PI/SCI/VR Issue: 1.1 Date: 18th December 2019 File: NWC-CDOP3-GEO-MF-PI-SCI-VR-Convection_v1.1.odt Page: 13/67
---	--	---

2 CONVECTION INITIATION (GEO-CI) VALIDATION

2.1 OVERVIEW

2.1.1 General objectives of the validation

The main objective of this section is to document Convection Initiation product accuracy. The method used has to compare POD and FAR scores to the threshold accuracies listed in the NWCSAF product requirements document [AD.4] : FAR<0.6, POD>0.4

2.1.2 Methodology outline

The following validation of the CI product has to be performed:

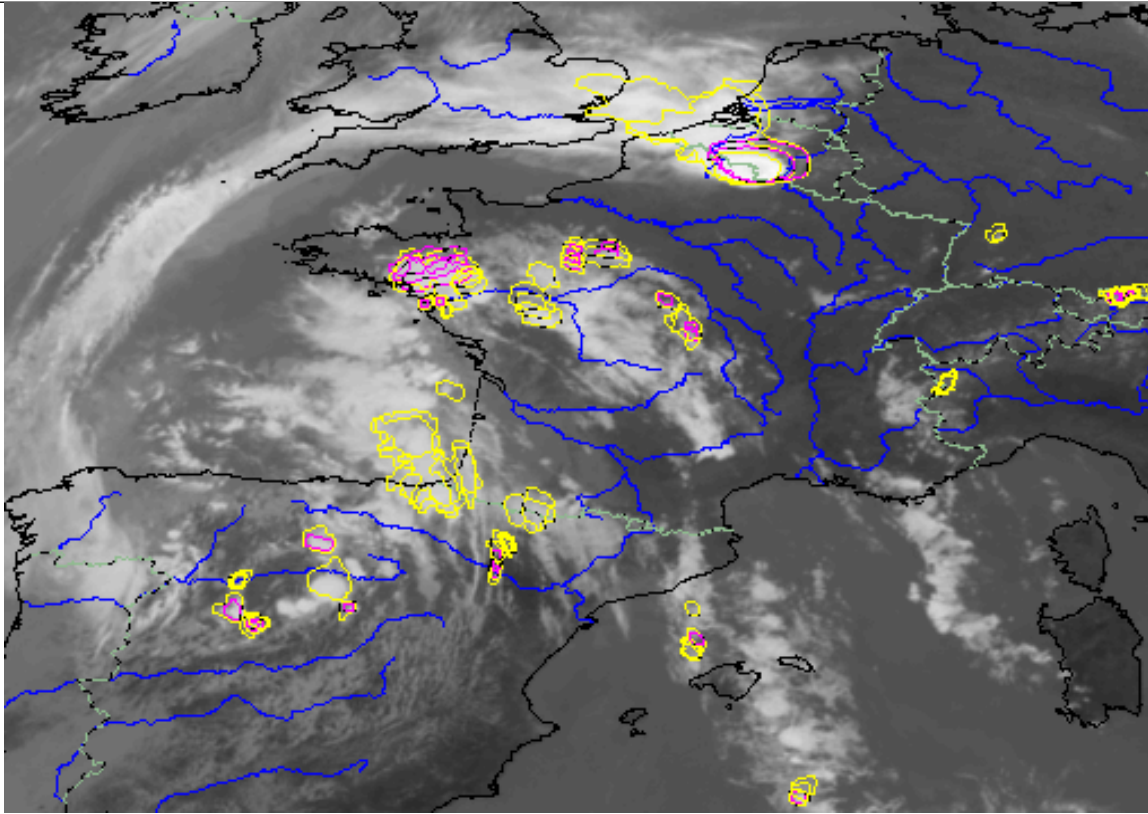
- The CI probabilities over identified pixels will be assessed regarding the evolution of convection during the following corresponding period over those pixels: 30 minutes for parameter ci_prob30, 60min for ci_prob60, etc.
- Presence of convective cloud cell from RDT-CW product will first be used as ground truth to assess the product. Smoothed path tracks of convective cloud cells over the corresponding period will allow to define areas of pixels where convection has been observed from a satellite point of view.
Using radar data above 30 dBZ or lightning data strokes will complement this ground truth, but only inside specific coverage areas (French radar or lightning network areas). In order to take into account representativeness issues, those data will be cumulated over the corresponding periods, smoothed and enlarged.
- Once convective masks have been elaborated for each slot over the corresponding periods, each CI parameter is compared to the ground truth of the corresponding period.

2.2 CI VERIFICATION

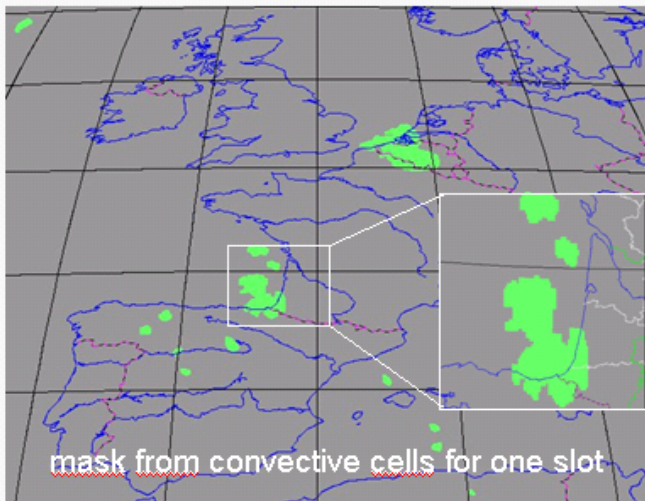
RDT cloud cells are not always defined by the same temperature threshold from one slot to another. The most realistic approach to identify “convective” areas during a given period is to gather successive contours of a given convective cloud cell and process a convex hull of those elements, producing a whole path track over the period. Such an approach provides a “convective mask” valid for a given period, with pixels sets to 0 or 1 depending on their position relative to the convective path track (see Figure 1).

Similar approach is undertaken with radar images, taking a threshold at 30 dBZ, then smoothed (median filter over 3 km) and enlarged (dilation operation over 3 km) to take into account uncertainty and tolerance. Corresponding pixels provide a radar convective mask over the period.

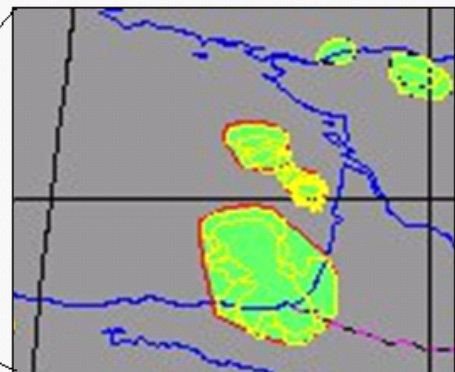
Finally, lightning data network allow to complete this approach, with enlarged strokes (10 km) during a given period providing a convective lightning mask.



RDT contours cumulated over 30min, overlaid with IR image of 11h00Z slot on 25/05/2009

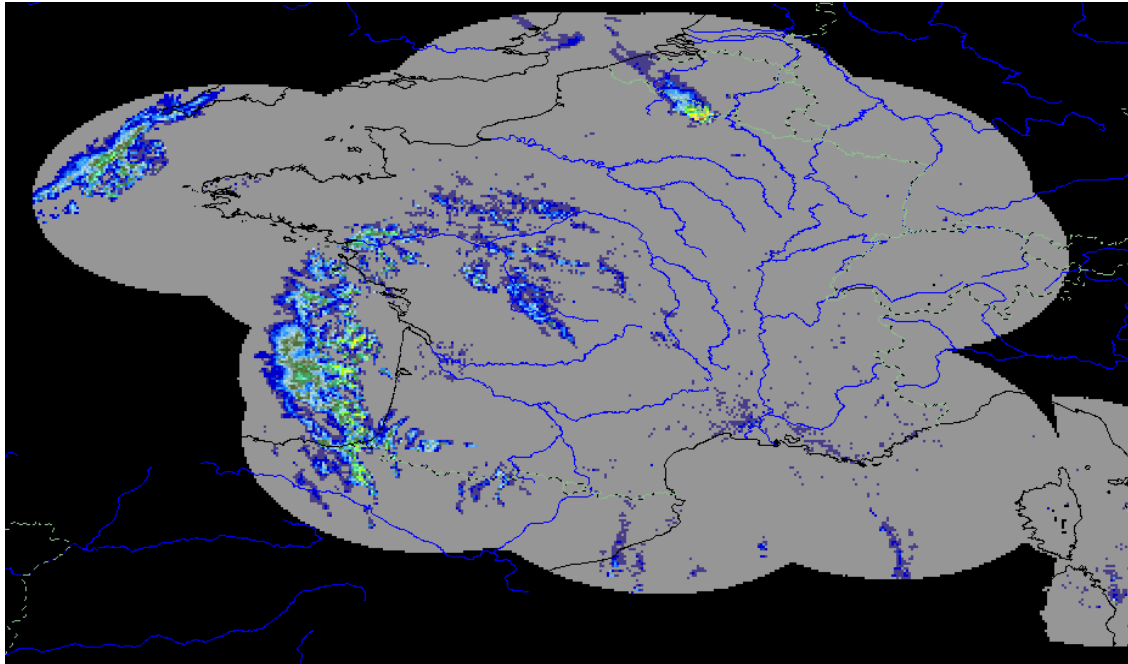


Convective mask from RDT
Smoothed Path tracks from successive convective cells

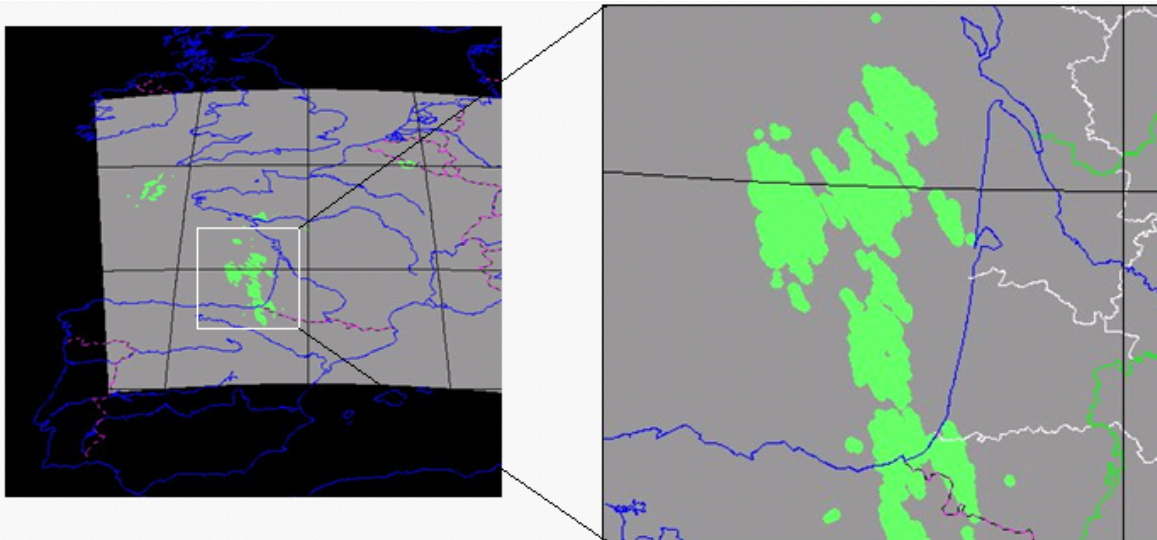


mask from accumulated convective cells for 3 slots included in a 30 minutes period

Figure 1: Elaboration of RDT ground truth for CI. A convex hull for accumulated contours over a given period identifies path tracks and thus areas of convective pixels



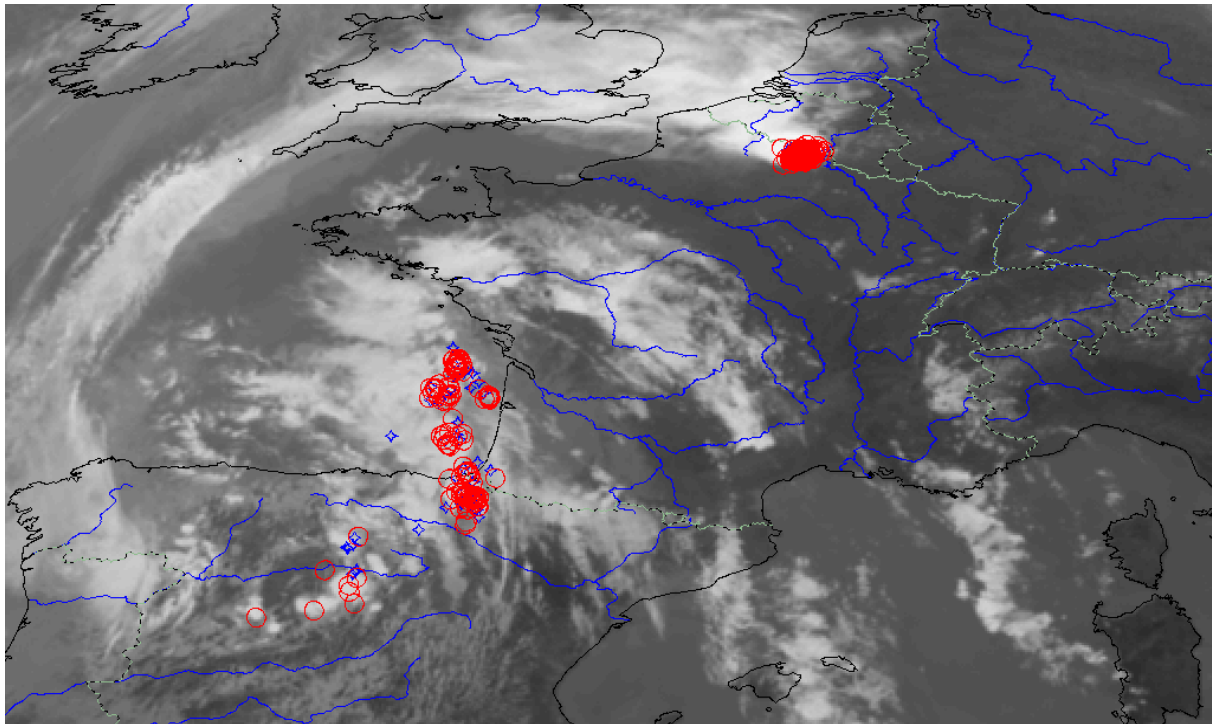
Radar reflectivity (dBZ) for 11h00Z on 25/05/2009



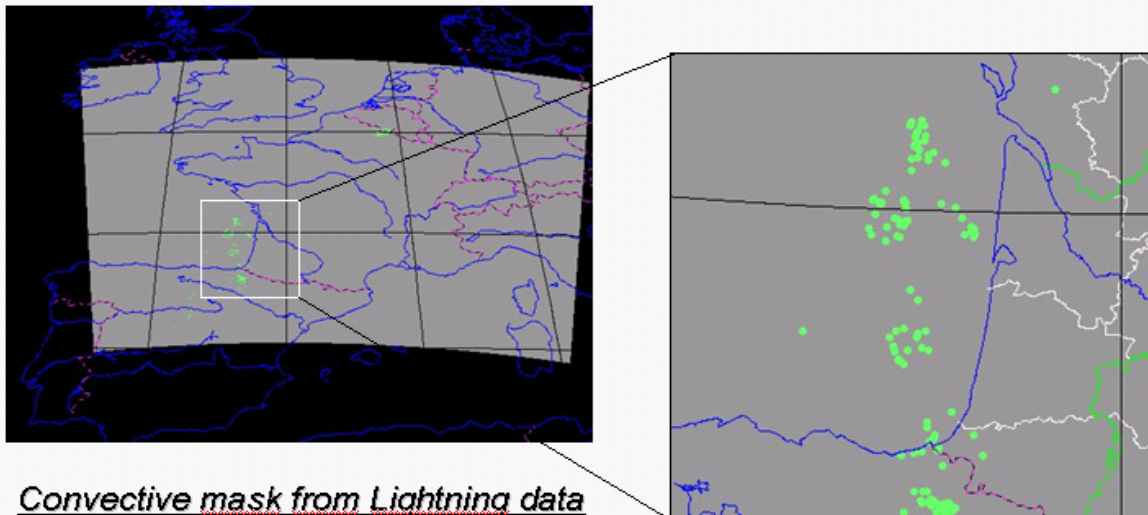
Convective mask from radar data

Smoothed path tracks from successive (5mn) significant pixels (>30dBZ)
for a given period

Figure 2: Elaboration of radar ground truth for CI over coverage area. Accumulated pixels with reflectivity over 30 dBZ during a given period identifies path tracks and thus areas of active pixels



Lightning strokes (red-negative, blue-positive) accumulated over 30min from 11h00Z on
25/05/2009



Convective mask from Lightning data
Enlarged (~10km) plots from cumulated
strokes for a given period

Figure 3: Elaboration of lightning ground truth for CI over specific coverage area. Accumulated and enlarged strokes over a given period identify areas of active pixels

2.3 SPECIFICITIES OF CI VERIFICATIONS

The verification method will have also a high impact on scores (see [RD.14.]

- Case study for convective days or large period,

	Validation report of the Convection Product Processors of the NWC/GEO	Code: NWC/CDOP3/GEO/MF-PI/SCI/VR Issue: 1.1 Date: 18th December 2019 File: NWC-CDOP3-GEO-MF-PI-SCI-VR-Convection_v1.1.odt Page: 17/67
---	--	---

- Double penalty issue taken into account or not,
- Threshold above which CI is verified (25%, 50% 75%),
- Day verification or day and night verification,
- Object or pixel-based verification,
- Verification of tracked clouds or verification of all clouds.
- CI below cirrus taken into account or not.
- Use of a rapid scan imager or not

For example in [RD.9] the POD varies from 0.32 to 0.72 depending on the way CI is verified.

Additionally high FAR are often attributed to difficulties inherent to CI problem. For example one CI object can dominate all other CI objects in the surrounding, as low-level convergence and upper-level divergence suppress other up-drafts. Very large FAR values can be found in literature.

2.4 OBJECTIVE VALIDATION

2.4.1 Context

Tropos (Leibniz Institute for Tropospheric Research) performed in Autumn 2018 a verification of CI v2018 in the framework of an Associated Scientist activity [RD.4].

2.4.2 Data and methods

The verification focused on 7 days with isolated convection over Germany. The verification is rather strict and is 100% independent of the learning data set. Identification of isolated convection with radar data is made using a method described in [RD.8]. HRV and 10.8 μ m SEVIRI channels are used to define the motion fields with optical flow techniques. At the final steps cloud objects are defined with HRV and radar data.

It is to note that this verification is highly independent of the training data set (some dates of the verification are common with the training data set but CI is trained with French radar data while it is validated with German radar data)

2.4.3 Results

Some case studies can be seen on <https://owncloud.gwdg.de/index.php/s/mqD75qzpPynel5m>

The report described some general features of the NWCSAF CI output in pixel-based approach: correlation between increased precipitation formation activity and number of issued CI detection, CI outside radar high-reflectivity areas, CI duration detection relatively short-lived especially for high probabilities, CI expected cloud type, repartition of CI in probability classes. It has been verified that

- CI warnings include regions with existing significant precipitations
- According to the definition of CI, temporal persistence of warning don't exceed the forecast horizon of CI product, especially for high probabilities

One problem identified in the report is that 50-75% and 75-100% classes are rarely filled in.

In object mode the less numerous classes are 0-25 % and 50-75 %.

Verification itself only concerns few cases and with POD ranging from 0,28 and FAR between 0,5 and 0.76 (see next figure), close the thresholds. The HSS (Heidke Skill Score) is above 0,3, CSI (Critical Success Index) is about 0,2.

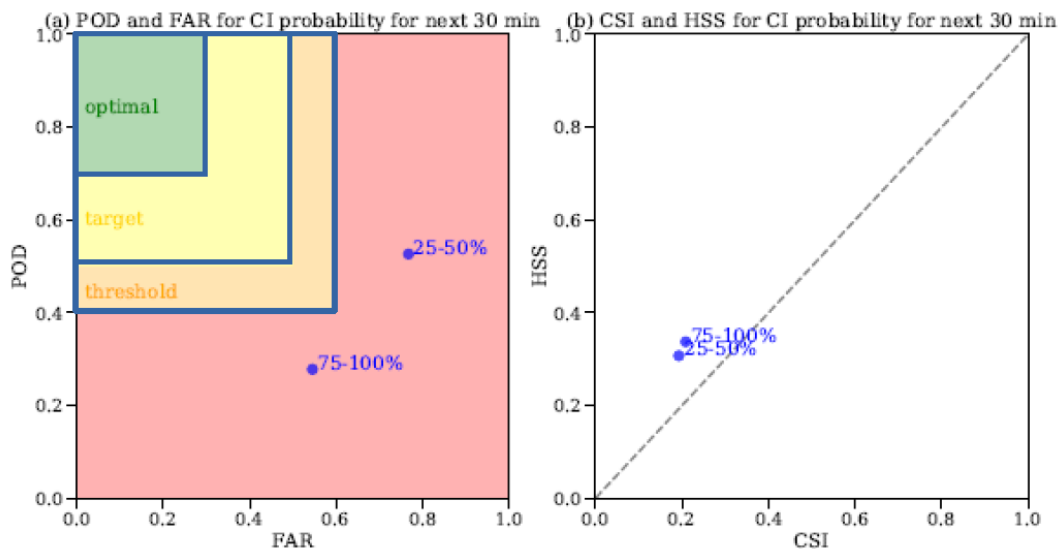


Figure 4: Plot of the POD FAR (figure on the left) CSI and HSS (figure on the right) of the validation of the v2018 CI 0-30' forecast product for the CI probability levels 25-50% and 75-100%. For the figure on the left the colour surfaces denotes the threshold values of POD and FAR given in PRD [AD.4]

The expert indicate that, in order to meet the requirement of product accuracy, further developments would be necessary through tuning of thresholds, refining definition of the CI areas, and use of rapid-scan data to enhance the confidence level of detection in future version.

A huge gap has been filled from v2016 to v2018 as several input data has been added corresponding to various physical properties of CI. Report from TROPOS indicates “v2018 CI product constitutes a clear improvement over its predecessor v2016, in particular considering the fact that our validation using ground-based radar fields is rather strict”.

2.5 CASE STUDIES

The methodology described above should be applied to situations where CI may be produced in full configuration mode, i.e. with CT product and an estimation of pixel movement as precise as possible, using NWP and HRW data to manage a movement guess field. Thus, 2010 situations with corresponding reprocessed products have been identified: 25/05/2010, 15/06/2010, 28/06/2010, 02-03/07/2010, 06-07/09/2010.

For other pre-selected dates (25/05/2009, 1-6/06/2013) identified, optional input data have been regenerated on the basis of available pre-v2018 source code.

CI and RDT product will have to be processed over those dates to undertake widest verification or validation data sets.

2.5.1 20100628 MSG Case Study

This case study illustrates the complexity to undertake a validation of CI product, taking into account a 30 minutes accumulation of radar data whose reflectivity are over 30 dBZ as ground truth.

Diurnal and orographic convection develops over France and moderate convective cells appear in Spain as illustrated below.

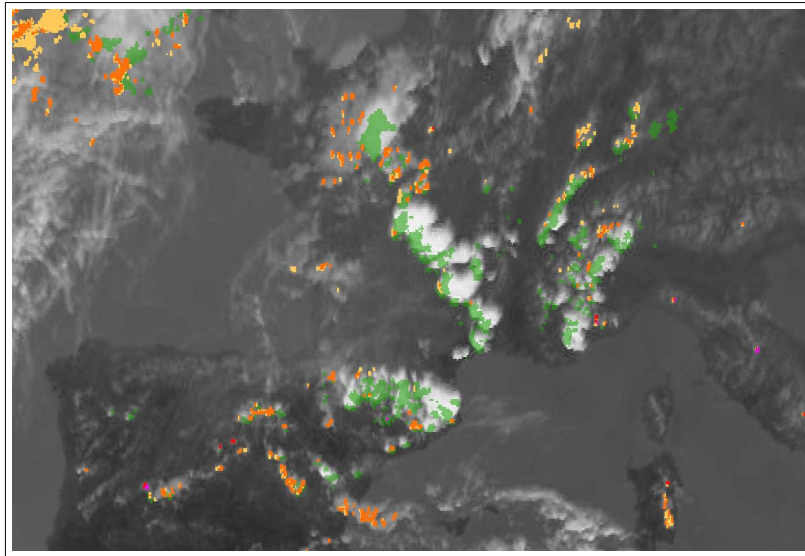


Figure 5: 20100628 CI Case Study - 13h00Z IR image, overlaid with with CI_prob30 and [13h00Z-13h30Z] accumulated radar > 30dBZ seen as ground truth (green shading). The colour code for visualization of CI is as follow: yellow for [0-25%] probability of Convection initiation, orange for [25-50%] probability of Convection initiation, red for [50-75%] probability of Convection initiation, magenta for [75-100%] probability of Convection initiation

Favourable cases are masked by a high number of false alarms. When regarding this situation at a finer scale, one can detect interesting features, giving a favourable credit to CI product. CI signatures are often not so far from radar information, collocation is a real issue, and thus “double penalty” consequence.

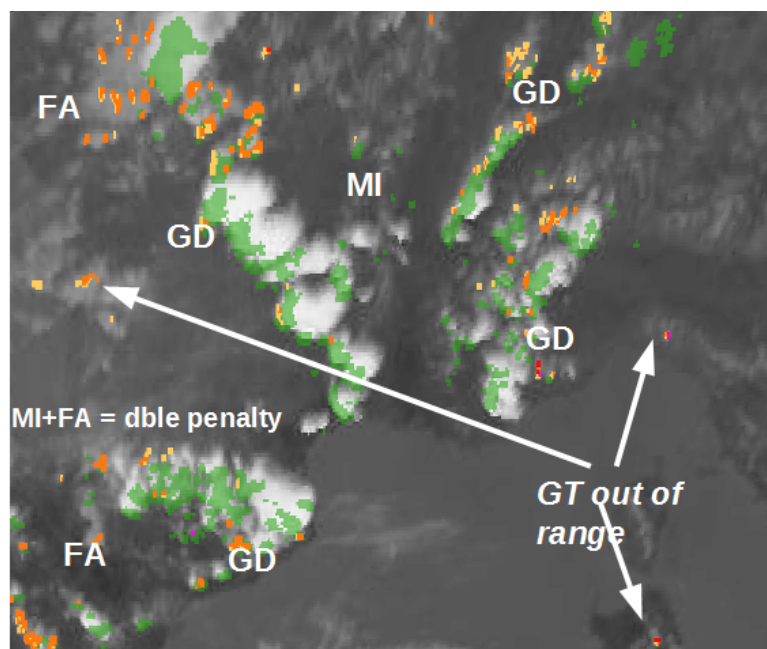


Figure 6: 20100628 CI Case Study. Same legend as Figure 5. Zoom allows to detect all cases : Good Detection (GD), miss cases (MI), false alarms (FA) and double penalty when MI and FA are inside the same area

2.5.2 20180702 MSG Case Study

This summer case study highlights deep orographic convection over the Alps and moderate convection over Pyrénées and Massif Central. One can note that CI signature is unfiltered and sometimes encountered on the edge of cloud systems.

Other signatures in isolated convection areas seem relevant, even if they don't fit exactly with the ground truth: the zoom on the convection area near the centre of the image illustrates this feature. A level 3 signature (red pixel - 50%-75% probability) fits perfectly with radar signature in the next 30 minutes (over pre-Alps), where another seems as a false alarm (over Massif Central), even if other highlighted pixels (levels 1 and 2, i.e. 0-25% and 25-50% probability) looks as good detections.

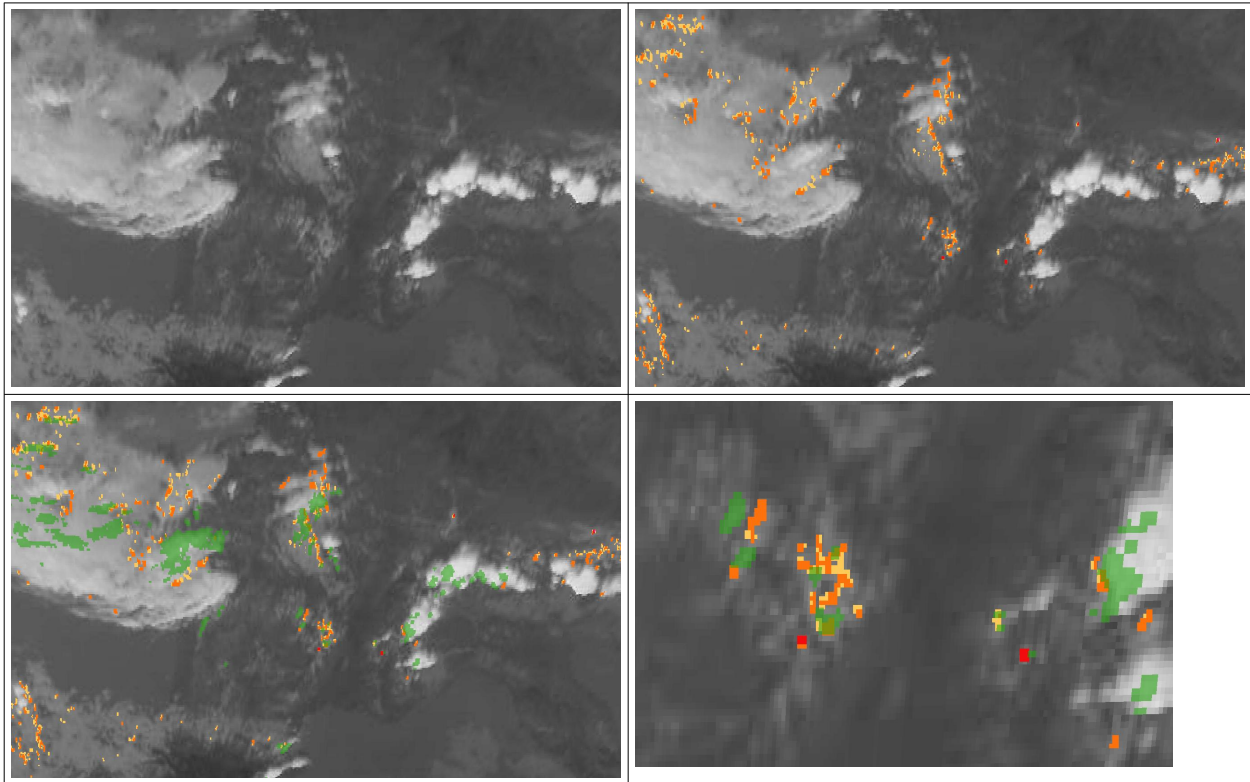


Figure 7: 20180702 CI Case Study, same legend as Figure 5 - 15h00Z 10.8 μm IR image (top left), overlaid with CI_prob30 (top right), and with [15h00Z-15h30Z] accumulated radar > 30 dBZ as ground truth (green shading bottom left). Zoom on moderate convection (bottom right)

Considering the same satellite slot and exploring the radar signature in the next 60 minutes instead of the next 30 minutes shows that some significant CI [0-30²] pixels are confirmed, beyond the 30 minutes forecast range. CI has caught a relevant signal far before radar signature. It changes in a positive way the impression of false alarm given when looking only a strict time-recovering between CI horizon and radar verification-period. It confirms that CI product may bring some valuable information, even far before an event occurs

Several significant CI are good detection from the moment radar signature occurs in the vicinity.

But it is an evidence that false alarm pixels are much more numerous than good detection ones. Moreover, the distribution of the levels of probability of CI products reveal a kind of anomaly : the product provides much more pixels in the [0-25] and [25-50] classes than in the two others (Figure 10). It confirms a result of the objective validation.

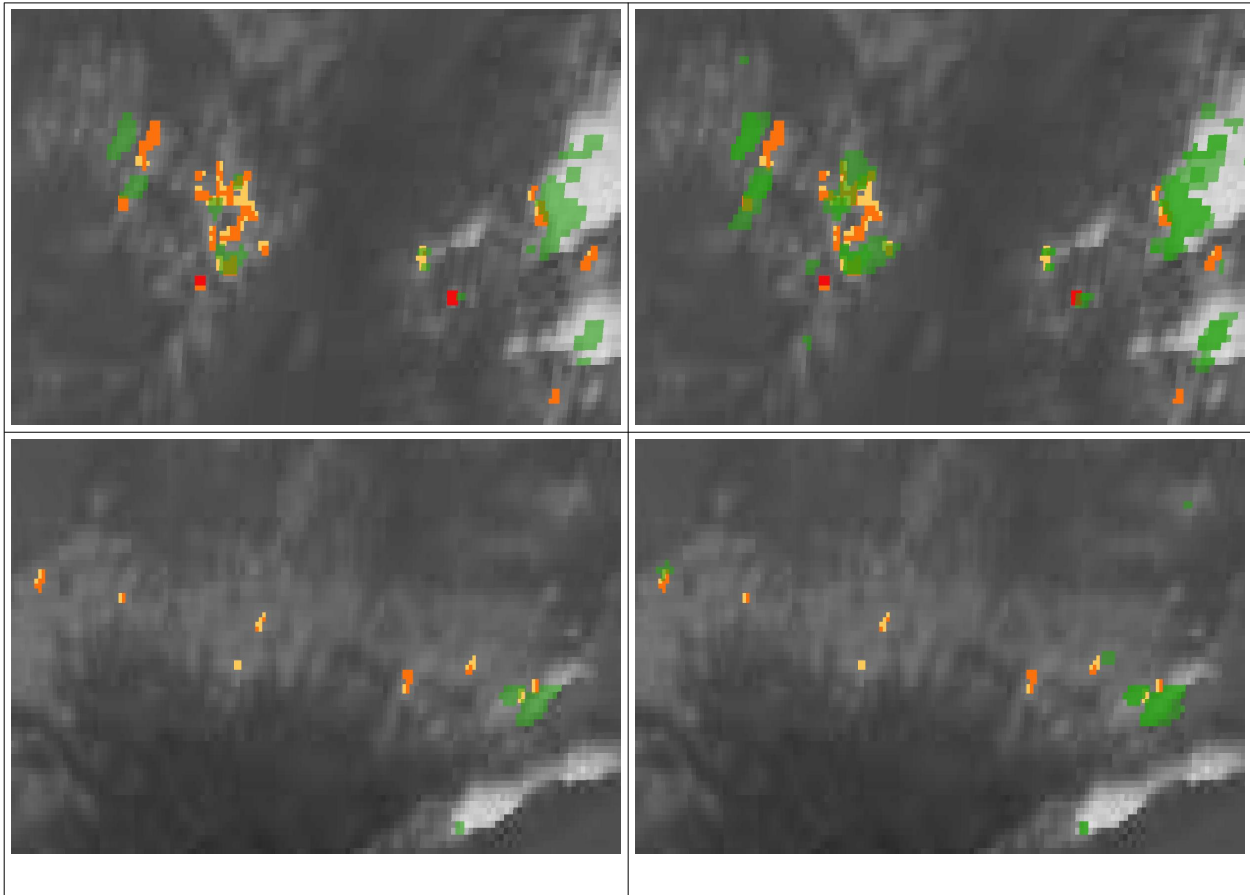


Figure 8: 20180702 CI Case Study, same legend as Figure 5 - 15:00 Z 10.8 μ m IR image overlaid with CI_prob30 and [15h00Z-15h30Z] accumulated radar>30dBZ (left), with [15h00Z-16h00Z] accumulated radar>30dBZ (right). Zoom centre France (top), over Pyrénées (bottom)

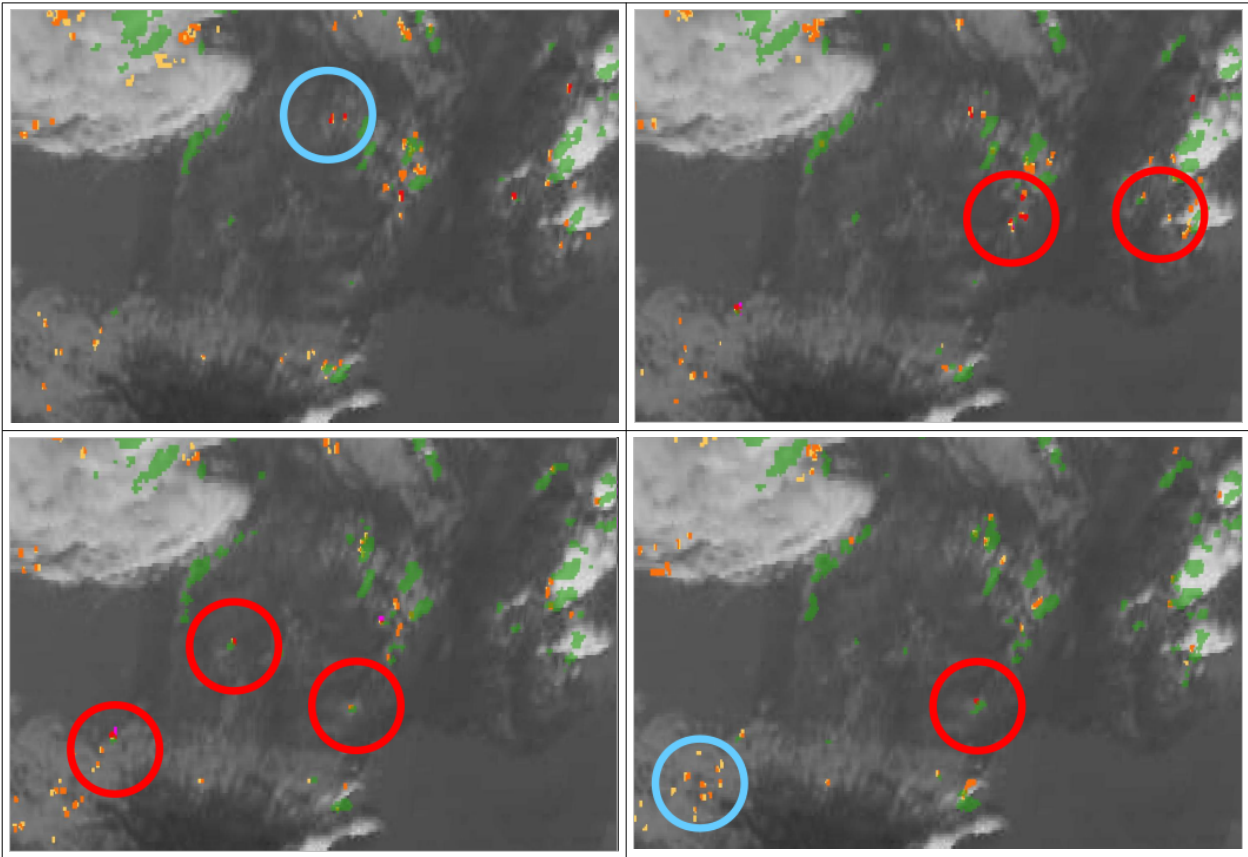


Figure 9: 20180702 CI Case Study, , same legend as Figure 5 - 15:00 Z 10.8 μm IR image overlaid with CI_prob30 and next 30 minutes accumulated radar > 30dBZ. Slots 15h15Z (top left), 15h30Z (top right), 15h45Z (bottom left), 16h00Z (bottom right). Good Detection pointed with red circles, false alarm with blue circles.

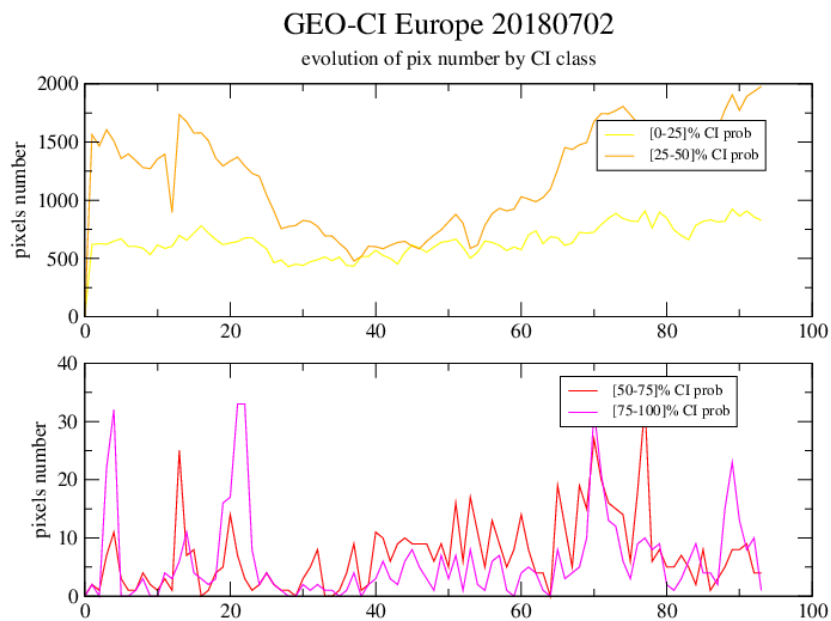


Figure 10: 20180702 CI Case Study - Time series of pixel numbers by probability classes. X-axis ranges from 00h15Z to 23h45Z,

2.5.3 20180513 MSG Case Study

This case study presents a cold unstable air mass intrusion in Biscay bay (Spain) behind a disturbance. We limit our analysis to this part of the image, on the West coast of France.

CI product identifies significant pixels mainly in southern (warmest) part of the air-mass. Despite obvious unstable cloud cells in the cold air-mass, GEO-CI does not identify convection initiation, leading to numerous "miss" cases.

This feature seems to be more important in the morning than in the afternoon, as illustrated in figure hereafter.

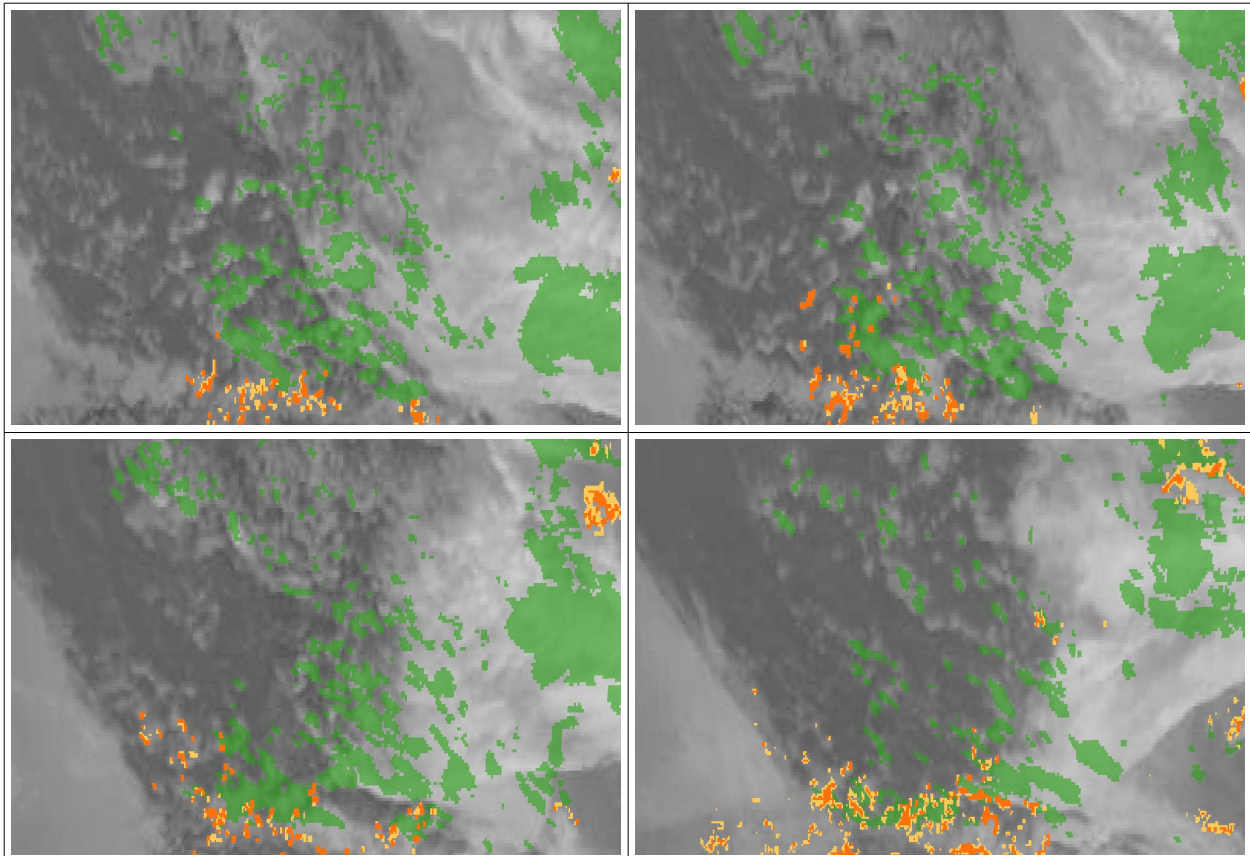


Figure 11: 20180513 CI Case Study - From Left to right and top to bottom, 11h00Z, 12h00Z, 15h00Z and 18h00Z, CI probabilities for next 30minutes (yellow and orange), radar ground truth (green shades)

CI product seems less relevant in cold air masses. It is likely linked to the filter which is implemented, limiting the analysis to warmest and lowest Cloud types, and ignoring in particular fractionated class of Cloud Type. Another explanation could be an insufficient precision of movement field in case of a rapid flow in low levels, leading to imprecision in trend estimates. This case provides clearly some ways of improvement.

One can note that we can hardly see CI pixels with a probability above 50%. The same unbalance between low probabilities and high probabilities can be found in this situation, as illustrated below.

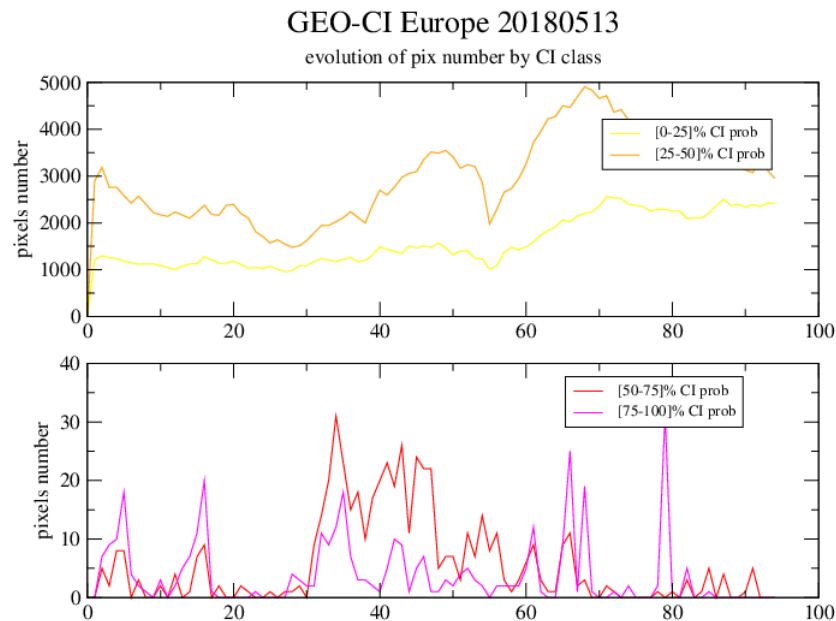


Figure 12: 20180513 CI Case Study - Time series of pixel numbers by probability classes. X-axis ranges from 00h15Z to 23h45Z,

2.5.4 GOES-16 CI verification - data and method

2.5.4.1 Case studies date and location.

Two case studies have been analyzed: October 2, 2018 and October 4, 2018. They focus on small parts of GOES16 ABI full disk, where French radar data is available to be used as ground truth.

Radar data in French West Indies is operated by Météo-France and covers Martinique and Guadeloupe islands. This is a 2km-resolution long-range radar mosaic. Both night-time and day-time part of CI algorithms are verified.

Radar data in French Guiana is operated by the French National Centre for Space Studies (CNES: Centre National d'Etudes Spatiales). This is a 1km-resolution radar close to Kourou launch pad.

2.5.4.2 Use of a radar-based product as ground truth.

Up to now [RD.10], 'raw' radar was used as ground truth when radar reflectivity reaches a value between 30 and 35 dBZ. We refine the definition of the ground truth towards a radar-derived convection object so as to consider:

- The birth of the convective cell. The CI focuses only on newly developing convective cells. It is a key feature of the new approach. It avoids CI product to be verified against cells already developed when CI is calculated. It also helps distinguish CI signage characteristics and CI forecast ones.
- The lifetime of the convective cell. The CI focuses on convective cells of lifetime over 30 minutes to consider the lifetime of a thunderstorm.
- The pairing of the convective cell with lightning. The CI focuses on convective cells that become thunderstorms. In that case, GLD360 lightning data [RD.11] is used for pairing.
- The cloud top pressure of the convective cell. The CI focuses on Cumulus that become Cumulonimbus, that is, on warm clouds defined here as cloud top pressure over 500 hPa.

Météo-France produces such radar-derived convection objects at a 5-minute frequency. Convective cells are delineated at different reflectivity thresholds (32, 36, 40 and 48 dBZ) and contain information about the tracking of the convective cell, the pairing of the cell with lightning, and the cloud top pressure derived ([RD.12]), in the present case studies, from MSG NWC SAF CTH product operated in version v2016 by Météo-France ([RD.13]).

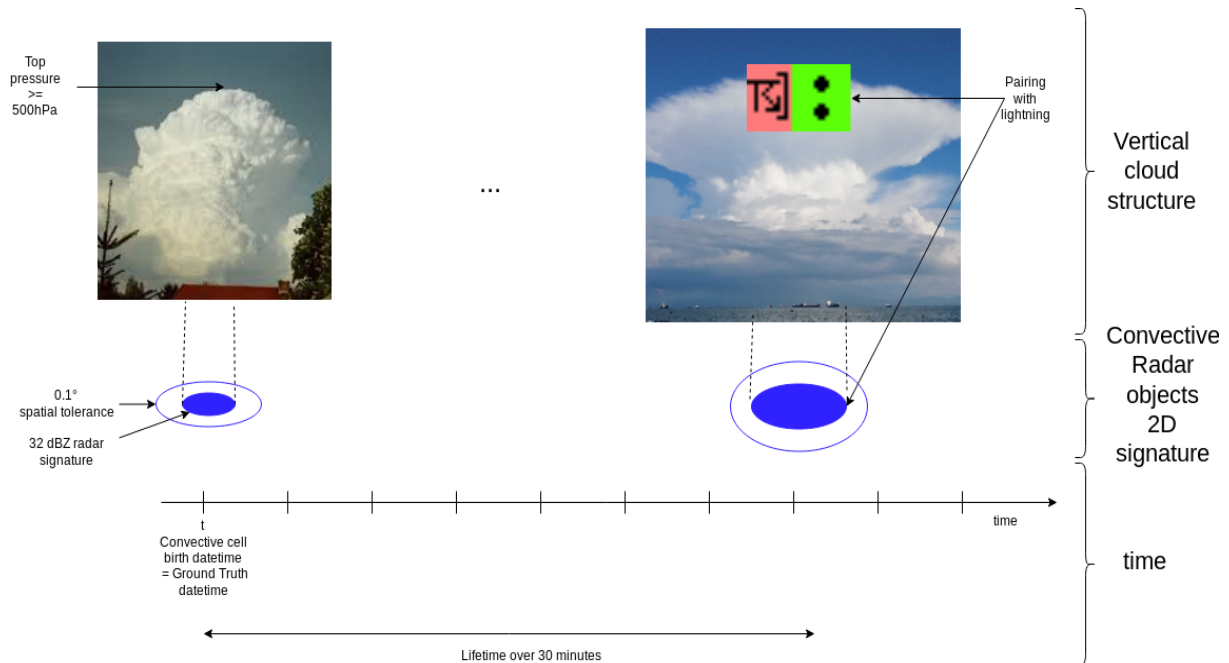


Figure 13: Ground Truth definition illustration

The ground truth is now defined as a radar-derived convection object, taken at the date time of its birth, paired with lightning, with a sufficient lifetime, embedded in a warm cloud (Figure 13).

The ground truths for the two case studies are displayed in Figures 14 and 15. The new definition of the ground truth considerably limits the amount of available ground truths for a single day, 14 for the 2018-10-02 case study (from 13:20 to 20:25), 10 for the 2018-10-04 case study (from 3:30 to 08:30 and from 16:15 to 21:45).

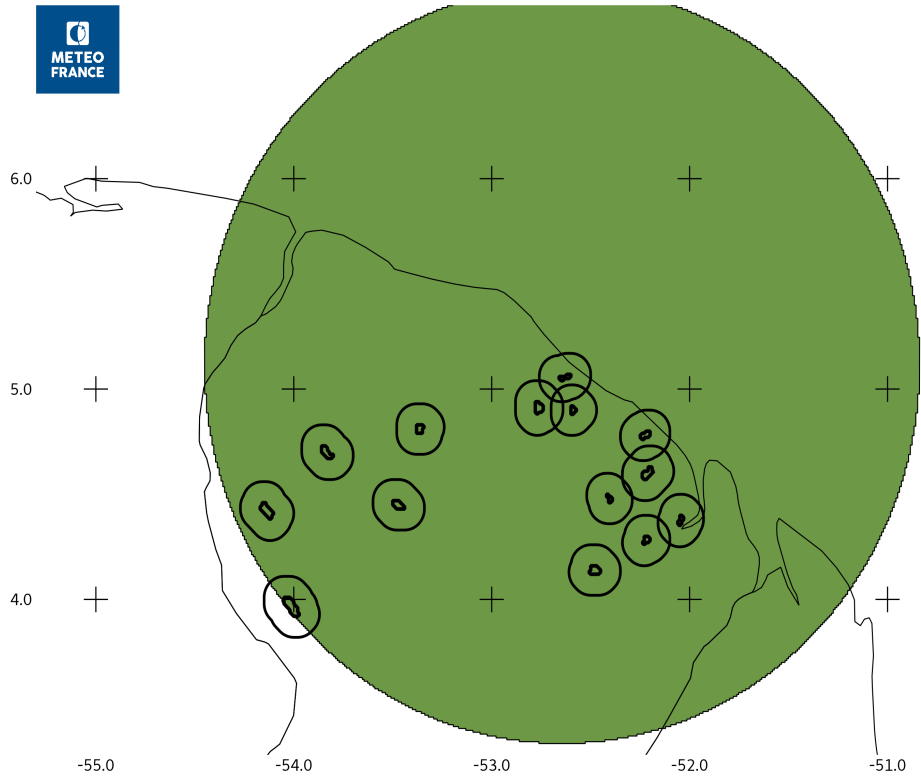


Figure 14: 2018-10-02. Ground Truths over French Guiana. Smaller objects delineate convective cells. Bigger objects delineate a spatial tolerance of 0.1° around each convective cell.

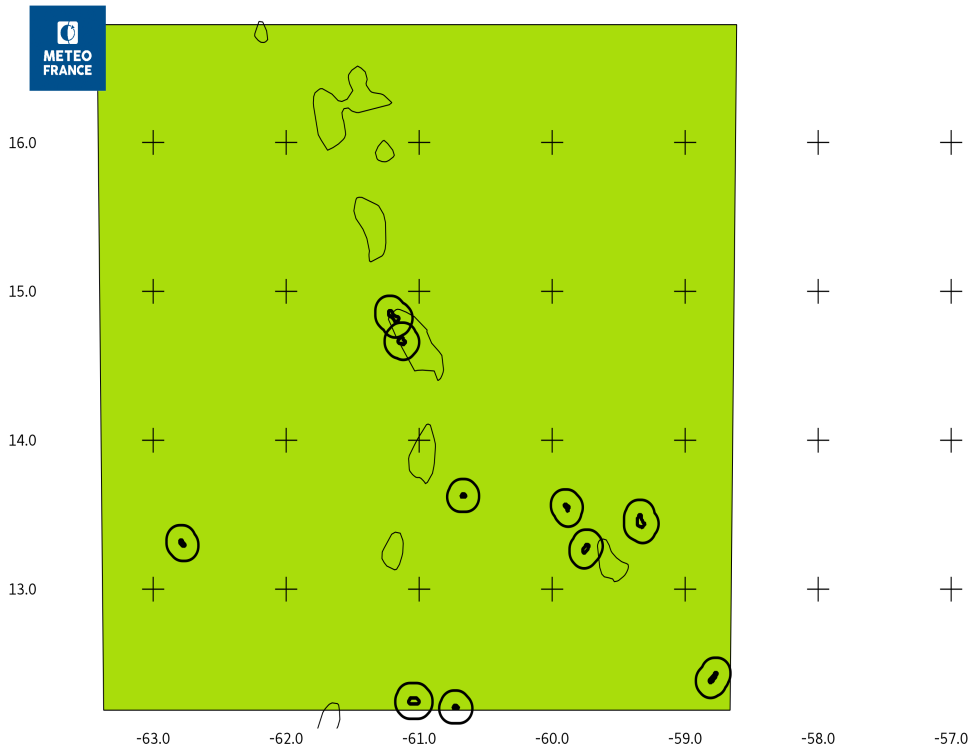


Figure 15: 2018-10-04. Ground Truths over Caribbean French West Indies. Same representation of objects as in previous figure.

 	Validation report of the Convection Product Processors of the NWC/GEO	Code: NWC/CDOP3/GEO/MF-PI/SCI/VR Issue: 1.1 Date: 18th December 2019 File: NWC-CDOP3-GEO-MF-PI-SCI-VR-Convection_v1.1.odt Page: 27/67
---	--	---

2.5.5 20181002 GOES-16 case study

2.5.5.1 CI default production

This case study focuses on French Guiana. Convection appears only overland.

The CI production configuration is the default one. IR11.2 μ m ABI band is used for cloud detection and tracking.

In this subjective analysis, we try to assess the performance of CI product for signage or for, as it is made for, forecast. When looking at a specific production date time 18:30 (Figure 16 top left), CI [0;30] forecast production depicts a high number of false alarms, as mentioned in NWC SAF v2018 validation report for convection product ([RD.10]) and somewhat inherent to convection initiation problem ([RD.14]). False alarms appeared at the edge of cold cloud systems. They are associated mainly with [25 %,50%] CI level of probability and contribute to the strong unbalance between the CI classes of probability (cf. Figure 17).

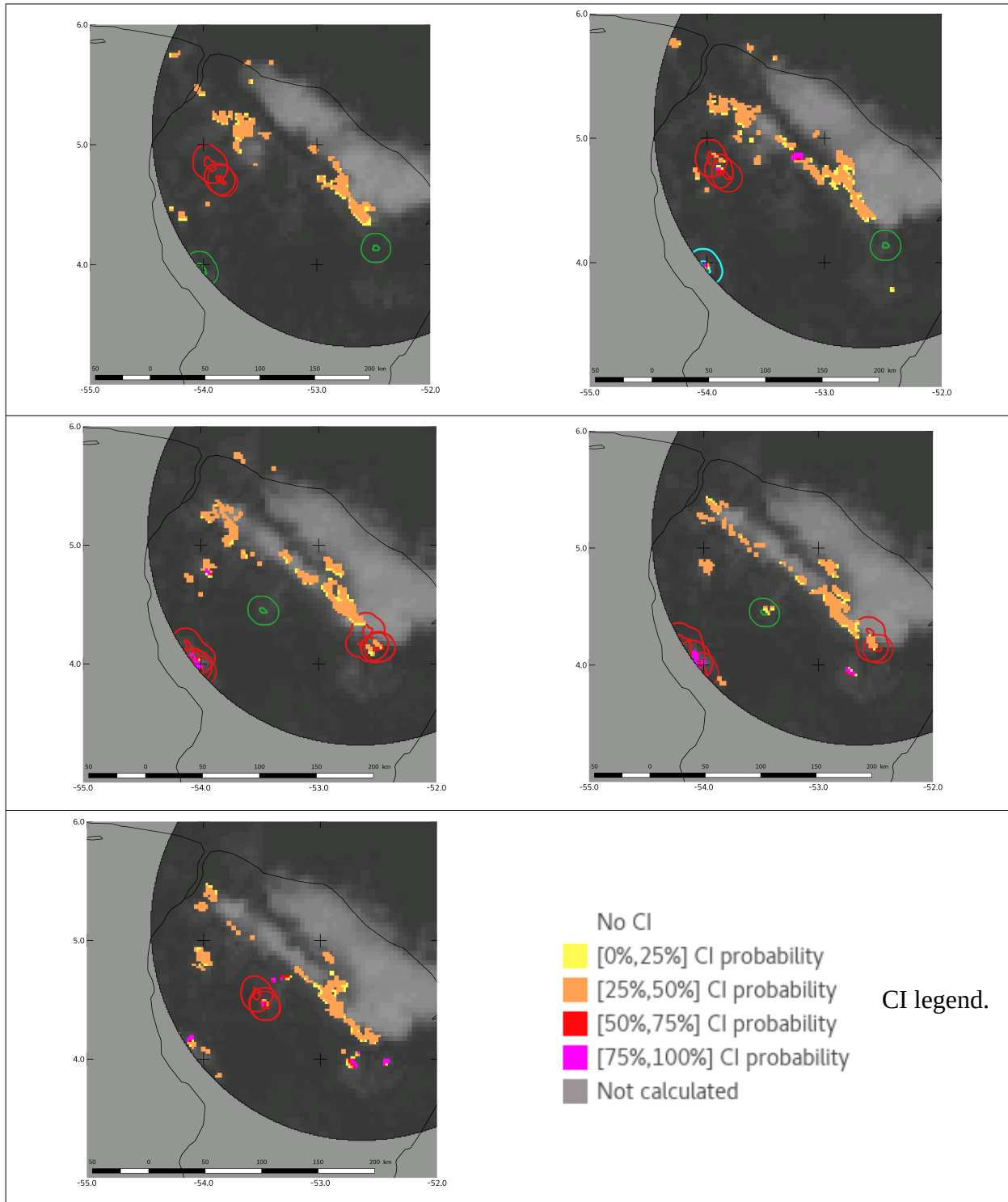


Figure 16: Zoom on French Guiana, 2018-10-02. Top Left: Time $t = 18:30:00Z$. IR10.8 satellite imagery at t , CI $[t+0;t+30min]$ forecast production (from yellow to magenta according to the class of probability to assess the forecast capacity of CI), Ground Truths at $t = 0$ in blue contours, at $[t+5;t+30 min]$ in green contours. Ground Truths at $[t-30;t+0min]$ and their evolution at $t+0min$ and $t+30min$ in red contours to assess the signage capacity of CI. From top to bottom and left to right: Same figures at times $t = 18:45:00Z, 19:00:00Z, 19:15:00Z, 19:30:00Z$

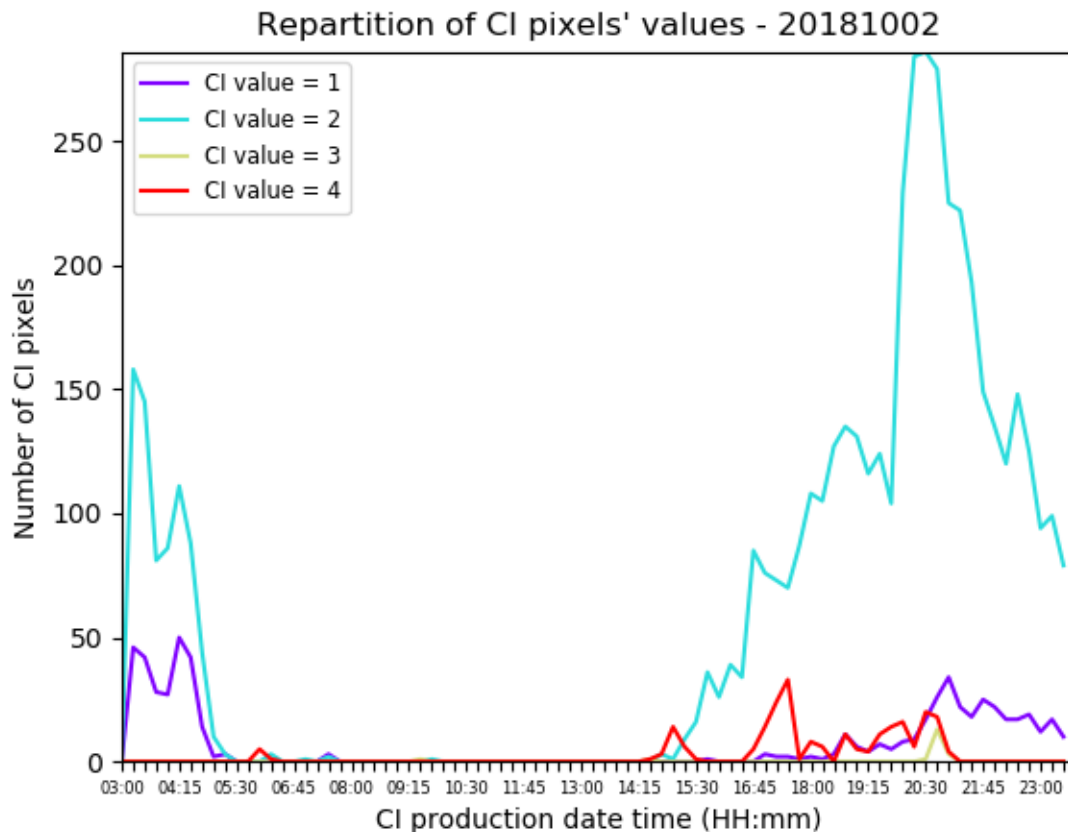


Figure 17: 2018-10-02. Repartition of CI pixels' values.

On top left, no CI pixels are forecast within a ground truth in green / blue / red contour: these are misses. Misses have however to be mitigated. When looking at next CI production (18:45, top right), the same ground truths appear and we notice that there are two good detections:

- Ground Truth in blue means that CI production time and ground truth time are the same. In that case, CI radar signature and CI satellite signature are simultaneous.
- Ground Truth in red means that CI production time exceeds GT birth time. GT is paired with CI in the vicinity of the radar signature, within the 0.1° spatial tolerance.

The second case occurs quite frequently (see following images). Radar convection initiation (ground truth) is often seen before the satellite one.

We also notice a match between CI pixels and GT green contours at 19:15. In that case, it means that CI [0;30] forecast is good because it overlaps with a newly developing cell within [0min;30min] time interval.

Figure 18 summarizes the CI / Ground Truth pairing for the 14 ground truths of the case study.

CI has very good skill to detect existing convective cells when taking into account a spatial tolerance around the ground truths. When looking at GT at [t-30min;t-0min[and CI forecast at [t+0min;t+30min], 80 % of GT are paired with CI. In other words, up to 80 % of ground truths are detected 30 minutes after the radar object's birth.

The radar signature of convection initiation precedes the satellite one. The production time frequency (15 minutes for satellite data vs 5 minutes for radar data) may play a role. The right part

of the curve (after the vertical line) illustrates the relatively poor capacity of CI to detect in advance the radar object.

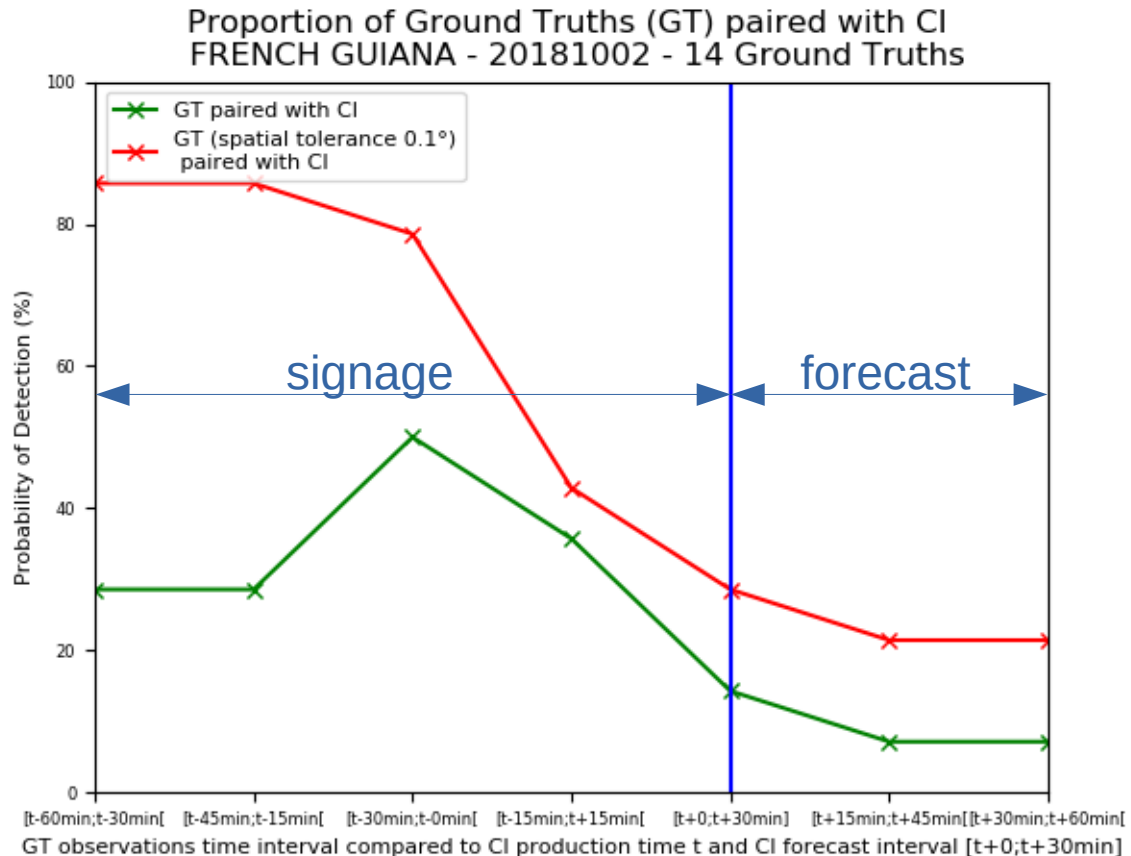


Figure 18: 2018-10-02 case study. Proportion of GT paired with CI.

For this case study we can say that CI provides useful information to detect convection when a radar network is not present. But CI hardly anticipates the convection and brings poor added value to radar network.

2.5.5.2 CI production with IR10.3 μ m

In this part, we want to assess the impact of using IR 10.3 μ m instead of IR 11.2 μ m for cloud detection and tracking.

Figure 19 is a representation of the same slots as Figure 16 using channel IR 10.3 μ m CI production.

CI production with IR 10.3 μ m exhibits similar behaviour to CI production with IR 11.2 μ m. So similar results are applicable to IR 10.3 μ m channel:

- Large number of false alarms at the edge of cold cloud systems,
- Good pairing with ground truths when taking into account a 0.1° spatial tolerance and a temporal tolerance (GT at time [t-30min ;t-0min]). It highlights the signage capacity of the CI.

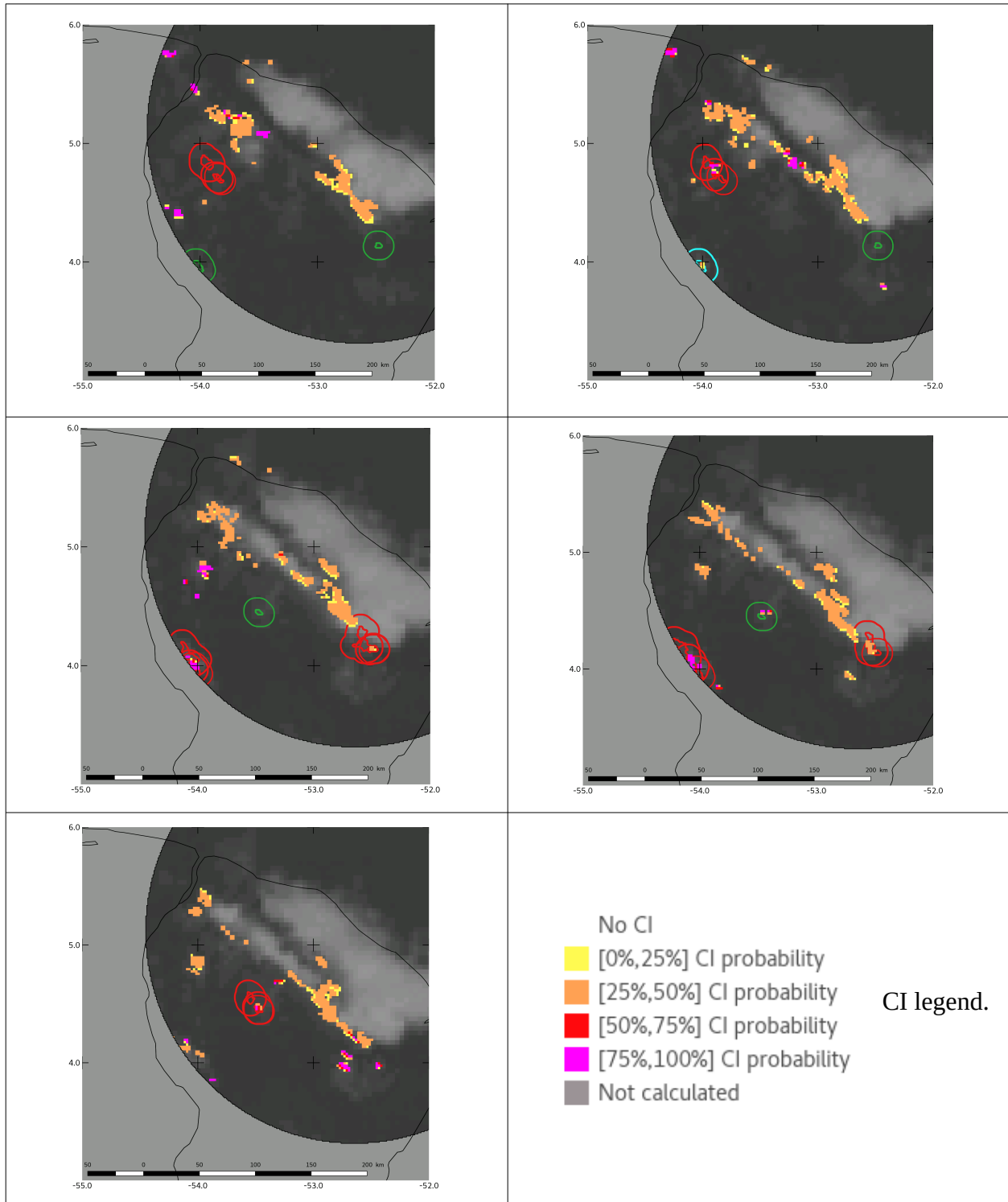


Figure 19: Zoom on French Guiana, 2018-10-02. Same as Figure 16 with channel IR10.3 μ m

All ground truths considered, the proportion of GT paired with CI is nearly equivalent to IR11.2 regarding the spatial tolerance (Figure 20). The only difference is for GT interval [-45;-15min[. It corresponds to the 14:00 ground truth for which a CI pixel is forecast within the ground truth with IR11.2 and not with IR 10.3.

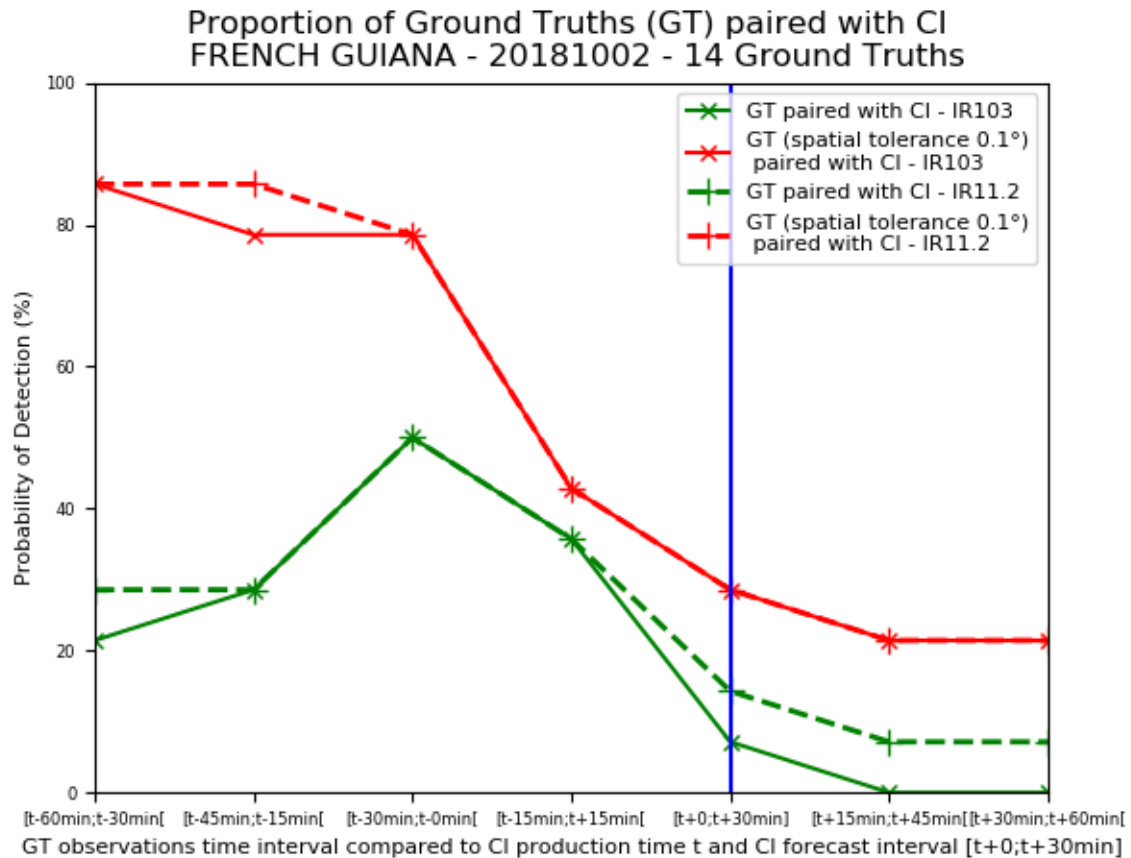


Figure 20: 20181002 Case Study Proportion of GT paired with CI – channel IR10.3 compared to channel IR11.2

As a whole, CI production with IR10.3 generates less false alarms than CI production with IR 11.2 (Table 3).

	CI production with IR11.2	CI production with IR10.3
Total number of pixels of interest	110 532	110 634
Total number of CI pixels before advection	5 733	4 355

Table 3: Comparison of CI production between IR11.2 μ m and IR10.3 μ m in terms of number of CI pixels.

CI production with IR10.3 is similar to CI production with IR11.2 in terms of good detections and significantly reduces false alarms (around 25 % less). So we recommend to use channel IR10.3 μ m as main channel for cloud cell detection and tracking.

2.5.6 20181004 GOES-16 case study

2.5.6.1 CI default production

	Validation report of the Convection Product Processors of the NWC/GEO	Code: NWC/CDOP3/GEO/MF-PI/SCI/VR Issue: 1.1 Date: 18th December 2019 File: NWC-CDOP3-GEO-MF-PI-SCI-VR-Convection_v1.1.odt Page: 33/67
---	--	---

This case study focuses on French West Indies. Convection appears mainly in the ocean. The CI production configuration is the default one. IR11.2 μ m channel is used for cloud detection and tracking.

Figure 21 depicts a series of CI production slots over the region (from 06:30 to 07:45), with two ground truths, one at 07:05 on the south of the image and the second at 07:15 on the east (top right, in green).

As in the 2018-10-02 case study, a large number of false alarms appear at the edge of cold cloud systems. Moreover, at almost each slot, some CI pixels are paired with ground truths. Focusing on GT at the south of the image, good detections occur before the 07:05 GT (from 06:30 to 07:00) and seem relevant. But pairings in the vicinity of the GT from 07:15 to 07:45 should rather be considered as false alarms at the edge of already developed cold cloud systems.

The analysis for the other GT is difficult to achieve: GT appears in a developing large cloud structure in which, at the end (07:15 to 07:45), CI pixels seem related to false alarms.

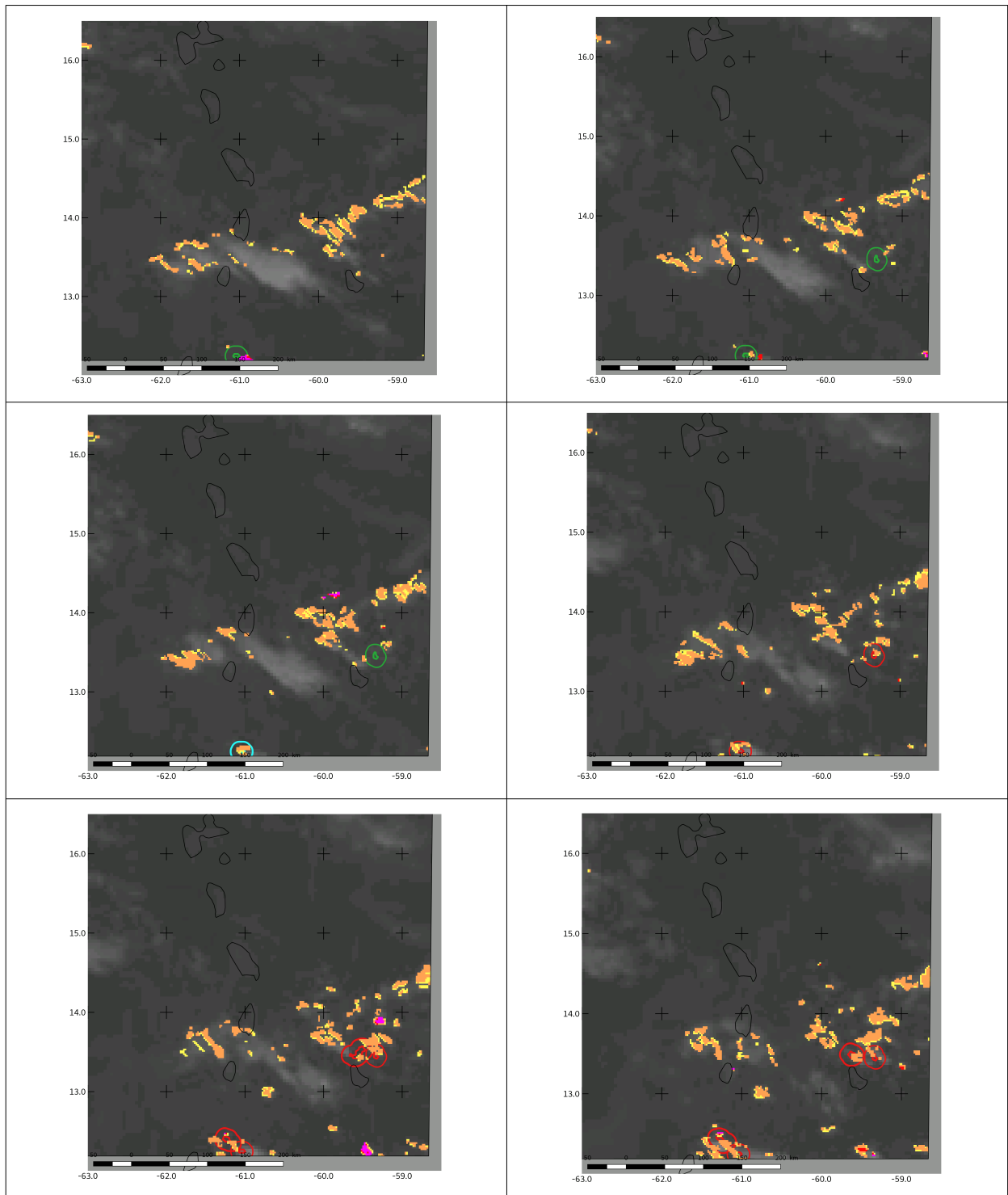


Figure 21: Zoom on French West Indies, 2018-10-04. Top Left: Time $t = 06:30:00Z$. IR satellite imagery at t , CI $[t+0;t+30min]$ forecast production (from yellow to magenta according to the class of probability), Ground Truths at $t = 0$ in blue contours, at $[t+5;t+30 min]$ in green contours. Past Ground Truths and their evolution at $t+0min$ and $t+30min$ in red contours. From top to bottom and left to right: Same figures at times $t = 06:45:00Z$, $07:00:00Z$, $07:15:00Z$, $07:30:00Z$, $07:45:00Z$

Overall, CI has skill to detect new convective cells for signage and also sometimes for forecast. Forecast skill is more obvious for this case study than for the 20181002 case study (Figure 22).

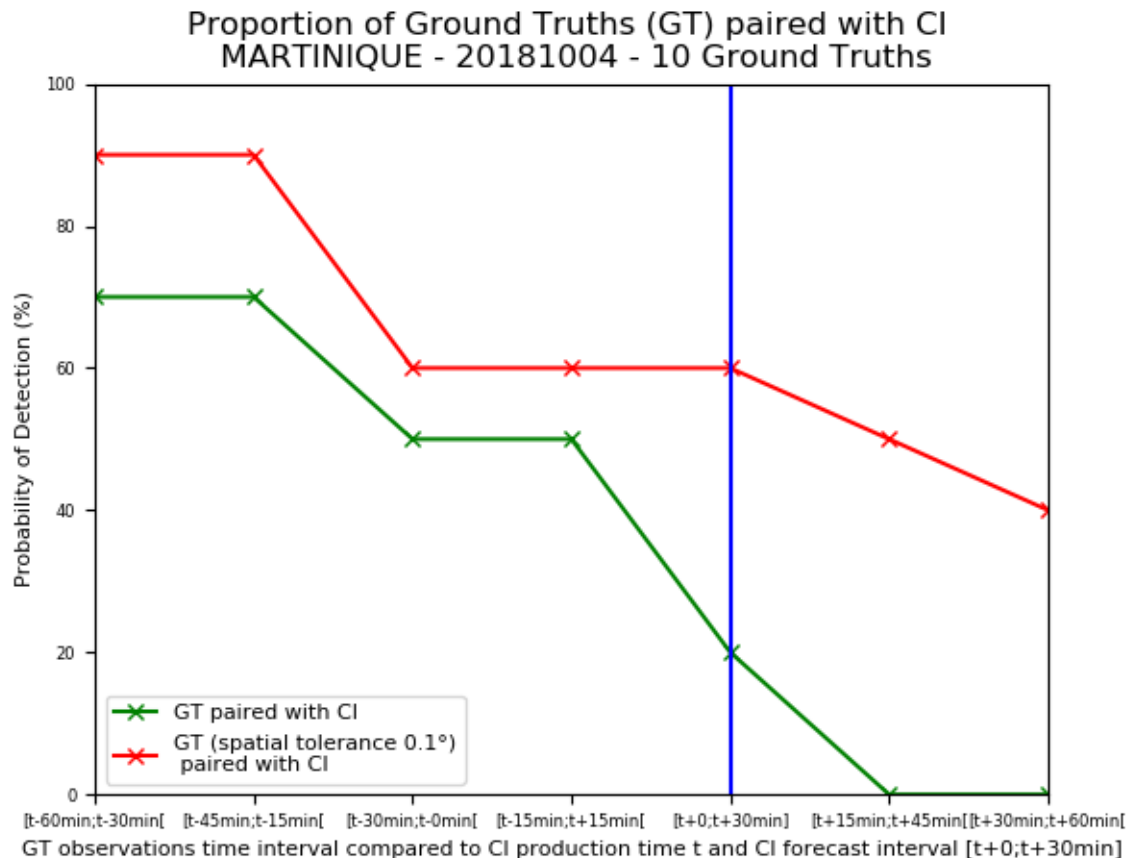


Figure 22: 2018-10-04 Case Study. Proportion of GT paired with CI.

2.6 CONCLUSION AND COMPLIANCE REQUIREMENTS

After CI v2016 first delivery of the product, v2018 exhibits major improvement and an effort on validation has been made. Improvements are illustrated in [RD.5].

MSG subjective evaluation highlights some strength of CI product for identifying significant pixels in areas of growing isolated convection, but points also some false alarms cases, especially in the edge of larger cloud systems, or in cold air masses. An analysis at fine scale shows also how relevant CI pixels are not always collocated with radar signal. In some cases, spatial or temporal tolerance can be considered, and could lead to consider some cases rather as good detection than false alarm. Nevertheless, improvements are still required to lower the number of false alarms, reduce the unbalance between probability classes, and better take into account the movement field.

MSG objective evaluation from TROPOS ([RD.4]) suggest FAR and POD not reaching the accuracy but remain close of them. The report points out that this “validation using ground-based radar fields is rather strict” and that the motion field used for reference and product are different, as it can also be a very sensitive point to improve in further validation studies. Sample size would have to be increased in future validation processes.

GOES-16 CI subjective validation has been undertaken in tropical regions using a new stricter ground truth based on radar convective cells. Some conclusions are common with the MSG CI

 	Validation report of the Convection Product Processors of the NWC/GEO	Code: NWC/CDOP3/GEO/MF-PI/SCI/VR Issue: 1.1 Date: 18th December 2019 File: NWC-CDOP3-GEO-MF-PI-SCI-VR-Convection_v1.1.odt Page: 36/67
---	--	---

production, whose validation has been made over Europe (France). CI has good skill to detect new developing convective cells for signage and sometimes for forecast. We recommend the use of IR10.3 μ m channel for cloud cell detection and tracking, instead of IR11.2 μ m.

Thanks to both objective and subjective validation the knowledge of the product has been highly increased. Nevertheless there is still room for improvement and new validation exercises to clearly outreach the requirements thresholds.

The CI v2018 confirms promising output of previous version. The validation effort has been largely increased leading to a much better knowledge of the output. The subjective validation confirms the usefulness of the product for forecasters.

We consider CI product at the boundary of the requirements.

	Validation report of the Convection Product Processors of the NWC/GEO	Code: NWC/CDOP3/GEO/MF-PI/SCI/VR Issue: 1.1 Date: 18th December 2019 File: NWC-CDOP3-GEO-MF-PI-SCI-VR-Convection_v1.1.odt Page: 37/67
---	--	---

3 RAPIDLY DEVELOPING THUNDERSTORM – CONVECTION WARNING (GEO-RDT-CW) VALIDATION

3.1 OVERVIEW

The main objective of this section is to document RDT convective discrimination accuracies and compare them to the threshold accuracies listed in the NWCSAF product requirements document [AD.4]. As the RDT discrimination scheme has been enriched between v2016 and v2018.1, with an additional calibrated scheme, new graphs and comments in this report will refer to this new approach (CAL). However, one still can refer to the previous validation of so-called generic (GEN) scheme over European areas, which can be still used in specific configurations (un-calibrated satellite, invalidated statistical model).

Concerning the forecast capabilities (forecast products) included in RDT-CW code (CW part) it is to note that thunderstorm conceptual models often show a rapid morphological evolution and intensity variability, for which satellite data bring not enough information. A subjective evaluation based on cases study is undertaken for an analysis of the localization of extrapolated cloud cells, depending on moving speed estimate accuracy and morphological evolution of the cloud systems. An objective validation has been made in a scientific report [RD.3].

3.2 VALIDATION OF GEN DISCRIMINATION DIAGNOSIS

3.2.1 Context

The GEN discrimination diagnosis has been fully described in previous validation report and results are still available as this choice of validation is still proposed to end-users. Hereafter a summary of the validation.

3.2.2 Data and methods

The configuration of discrimination verification is following

- Domain Europe
- Ground truth given by EUCLID network
- Period including intermediate season: June-August 2008 + April-October 2009)
- Section approach where trajectory is split in convective and non convective sections
- Trajectories with light electric activity suppressed of the sample
- H2 hypothesis where RDT-CW early diagnosis (before an electric section) and continued diagnosis (after an electric section) have a positive impact on scores. It meets the requirement of “30 minutes detection after first lightning occurrence”
- RDT v2011 operated without lightning data to force the discrimination process.
- Results applicable to v2018 with GEN discrimination option

3.2.3 Results

POD	77 %
POFD	4 %
FAR	28 %
TS	59 %

Table 4: RDT v2011 Discrimination skill table

The figure below points out that more than 50% of good detection are already classified at the time of the first lightning occurrence, 80 % thirty minutes after. Nevertheless, only 25% are classified before the first flashes stroke (15 min before).

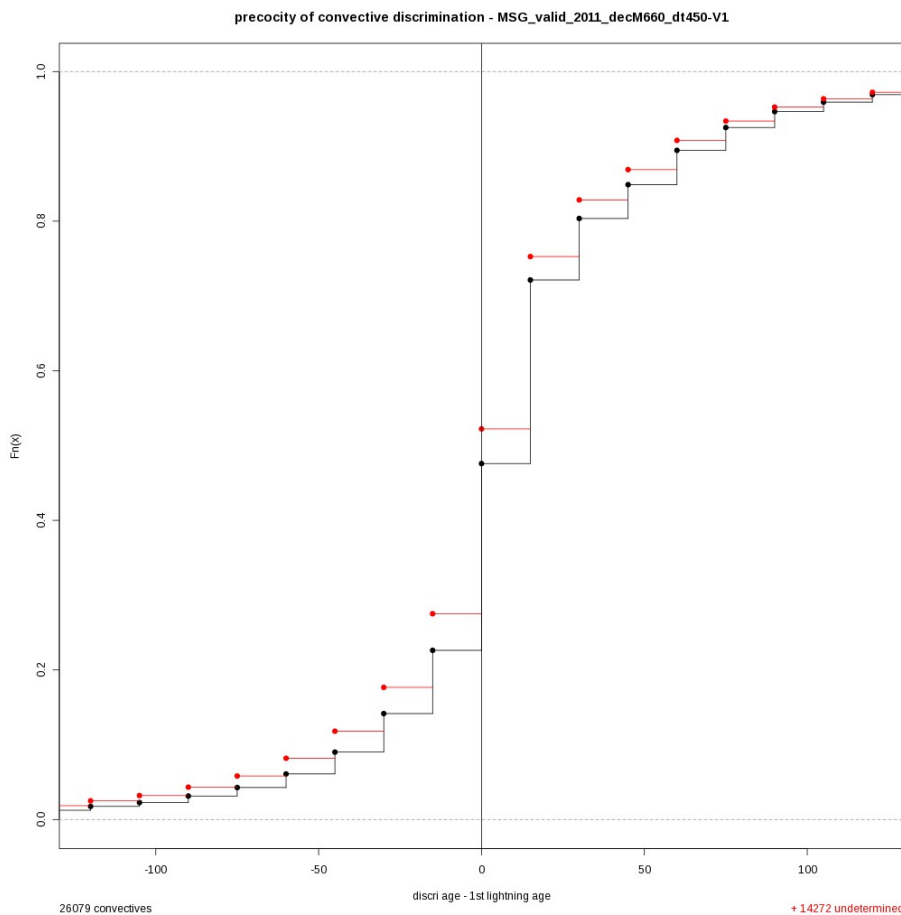


Figure 23: Precocity of RDT v2011 discrimination for moderate (black) and low (red marks) ground truths.

3.2.4 Conclusion

Threat Score is above 50% (above threshold accuracy of overall thunderstorm detection skill of 50%) and POD of 77% (above target detection 30 minutes after first lightning occurrence 50%). For this option GEN, the early diagnosis is still of 25% (threshold of the target requirement).

We consider that RDT follow the requirement. The versions associated with GEN discrimination scheme only are “operational” in EUMETSAT sense. Details and complete verification are in scientific report [RD.7] and previous verification report [RD.6].

	Validation report of the Convection Product Processors of the NWC/GEO	Code: NWC/CDOP3/GEO/MF-PI/SCI/VR Issue: 1.1 Date: 18th December 2019 File: NWC-CDOP3-GEO-MF-PI-SCI-VR-Convection_v1.1.odt Page: 39/67
---	--	---

3.3 THE VALIDATION OF CAL DISCRIMINATION SCHEME

3.3.1 Context

The primary purpose of v2018 release of GEO RDT-CW is to provide calibrated discrimination for each geostationary satellite and each scan rate. As mentioned in ATBD ([AD.11.]), it has not been possible to run and gather dataset long enough for each satellite for that purpose. That is why mainly current available satellites and scan rates have been taken into account: MSG4 every 15minutes, MSG1 every 15 minutes, MSG3 every 5 minutes, Himawari-8 available at Météo-France every 20 minutes, GOES16 every 10 or 15 minutes (depending on the date). Despite all, the length of v2018 datasets has limited the tuning possibilities. The same fact can be note for validation purpose. Thus, mainly subjective validation is presented hereafter.

Moreover, lightning data remain the ground truth used to tune and to validate (on objective or subjective basis) RDT-CW. Those data are usually provided by a ground lightning network. Meteorage lightning network data allow to get reliable information over Europe, providing a high-quality ground truth. For all other regions or satellites configurations, the only possibility was to use data from a global network. WLLN global network data are available at Météo-France, especially for the needs in overseas territories. Compared to Météorage, the quality of detection and precision of localization are however limited in that case. Long term processing will be held to gather dataset long enough for each satellite and scan rate configurations.

3.3.2 Cases study

It must be reminded that those cases study rely on RDT-CW processing whose discrimination scheme is based on satellite data only, after NWP filtering (stable areas excluded). Lightning data are paired with cloud cells, but without any change of convective diagnosis. Satellite image and lightning data will be hereafter to synthesize ground truth.

3.3.2.1 RDT-CW discrimination using MSG4 0°

Runs for MSG4 case are illustrated over Europe. METEORAGE lightning data can be considered as reliable enough, from a precision or detection point of view.

3.3.2.1.1 Inter-comparison between discrimination schemes

Figures 24 to 27 below illustrate a convective situation over Europe. One can note that almost the totality of electric phenomena are identified as convective clouds with RDT-CW, whatever the discrimination scheme. However differences can be seen between GEN and CAL discrimination schemes, which have been observed also on other situations:

- CAL scheme seems to generate a little bit more of false alarms on this situation.
- GEN discrimination scheme seems to provide a little bit more Yes convection diagnosis in the lowest categories
- Both discrimination schemes are able to provide diagnosis for cloud cells obviously convective but not yet electric
- The number of cloud systems diagnosed as convective appears less important with CAL scheme when compared to GEN. It seems to compensate a kind of overestimation of convective diagnosis with GEN discrimination scheme.

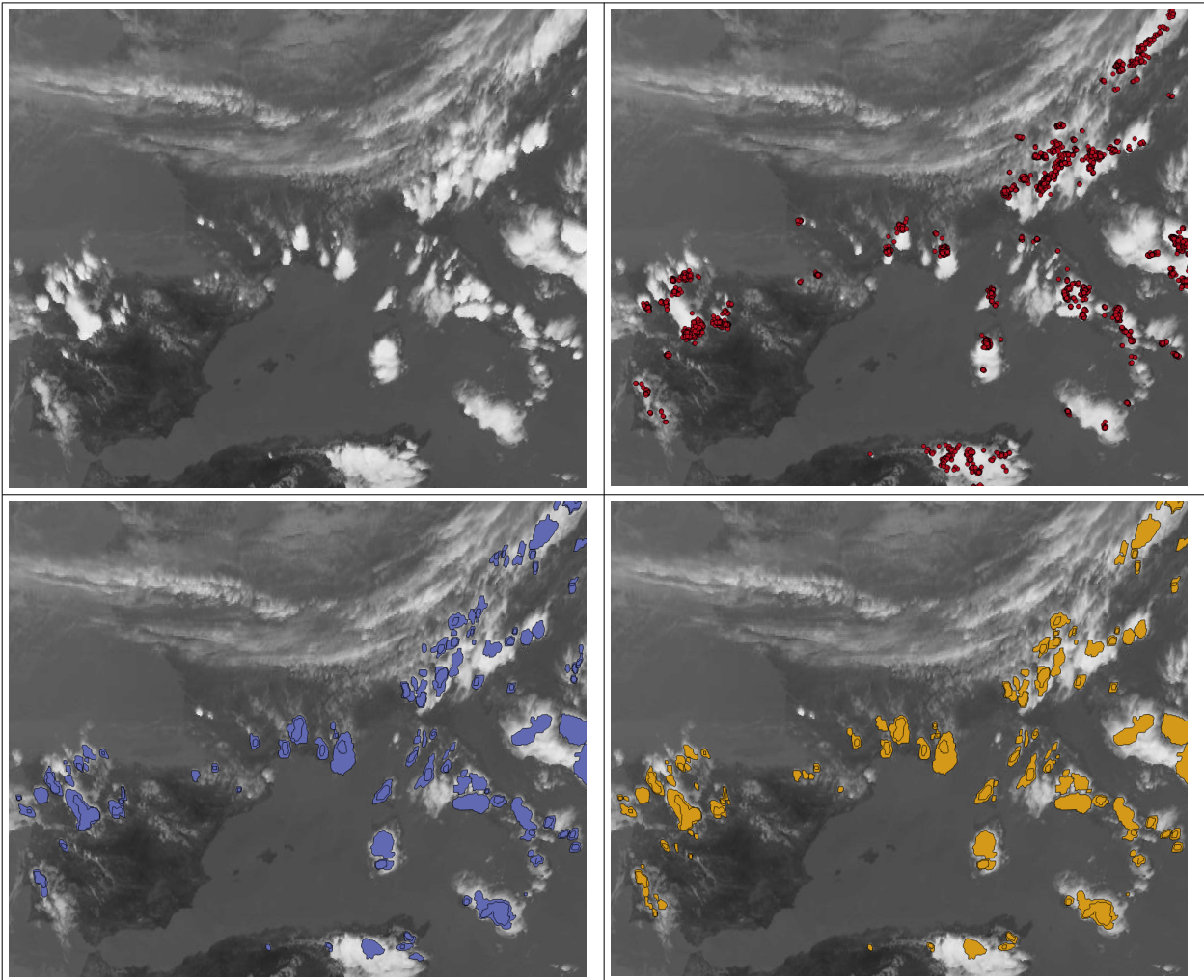


Figure 24: MSG4 case study for 12h00-15h00Z on 20180621. 15h00Z IR image (top left), 30min accumulated METEORAGE impacts around 15h00Z (top right), CAL (bottom left) and GEN (bottom right) results for 15h00Z.

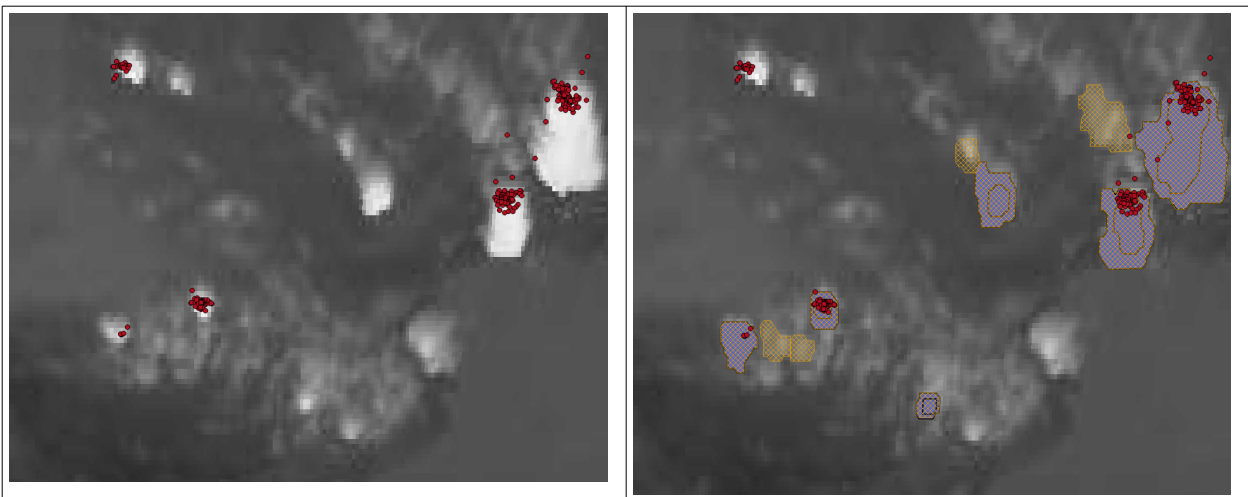


Figure 25: MSG4 case study for 20180621 12h00-15h00Z, zoom on South of France. IR and lightning on the left, CAL (plain blue cells) and GEN (orange dashed) on the right. One can note a miss near Bordeaux (top left cloud) with both CAL and GEN schemes, an early good detection more or less in the centre of image.

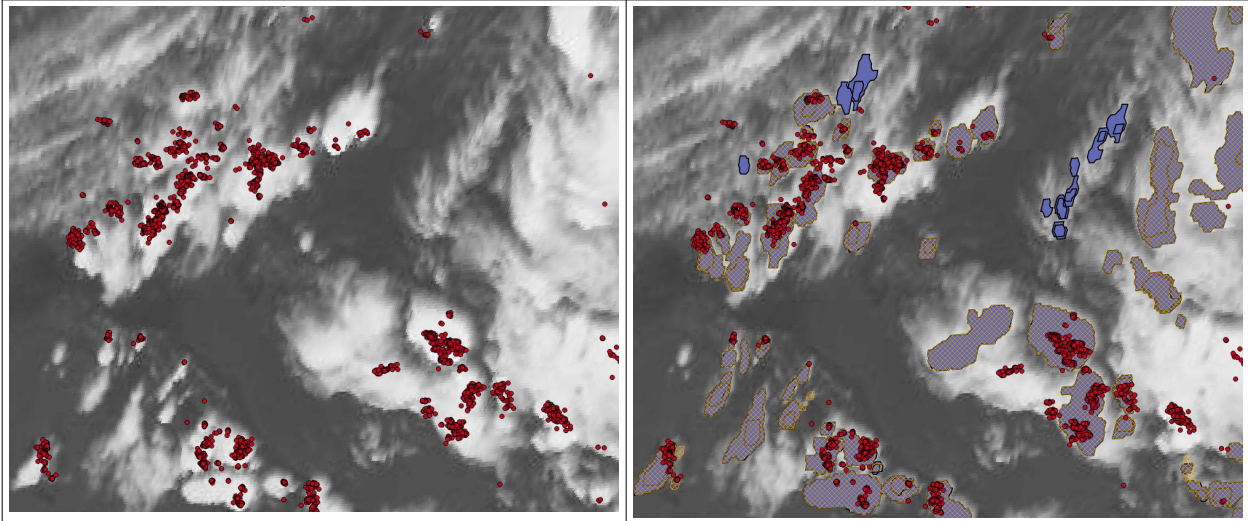


Figure 26: MSG4 case study for 20180621 12h00-15h00Z, zoom on Central Europe. IR and lightning on the left, CAL (blue cells) and GEN (orange dashed) on the right. One can note some False Alarms with CAL on the edge of cloud systems

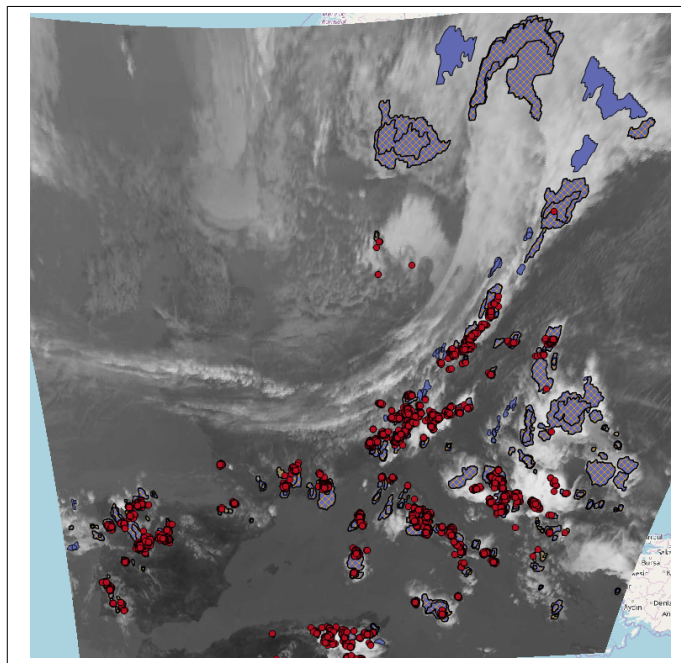


Figure 27: MSG4 case study for 20180621 12h00-15h00Z, large view. False Alarms suspicion in the North of the domain, more numerous with CAL (blue cells), in an area which seems out of lightning coverage area.

The time-series of convective diagnosis (Figure 28), starting from a cold start, shows again a stability of diagnosis after 4/6 slots (1 hour) of processing, and less numerous diagnosis with CAL scheme.

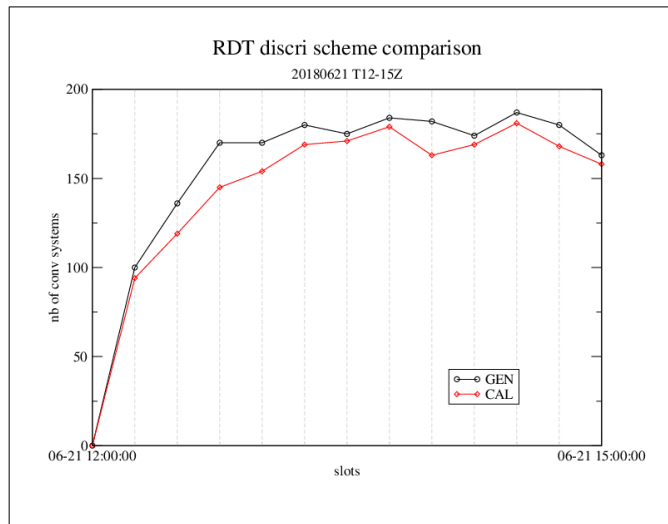


Figure 28: MSG4 case study for 20180621 12h-15hZ. Compared time series of convective cells numbers

3.3.2.1.2 20180702 over Europe

Only calibrated discrimination scheme is here considered. Figure 29 below illustrates a large and zoomed view of this situation.

Almost all electric clouds are discriminated as convective. Even for clouds with a low electrical activity (1 flash), RDT-CW identifies the whole cloud system as convective. In the middle of France, one can note a RDT-CW cell apparently correctly diagnosed as convective, even if no electrical activity appears yet. On the other hand, embedded cloud systems, as on the top left of the image, seem more difficult to separate and identify. Electrical activity is observed in several places, RDT-CW cells do not always correspond at that time for this complex system.

The cloud system at the edge of this cloudy area is tracked and identified from 14h15Z, and seems relevant even if not electric.

And if we consider RDT-CW from a temporal point of view, like in Figure 30, one can conclude that all electric cloud systems are identified by RDT-CW, and few false alarm are noted, if we consider the cell mentioned above as a false alarm.

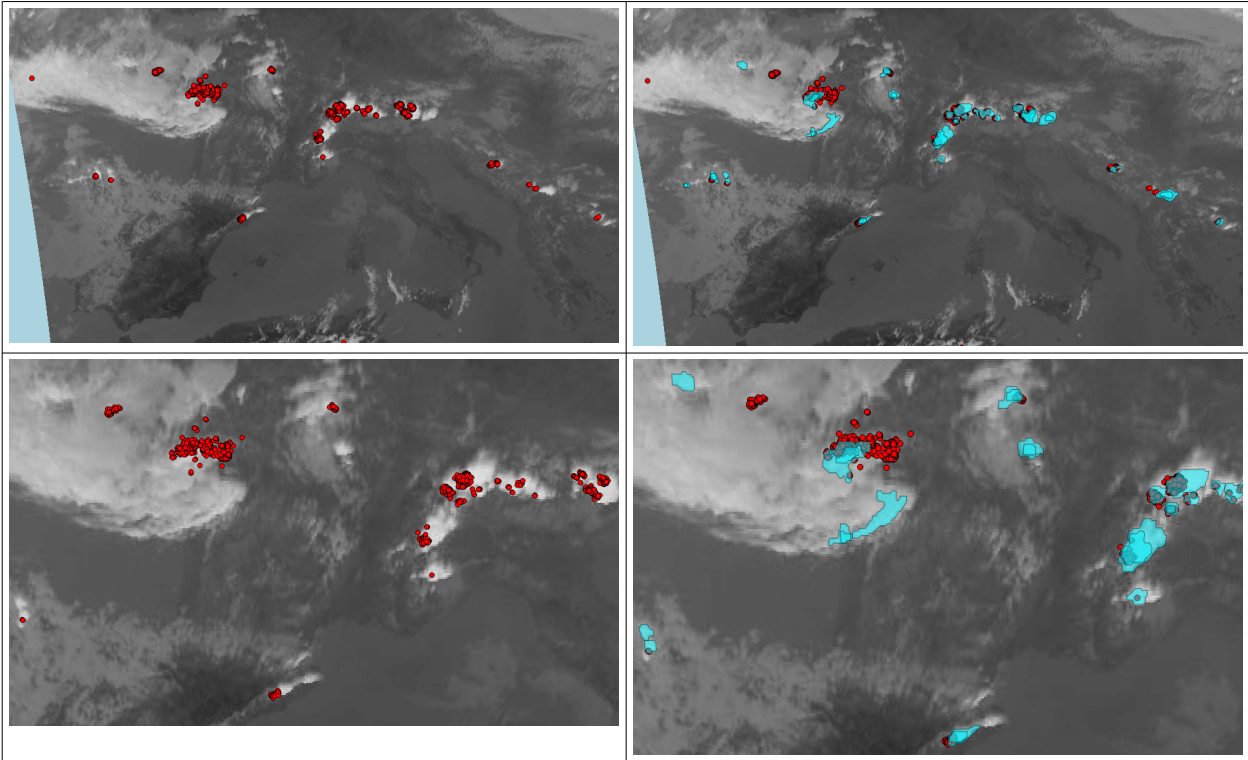


Figure 29: MSG4 case study for 20180702. 15h00Z IR image (top&bottom left) with METEORAGE impacts around 15h00Z , RDT-CW cells for 15h00Z with lightnings(top&bottom right).

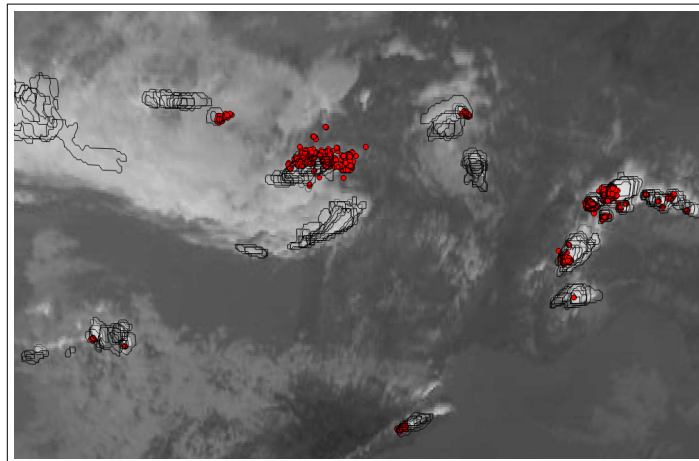


Figure 30: MSG4 case study for 20180702. 15h00Z IR image with 1h accumulated METEORAGE impacts and RDT-CW cells.

3.3.2.2 RDT-CW discrimination using Himawari-8

3.3.2.2.1 Intercomparison between discrimination schemes

In this case generic (GEN) and calibrated (CAL) discrimination are intercompared.

Figure 31 illustrates over Indonesia the large amount of cloud cells discriminated as convective, and the ground truth through WWLLN impacts. Even in this very active region, some diagnosis seem to be overestimated with the GEN scheme (see western part of GEN image) when compared to CAL

scheme. On the other hand, the North-Eastern part of this region shows isolated cloud cells which are identified with GEN and not with CAL. A deeper review shows that most active large cloud cells are discriminated by both scheme.

It is concluded that

- GEN discrimination appears to over-estimate convective activity
- CAL discrimination scheme shows same behaviour, but better fits to the available ground truth,
- The available ground truth seems to underestimate convective activity with same convective cloud

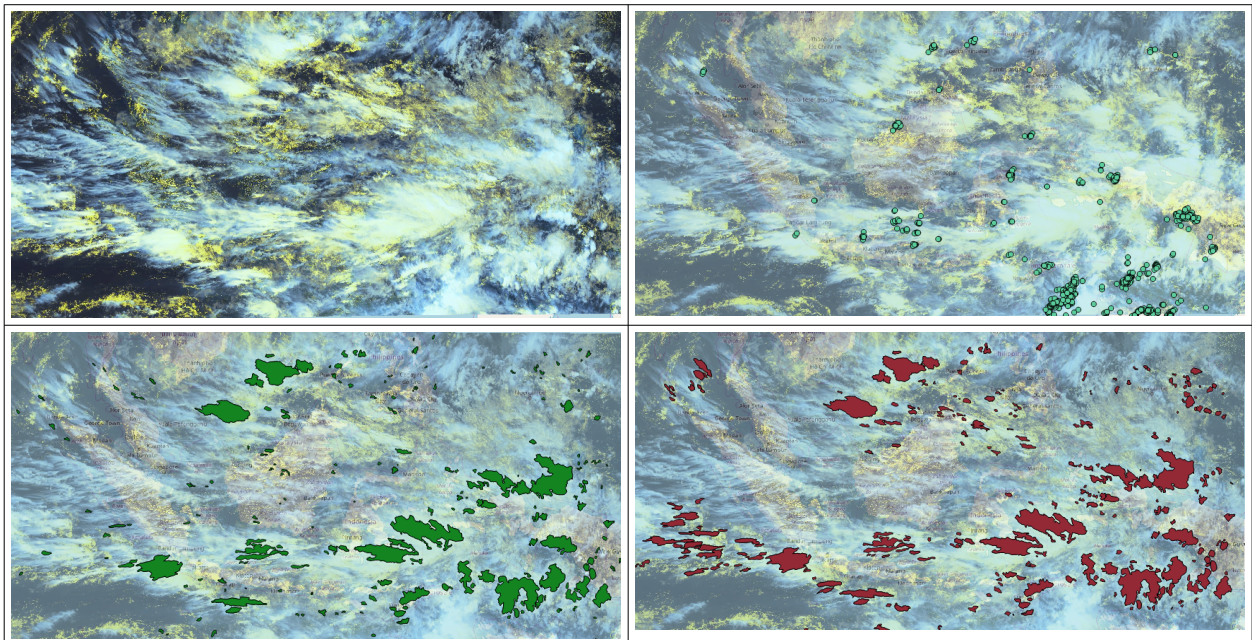


Figure 31: Himawari-8 case study for 03h00-06h00Z on 20180117. 06h00Z RGB image (top left), 1h-accumulated WLLN impacts around 06h00Z (top right), CAL (bottom left) and GEN (bottom right) results for 06h00Z.

An analysis of time-series of convective diagnosis numbers, starting from a cold start, shows a stability of diagnosis after 4/6 slots (1-2 hours) of processing (taking into account daily variation), and less numerous diagnosis with CAL scheme.

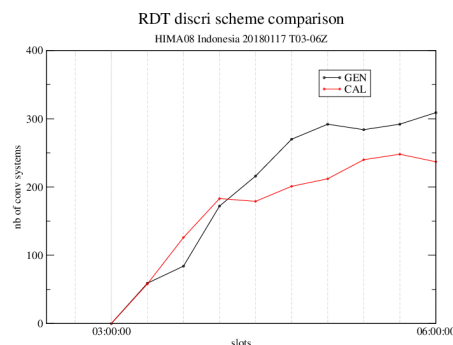


Figure 32: Himawari-8 case study for 20180117 03h00-06h00Z. Compared time series of convective cells numbers

3.3.2.2.2 Case study 20180702 over East Asia

During this situation, convective cells develop over land, and a tropical disturbance is moving northward.

Each large electric convective system is well identified by RDT-CW. Nevertheless, this calibrated discrimination scheme seems to overestimate convective activity, in the Northern part of disturbances, but also in some isolated clouds.

For lower, warmer, or isolated ones, RDT-CW and lightning activity are not exactly collocated, and RDT-CW seems sometimes overestimate convective activity in the warmest levels for small cells. But detection and localization of lightning data seem also sometimes doubtful in that case, and it is difficult to argue about the ground truth. Nevertheless, the display of 3h accumulated products in Figure 34 seems to confirm an excessive number of false alarms.

The specific calibrated tuning with Himawari-8 and WWLLN data clearly shows a need to further investigate to lower a false alarm ratio. It must be reminded here that Himawari-8 satellite data were available for this tuning at 20 minutes frequency.

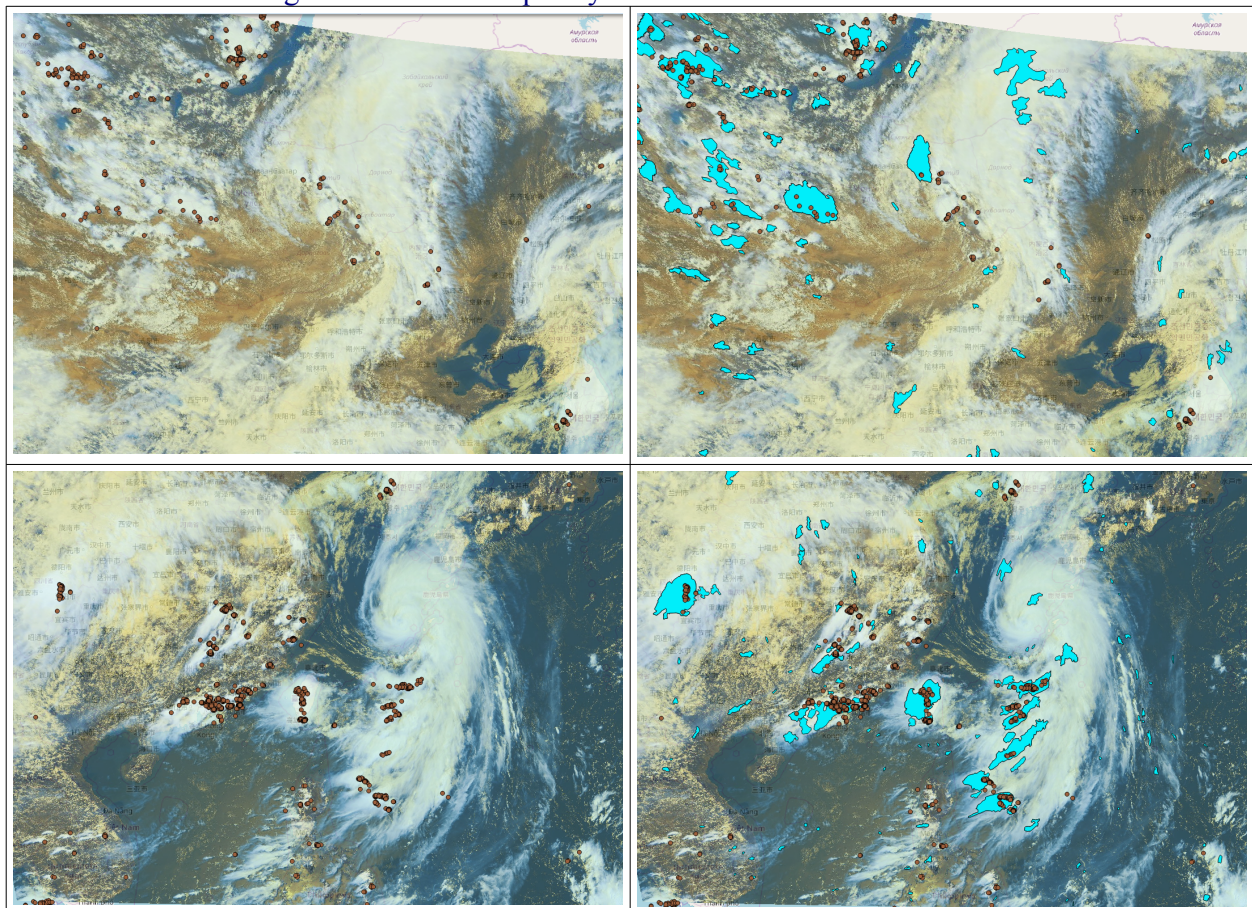


Figure 33: Himawari-8 case study for 20180702 03h00-06h00Z. 06Z RGB image with WLLN flashes (left) and overlaid with RDT-CW cells (right, blue cells). Northern inner land region on top images, Southern oceanic region on bottom images,

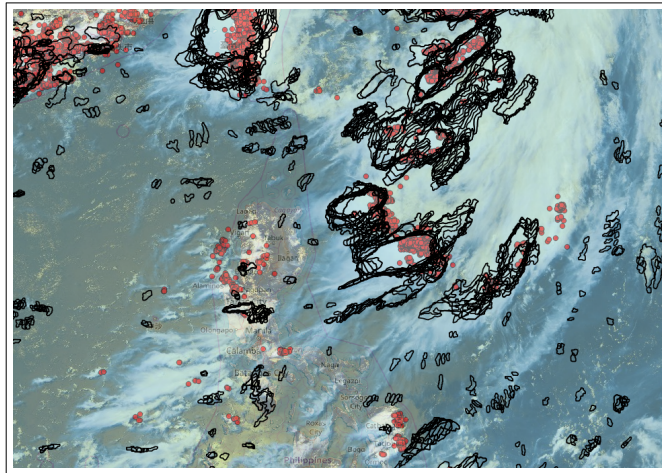


Figure 34: Himawari-8 case study for 20180702 03h00-06h00Z. 06h00Z RGB image overlaid with 3 hours-accumulated WLLN flashes and 3 hours-accumulated RDT-CW cells

3.3.2.3 RDT-CW discrimination using MSG3 - 9.5E° RapidScan mode

Like for MSG4 on this case study (20180702 over Europe), only calibrated discrimination scheme is here considered.

Here again all electric clouds are discriminated as convective. A comparison with MSG4 results in figure below shows a good coherency between both productions. One can note some additional small cloud cell identified as convective, whose relevancy seem difficult to assess.

One can note also that the edge of cloudy area on the west of the domain is also identified as convective.

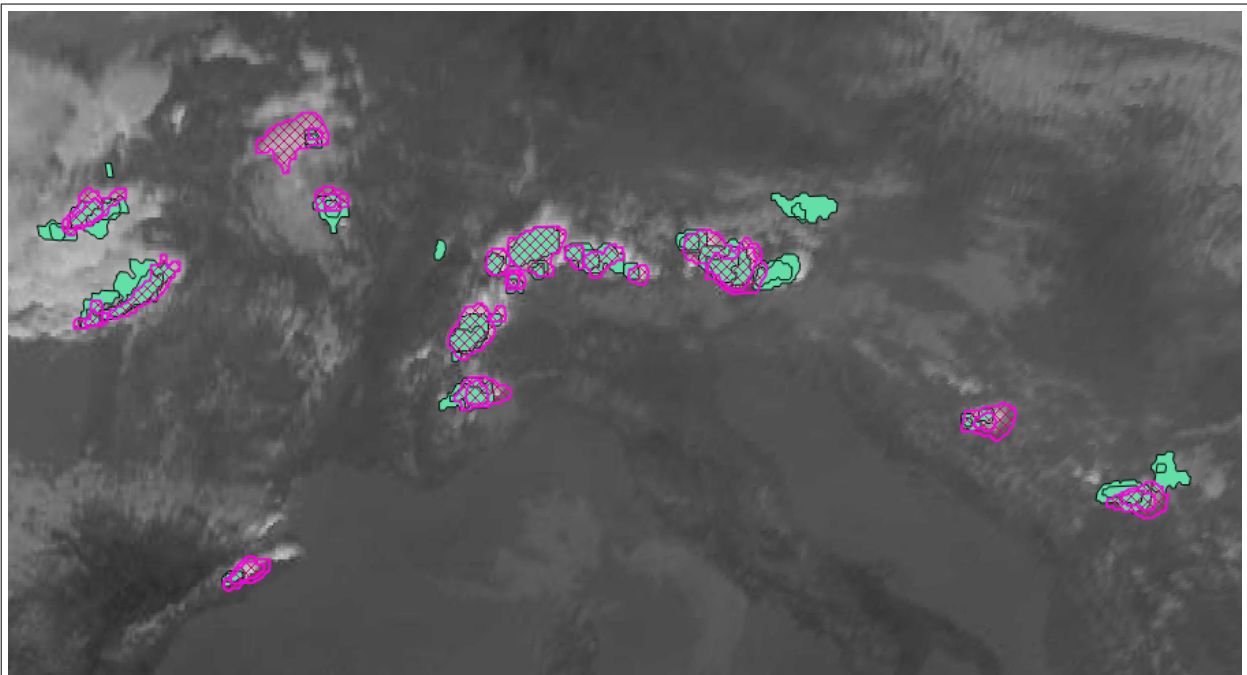


Figure 35: MSG3-RSS and MSG4 case study for 201800207 12h00-15h00Z. 15h00Z IR image overlaid with MSG3-RSS RDT-CW cells (green) and MSG4 RDT-CW cells (magenta dashed)

Figure 36 below shows contours accumulated within 1 hour consecutive RDT-MSG3-RSS products. Most convective attributes seem confirmed from one slot to another, almost all assessed by electric activity.

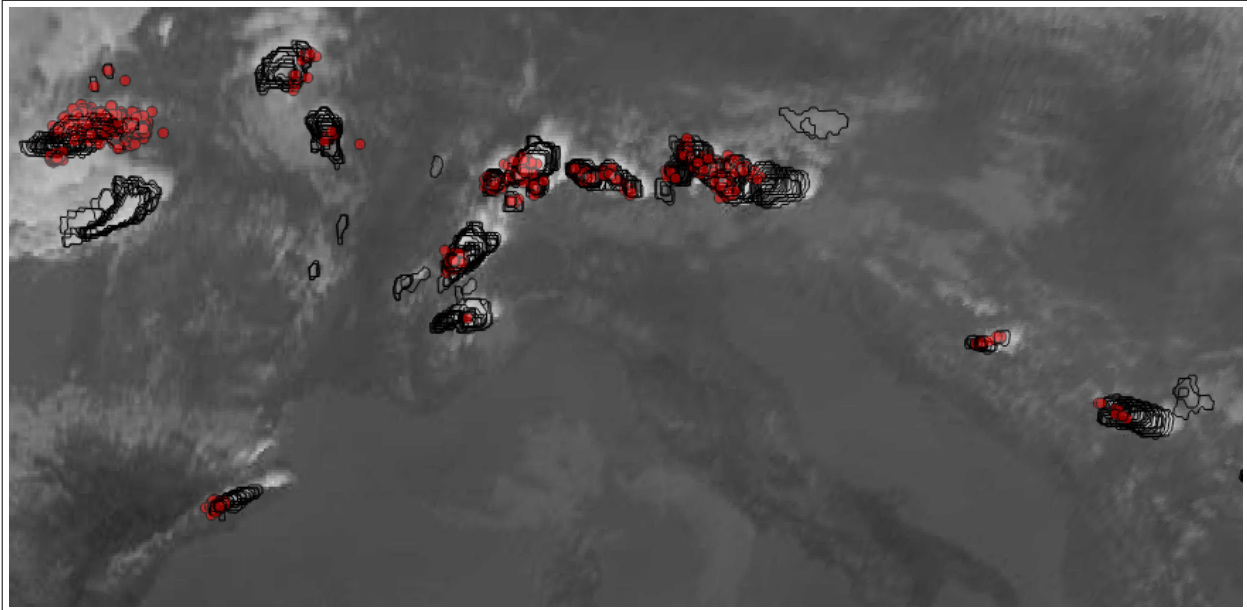


Figure 36: MSG3-RSS case study for 201800207. 15:00Z IR image overlaid with 1h accumulation MSG3-RSS RDT-CW cells (black contours) and lightning data (red)

3.3.2.4 RDT-CW discrimination using MSG1 - 41.5°E

The 20180121 case study over Indian Ocean illustrated below highlight two major problems:

- 1) On one hand RDT-CW seems to overestimate the number of convective systems, especially in the afternoon when diurnal convective activity is supposed to increase. It concerns mainly small cloud cells
- 2) On the other hand WLLN lightning data sampling (± 15 minutes around RDT-CW slot time) does not show the same tendency. Even with a proximity distance in pairing and a spatial uncertainty given to each lightning location, this has a negative impact for the pairing between cloud cells and lightning flashes for the tuning

The full set of WLLN data (bottom left image in Figure 37) presents an activity better in term of coherency with RDT-CW, but it concerns mainly large cloud systems. It is thus difficult to analyse which sensor brings the most reliable information

The calibrated discrimination scheme does not bring in this case full satisfaction for small systems.

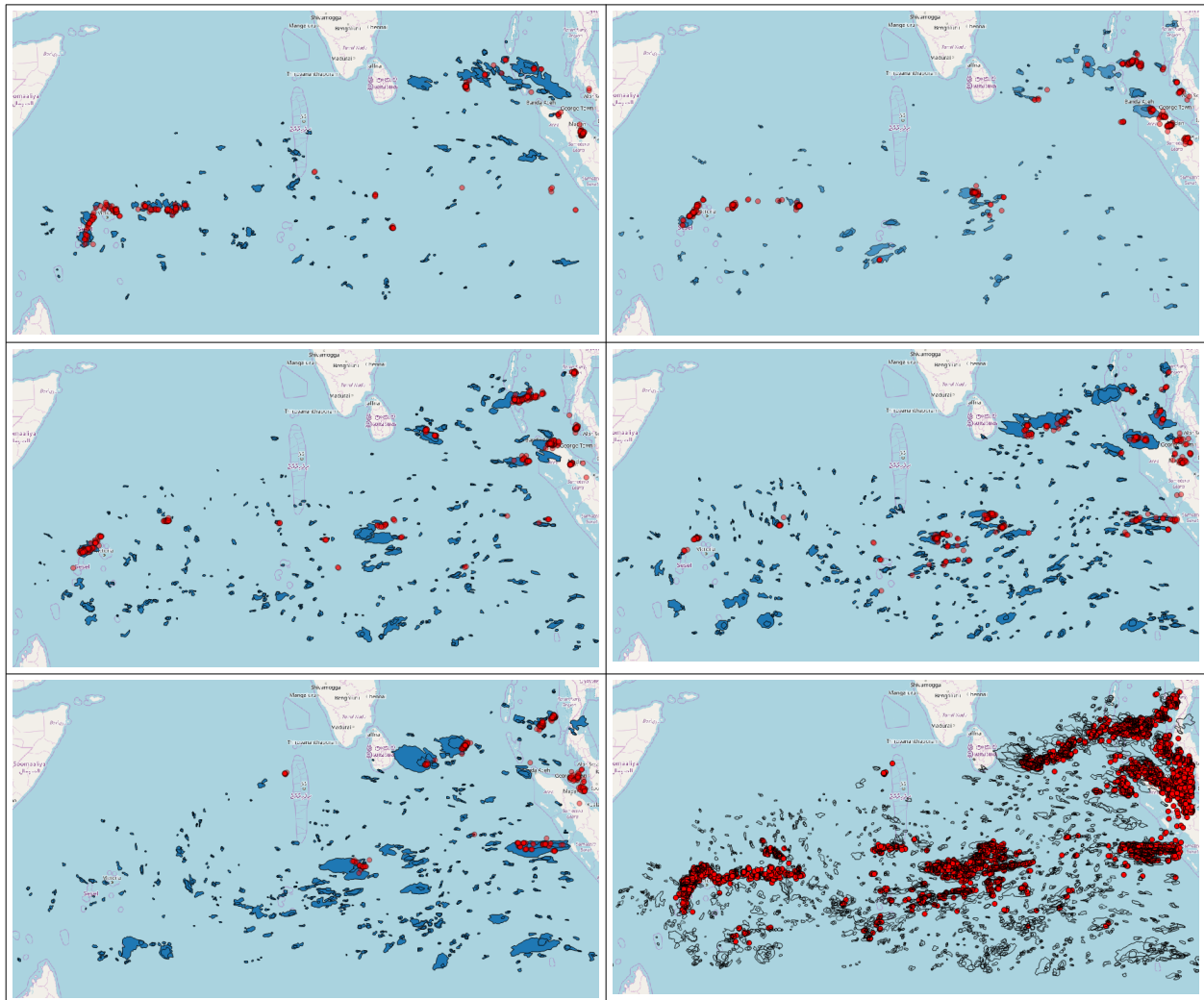


Figure 37: MSG1-41.5E case study for 20180121. Overlay of RDT-CW cell contours (black contours, blue cells) and WWLLN flash impacts (± 15 minutes, red spots). From top to bottom and left to right: 09hZ, 12hZ, 15hZ, 18hZ, 21hZ, 09-21hZ

3.3.2.5 RDT-CW discrimination applied to GOES16 with 15 minutes scan rate

The 20181008 case study between 15hZ and 20hZ over mid-tropical band over Central America and Caribbean Sea is illustrated below. The RDT product is regarded against electrical activity provided by GLM sensor. It is to note that for this case study, those data are not filtered, explaining some isolated artefacts over South Pacific Ocean.

At first sight, for 15hZ illustration, RDT seems to correctly correspond to electrical activity over land, while cells over mid-Atlantic and Pacific apparently don't correspond to electrical activity. Though, some RDT cells over ocean show sometimes convective texture.

20hZ illustration shows how RDT perfectly fits diurnal activity over land, with a very large number of cells, but much electrical activity. Some previous false alarms over Pacific are confirmed with isolated flashes.

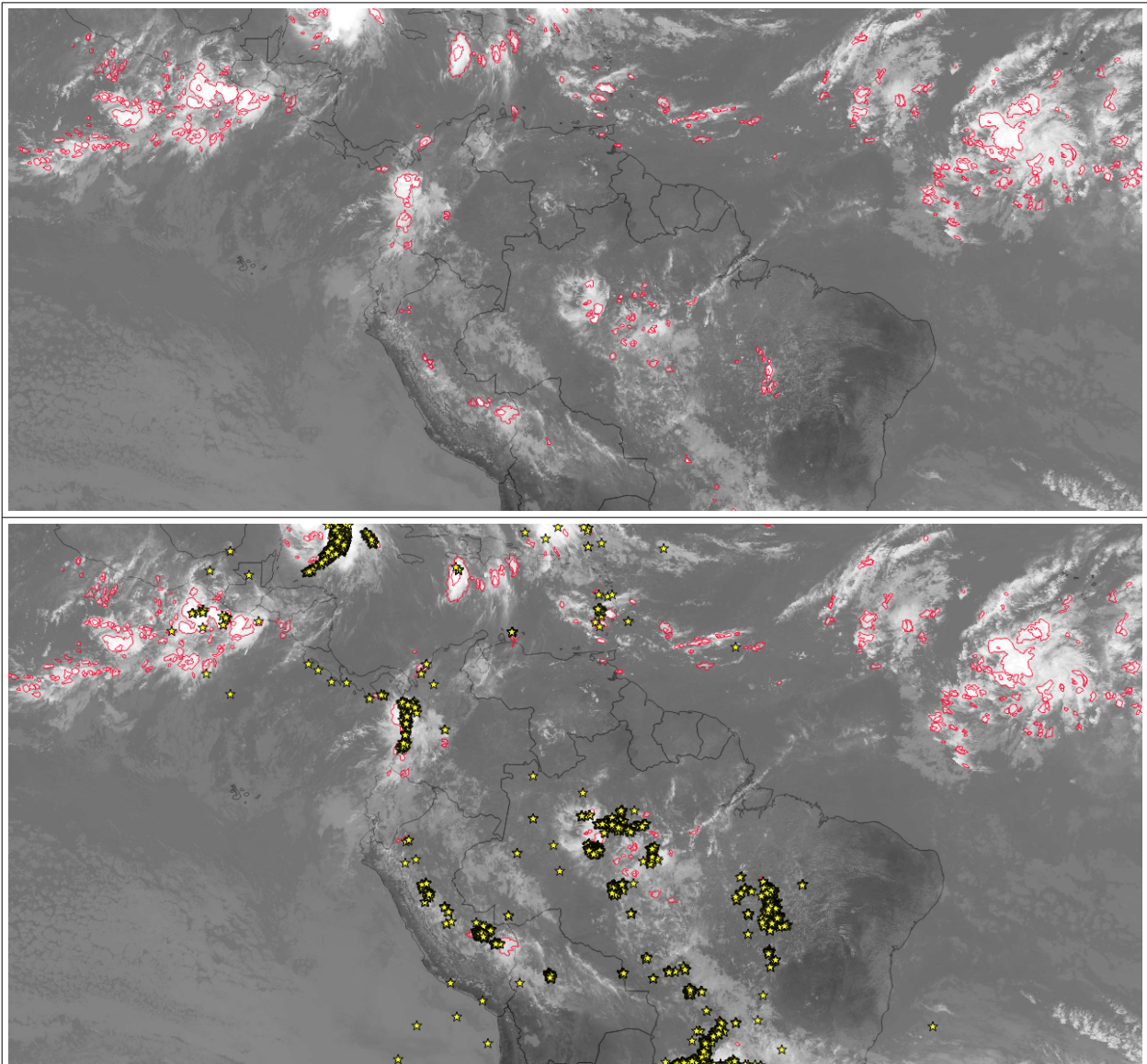


Figure 38: GOES16 case study for 20181008 15hZ. Top: IR image overlaid with RDT-CW cell contours (red contours). Bottom: idem plus GLM flash impacts in the next hour (15hZ-16hZ).

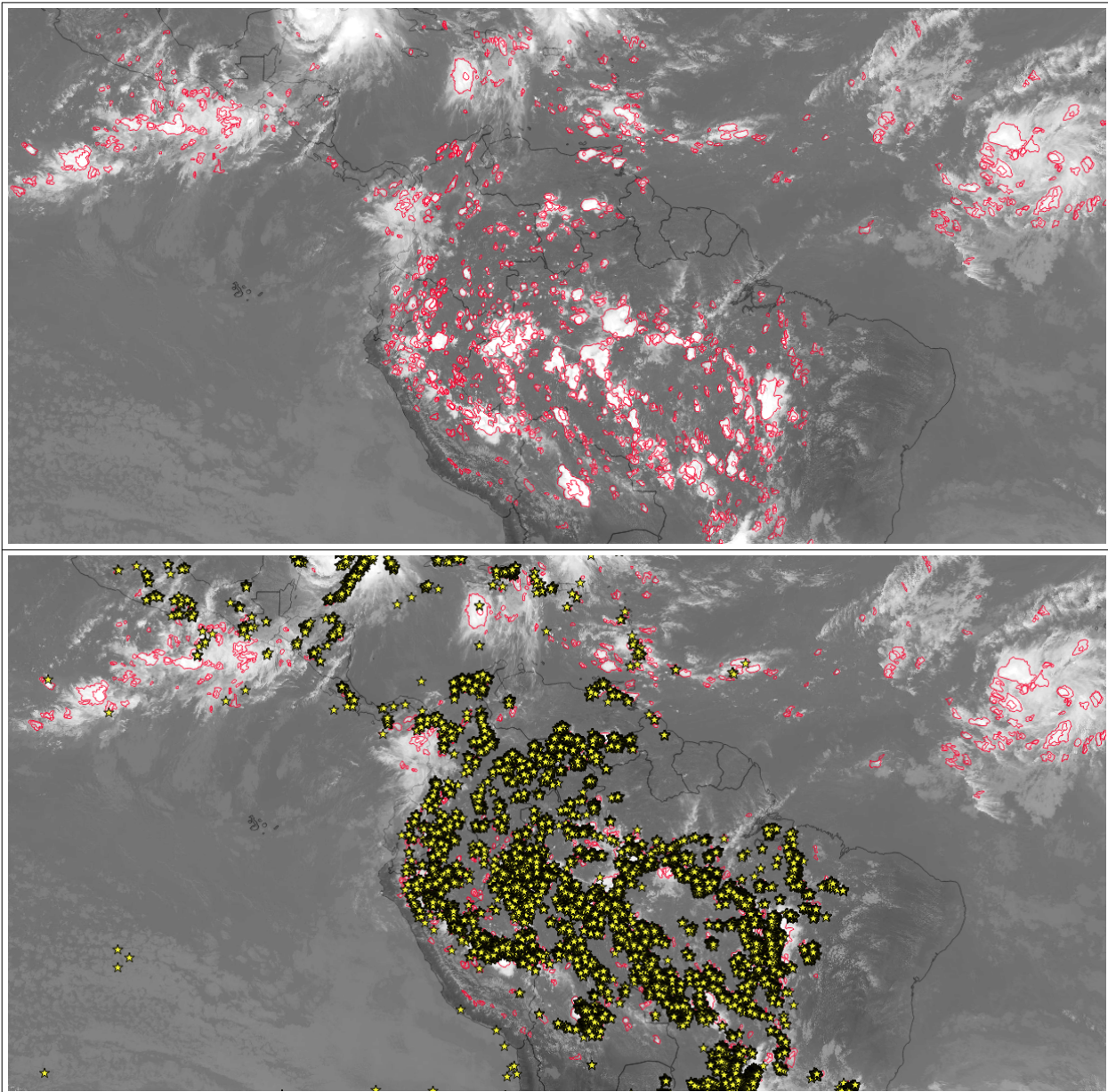


Figure 39: GOES16 case study for 20181008 19hZ. Top: SIR image overlaid with RDT-CW cell contours (red contours). Bottom: idem plus GLM flash impacts in the next hour (19hZ-20hZ).

A zoom over Caribbean Sea around 18h00Z shows how some convective systems are associated with no or very weak electrical activity. If we focus on convective systems apparently not associated with flashes, we can note that most of them are confirmed during next slots by flashes (blue arrows becoming green when electric): we are in the case of early diagnosis. Other systems could be false alarms (red arrows). There are few misses (yellow arrows).

Finally, almost all electrically active convective systems are correctly identified by RDT process, and a significant number of RDT cells are in the vicinity of electrical activity. It appears sometimes difficult to completely identify the false alarm cases.

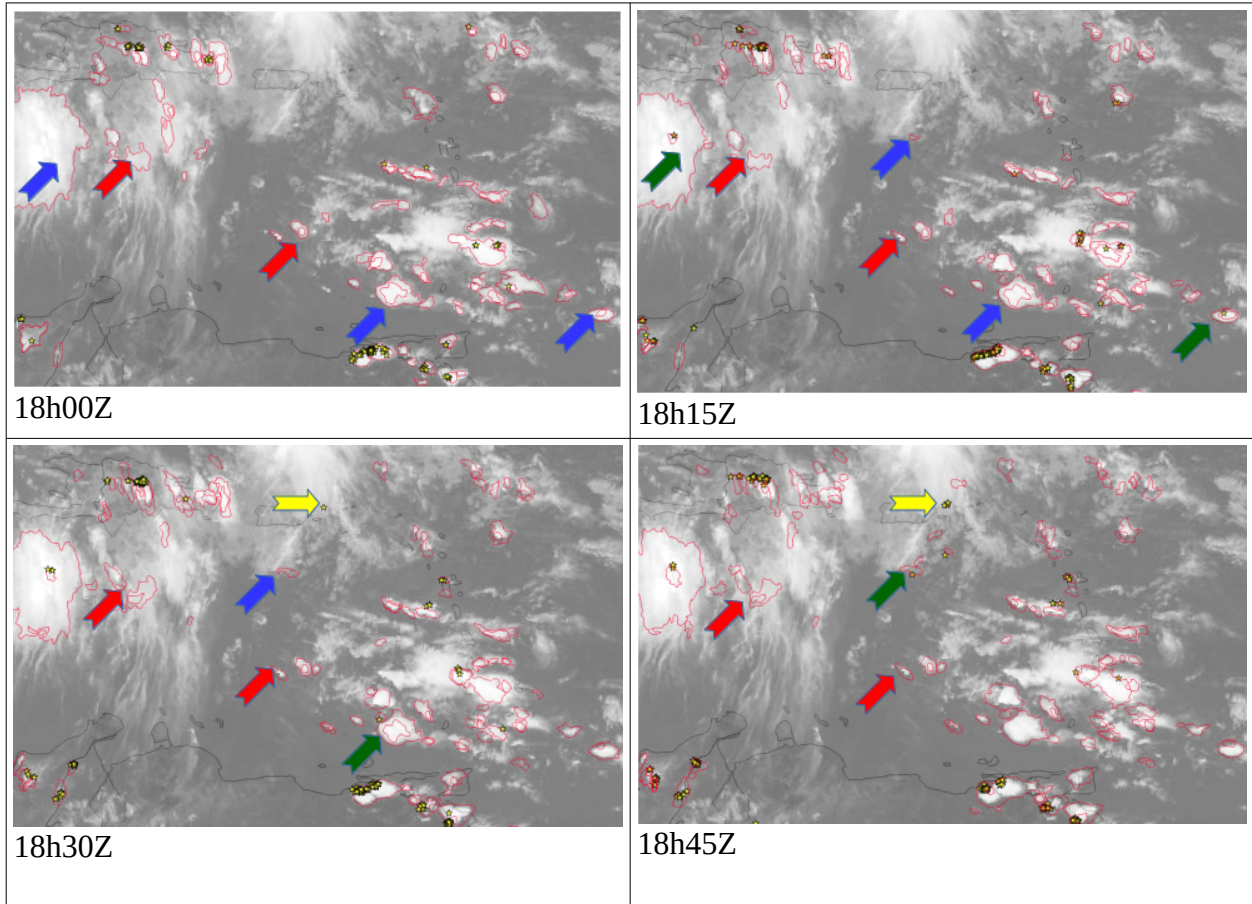


Figure 40: 20181008 Case study, 18h00Z to 18h45Z. GOES16 IR image overlaid with RDT-CW cell contours (red contours) and GLM flashes (yellow stars) .

3.3.2.6 RDT-CW applied to GOES16 with 10 minutes scan rate

20190419 date as been tested as case study to assess RDT-CW discrimination tuned with 10 minutes scan rate, and to analyse results regarding main IR window channel used for detection, tracking and discrimination in RDT-CW code.

For this case study lightning data from WLLN ground network have been taken into account.

Looking at several successive slots (from 12hZ to 14hZ), we can identify areas of apparent false alarms. Other isolated cases of apparent over-discrimination are not so obvious since they occur either in the vicinity of other active systems (some of them following split consecutive to temperature threshold adaptation). They may also represent an early diagnosis (for example French Guyana coast, 14hZ, from red dashed circle t green arrow).

RDT diagnosis must be regarded with a spatial and temporal tolerance, and also take into account performances of the lightning network for verification. For example, convective activity is obvious in equatorial Pacific area, but a large part of RDT cells are not co-localized with flashes. The same feature appears in the Peruvian mountains, where the number of flashes is low.

RDT-CW generally correctly identifies all active convective areas. But a correct quantitative estimation of false alarms remains a challenge. Moreover, the gain of a RDT tuning with 10 minutes scan rate compared to a 15 minutes scan rate is difficult to measure.

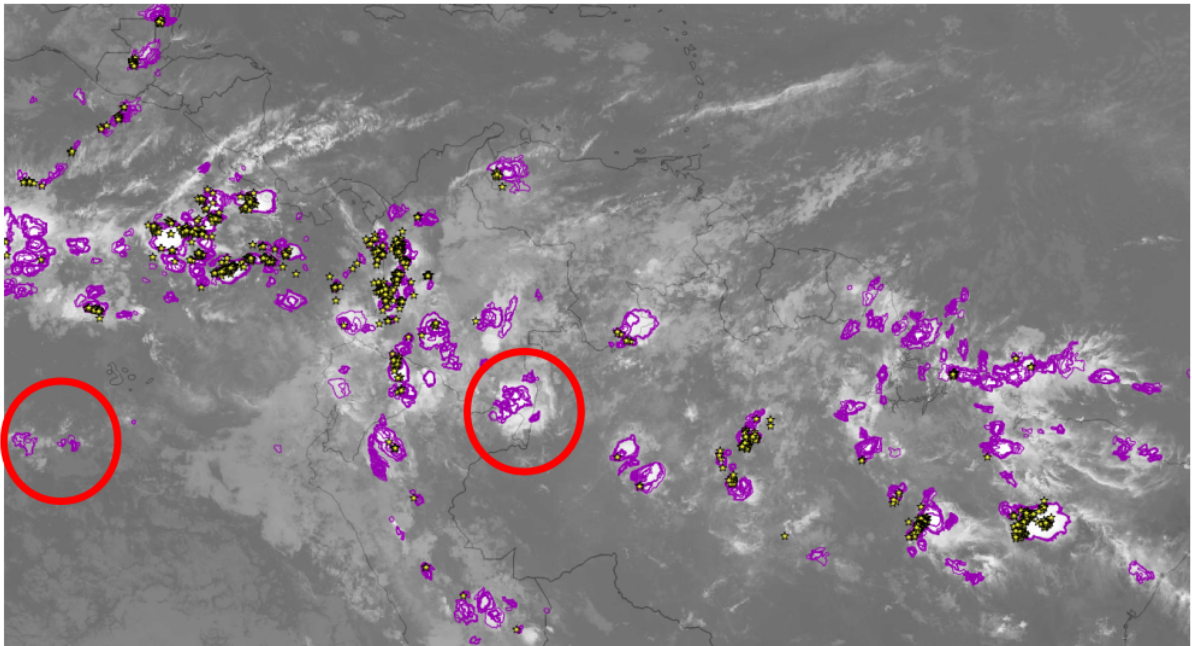


Figure 41: 20190419 Case study, 12h00Z GOES16 IR image overlaid with RDT-CW cell contours (magenta contours) and WWLLN flashes (yellow stars) in the 50 following minutes. Confirmed areas of false alarms in red circles, green arrow points good detection by RDT-CW with large anticipation

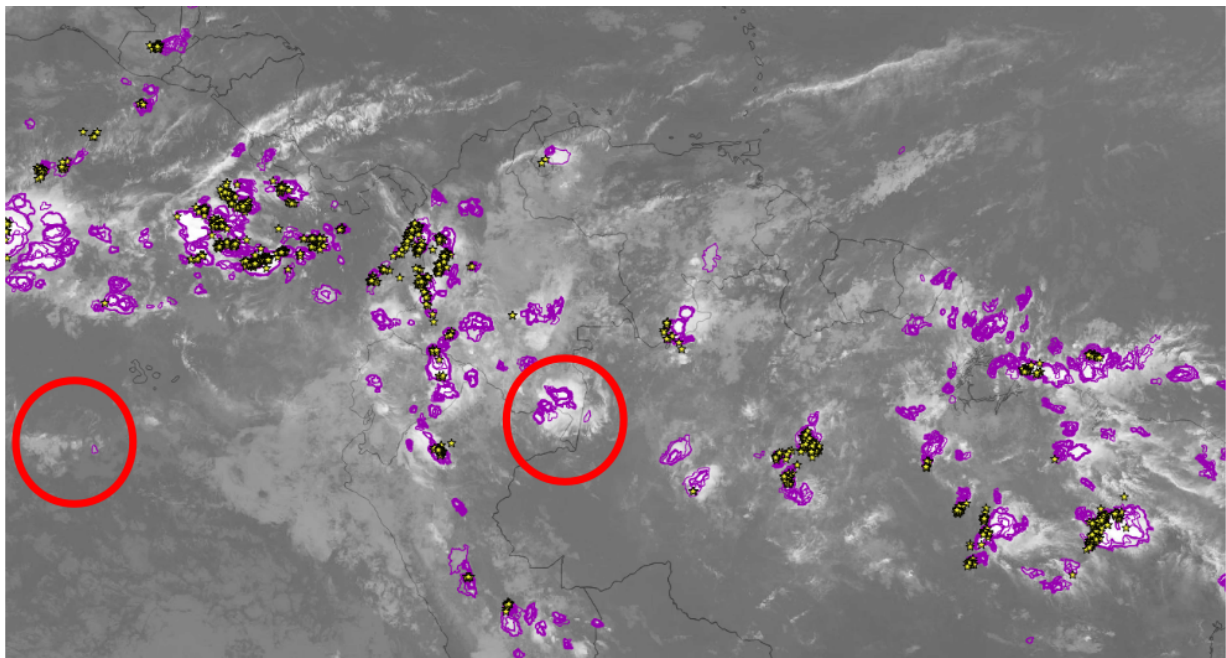


Figure 42: same as previous figure but for 13h00Z

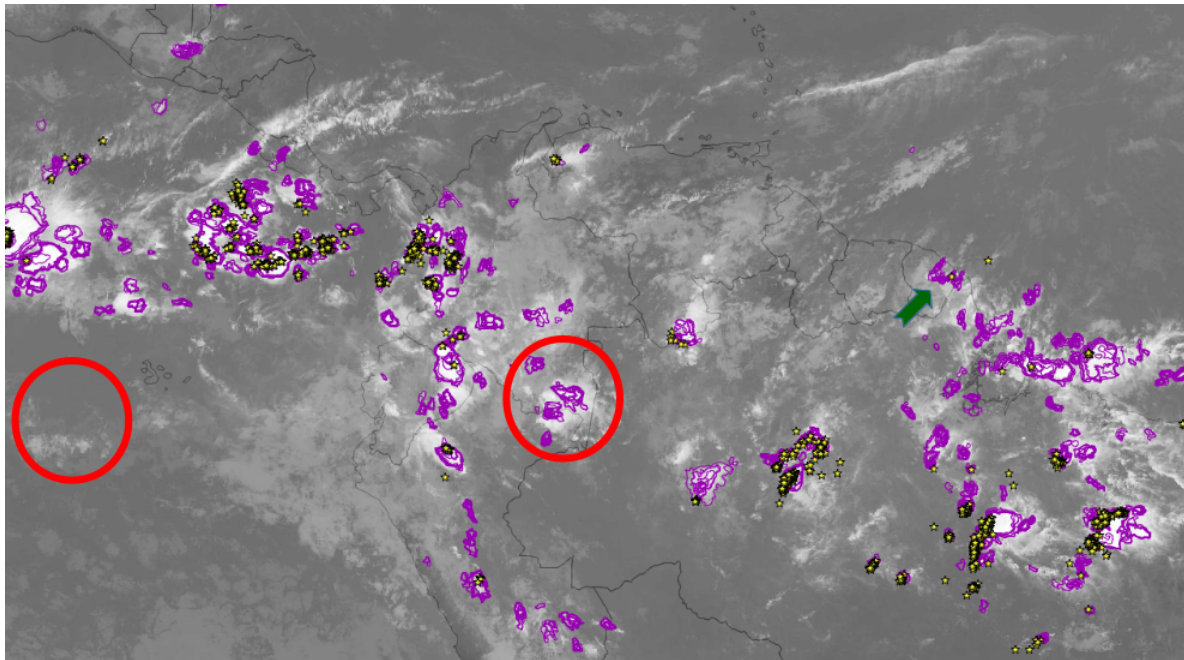


Figure 43: same as previous figure but for 14h00Z

3.3.2.7 Processing RDT-CW using IR10.3 (channel #15) or IR11.2 window channel (#16)

The availability of two IR window channels with GOES16 rose the question of the main channel to use. Up to now, channel #16 (corresponding to 10.8 μ m for MSG) was the main channel for detection, tracking and discrimination. After adaptation of RDT-CW code to the use of channel #15 (IR10.3 μ m for GOES16) as alternative channel, two different corresponding tunings have been undertaken for the convective discrimination. Then, the same case study has been processed for each branch .

It appears that the number of cells diagnosed as convective using IR11.2 μ m is larger than with IR10.3 μ m.

The figure below illustrates, for a given slot, a kind of over-discrimination with IR11.2 μ m. Each 10.3 μ m cell corresponds to a 11.2 μ m one. But all isolated unpaired 11.2 μ m cells are non electric: it indicates that the number of false alarm should be lower using channel #15 for RDT-CW.

This will be the default mode for GOES16 satellite.

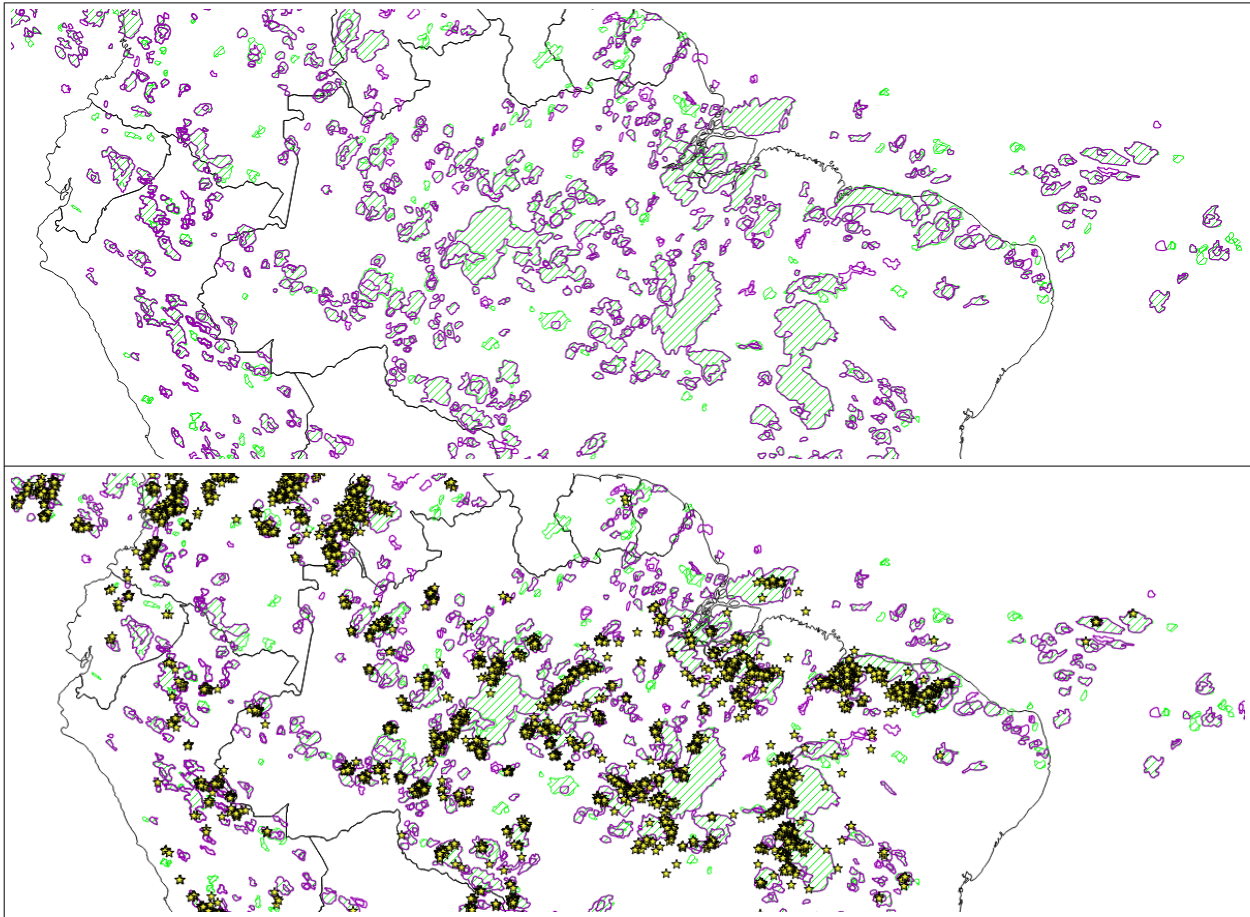


Figure 44: 20190419 Case study, 19h00Z . Top: IR10.3µm-RDT-CW cells (empty magenta contours) overlaid with 11.2µm-RDT-CW cells (green dashed contours). Bottom: same with WLLN lightning flashes over [19hZ-20hZ] period.

3.4 OVERTHROUING TOP DETECTION

As detailed in [AD.11], Overshooting Top Detection (OTD) in RDT-CW code is undertaken in two steps. First, morphological analysis of cloud cells allows identifying cell's list of so-called "OT-candidates". Then, OT candidates are eliminated or confirmed considering gap to tropopause or criteria more severe than those in first step.

Criteria are inspired from existing bibliography about OTD, and have been adjusted on case studies. With OTD, we have the first use of visible channel in RDT algorithm (VIS 0.6). Hereafter are some examples of these subjective tuning and validations. The expert subjective validation requires HRV images (that are not use in OTD).

3.4.1 Pre selection step

The static thresholds used for IR10.8 BT and $BTD = WV6.2 - IR10.8$, and the morphological analysis of cloud cell top lead to identify possible overshooting tops for convective systems. A balance had to be found between restrictive or more tolerant values of thresholds. The first option lead to missing some overshooting tops, the second one implied a necessary further confirmation through additional criteria. The second option has been chosen and the step are called "pre-selection" and "confirmation".

The figure below illustrates a case study over Austrian-Slovenian border, on the 25th of May, 2009. Only pre-detected OT are plotted, overlaid with an enhanced IR image. The convective system containing several convective cells exhibits some OT signatures. The corresponding OT's extensions vary from one to a tenth of pixels, all located on an extremum of IR10.8 BT.

A comparable approach concerning overshooting tops was also examined, for cross comparison. The same case study has been analysed by Bedka and al (here extracted from “Best Practice Guide” [RD.2.]), figure below exhibits HRV channel with result of OT detection. In this case, all four OTD appear also inside the pre-selected OT set. Some more interesting points are proposed with RDT-CW code, these points need a confirmation, which is the aim of next step of the algorithm.

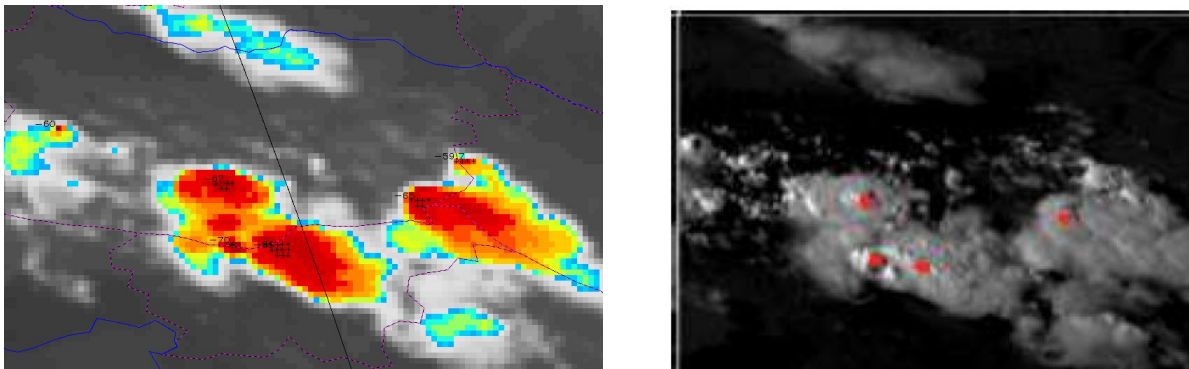


Figure 45: 25th May 2009, slot 16h00 UTC. Zoom over Austrian-Slovenian frontier. Left: Enhanced IR10.8 image with plotted pre-selected OT. Right: HRV image with highlighted OTD from Bedka method in [RD.2.]

3.4.2 Confirmation step

NWP input is used by RDT-CW code for guidance and for a more efficient discrimination step. With OTD, NWP data have now a new role in RDT. Tropopause pressure and temperature are read or re-processed (diagnosed) during the managing phase of NWP data. This parameter is a key attribute for confirming or filtering overshooting top candidates, since a relevant gap over tropopause is generally expected and observed with overshooting tops.

Several attempts and case studies, based on ARPEGE NWP data over Europe, have lead to set a first threshold to a value of 5°C to define what is a significant gap over tropopause. The value of 10°C, generally admitted, would filter almost all OTs from this situation.

For pixels slightly above tropopause level (i.e. gap between 0° and 5°), a complementary set of criteria mixing high BT, high reflectance and large gap between average and minimum temperature of cloud cell, allows to keep some overshooting tops with different marked signatures.

The figure below illustrates the differences between pre-selection and confirmation steps, highlighting in particular how the OTD takes advantage of tropopause diagnosis.

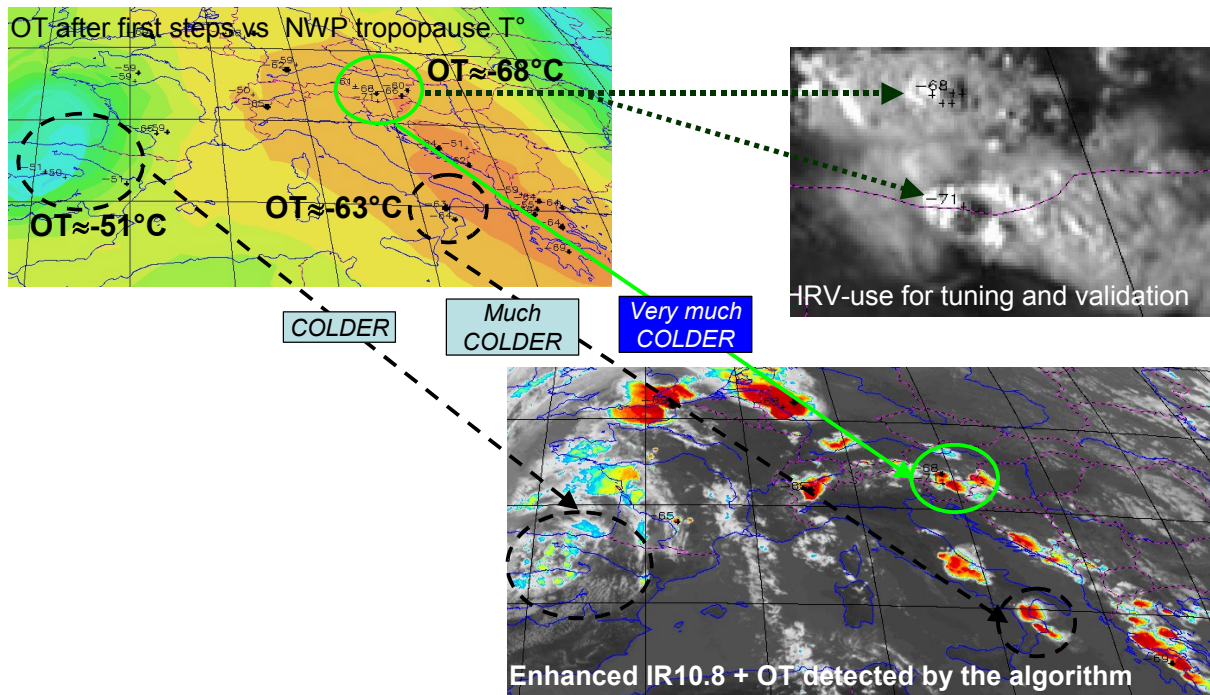


Figure 46: Left-above : OTD after first step plotted over NWP tropopause T°C (blue>-50, green[-50,-60], yellow-green[-60,-65], orange[-65,-67], dark orange<-67). Right above: HRV image confirming two OT (HRV not used by the algorithm). Below: the HRV OT are also found by the algorithm that takes into account (among other criterias) the gap between OT temperature and tropopause temperature.

3.4.3 Subjective validation

We only consider in this chapter the OT confirmed after the confirmation step. Only these OT are described in RDT-CW output. Mainly low resolution visible, HRV and IR10.8 enhanced images have been used to validate the OT. For most cases, overshooting top detection appears close to high reflectance spot, and can be considered as validated as in in figure hereafter.

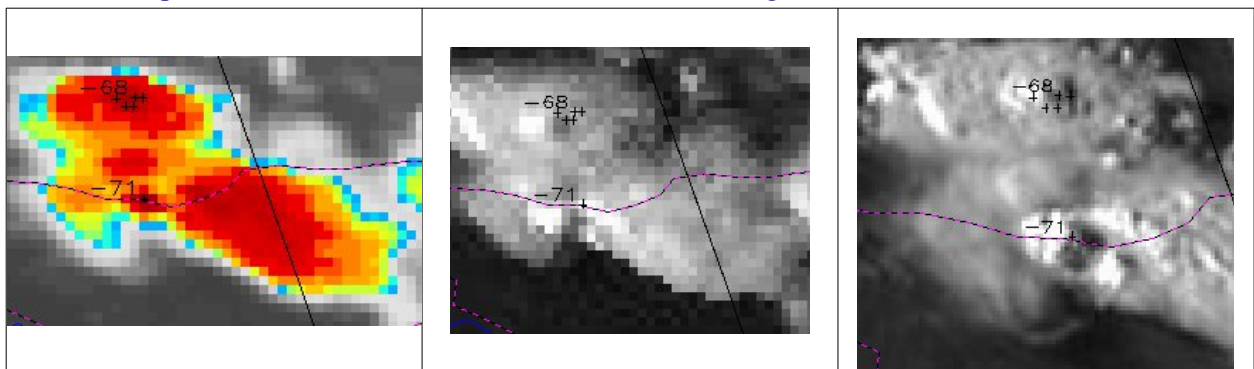


Figure 47: OTD plotted on raw IR10.8 enhanced images (left), on low resolution VIS parallax-corrected images (middle), and on raw HRV image (right).

On figure above Two OT have a temperature of 3-4°C below tropopause temperature. They are associated with high values of reflectance, even if those “spots” are not exactly collocated on parallax-corrected images. Detection can be considered as validated when looking at buddings on HRV images

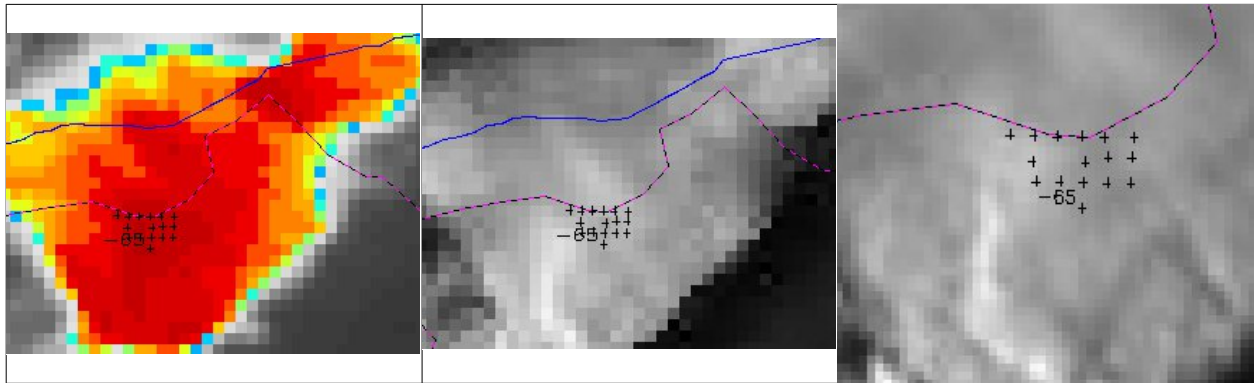


Figure 48: As in previous figure

Figure above indicates that the reflectance values are not very high on LR and HR VIS images, and located rather southward of the detected OT. This one is slightly above tropopause level but largely colder than surrounding pixels.

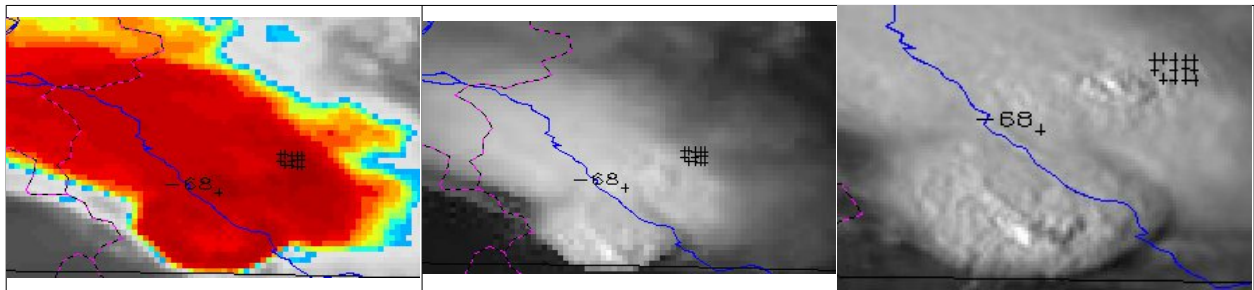


Figure 49: As in previous figure

On figure above “twin” OT, both with temperature extrema and BTD maximum, don't show high co-located reflectance (except for one pixel close to the eastern one), even if the texture seem obviously above an anvil. One can suspect a secondary extremum on the southern edge of the cloud cell, where white spot in HR visible appears.

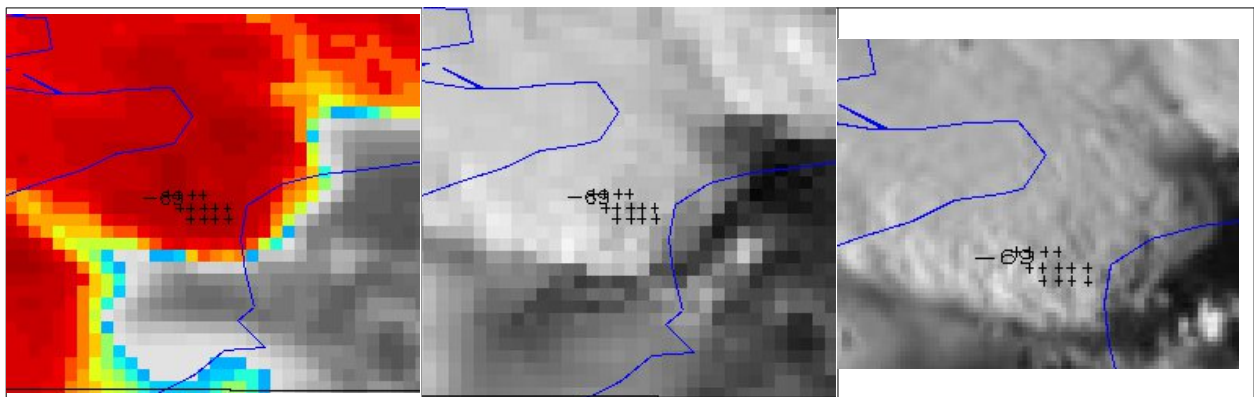


Figure 50: As in previous figure

Moderate reflectance appears here slightly south of the IR-detected OT, on the edge of the cloud system. Visible channels hardly confirm this detection. .

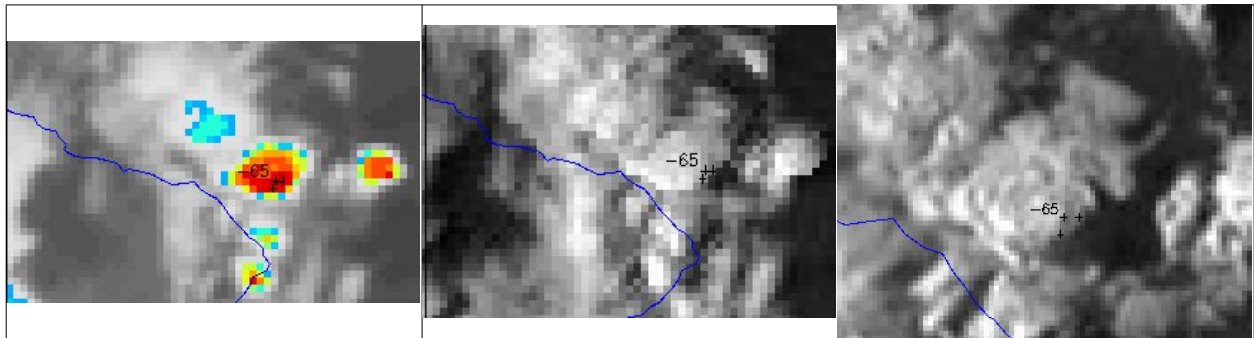


Figure 51: As in previous figure

On figure above OT is associated with high value of LR VIS reflectance. HRV signal appears more on the western edge of the cloud cell. The cell is quite small, but clearly above tropopause (gap of 5°), justifying the OT detection.

To conclude, the Overshooting Top Detection implemented in RDT-CW code fits its objective for the cases studies which have been analysed. The first step allows selecting all kind of interesting pixels and the confirmation step allow to focus on the most relevant ones.

3.4.4 Applicability to tropical regions

Brightness temperature, but also size and distance thresholds have been adapted when applying OT detection to tropical regions. Deep convection associated with high and cold tropopause has lead to consider rather at least double-size OT for the morphology analysis. indeed, the initial values of thresholds did not allow to fulfil the conditions for most cases.

Thus temperature threshold of -70°C and typical OT size of 100 km have set for latitudes below 30°. Below is an illustration of the result, with single pixel and extended OT which are compliant with morphology and tropopause value.

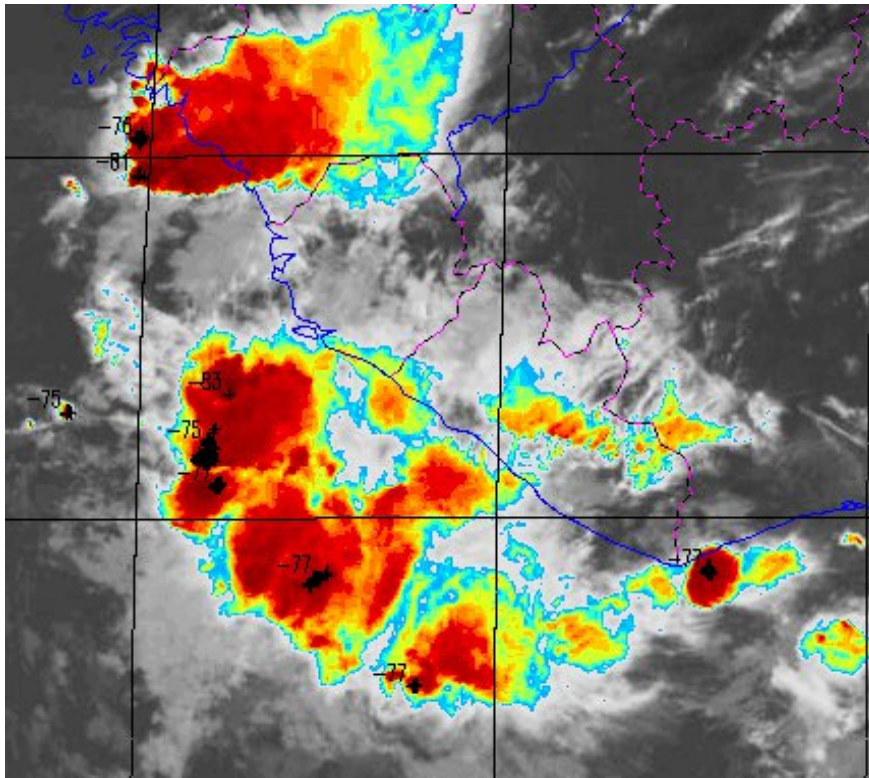


Figure 52: 06/06/2012 12h00 UTC, south-west Africa: OTD on enhanced IR image.

3.5 LIGHTNING JUMP DIAGNOSIS

A lightning jump detection has been implemented in version 2018 of RDT-CW, the algorithm (for details see [AD.11]) relies on minute lightning analysis inside RDT cell for a period of 12 minutes with a condition on lightning rate and lightning rate trend.

The main objectives of this diagnosis are to contribute to severity index and to be used as a precursor of hail.

Hereafter a figure with a severe convective cell crossing France on the 13th June 2017. The electrical activity of the cell over Haute-Loire region is extremely important, especially looking at Intra-Cloud numbers issued from Météorage network.

Total lightning activity (intra-cloud and cloud-to-ground flashes) is necessary for attempting to diagnose lightning jump. Moreover, it is necessary to change the time scale. RDT-CW time scale (i.e. satellite scan rate) allow to calculate a flash trend from one slot to another as current attribute. But in case of jump calculation, data are analysed at minute scale, joining flash time series of successive RDT-CW cells to explore the period associated to a given cell.

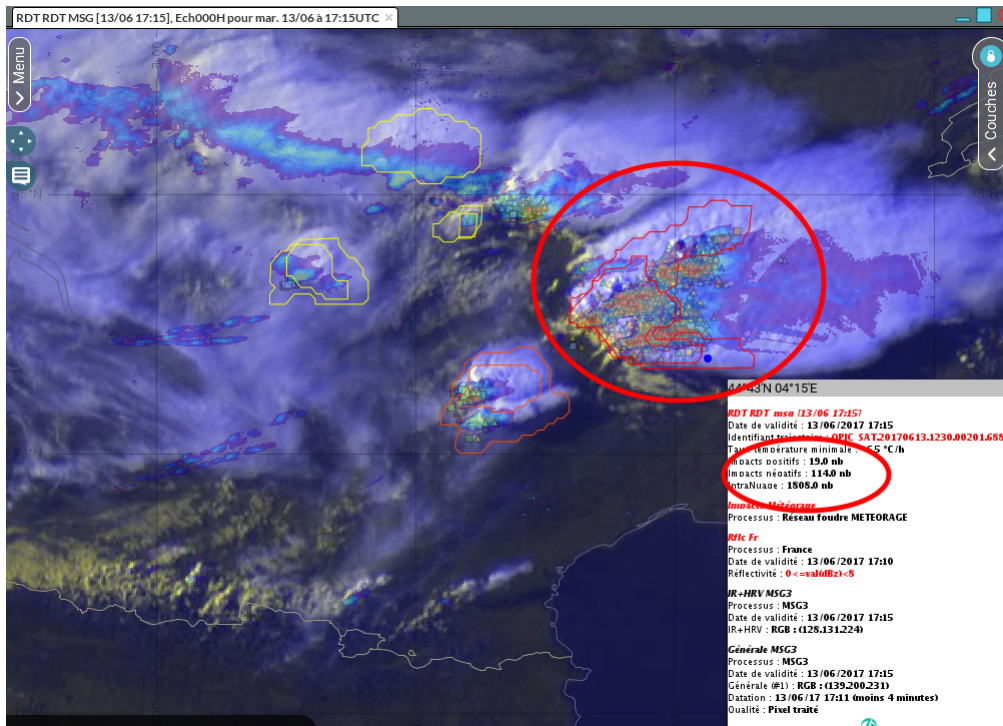


Figure 53: 13/06/2017 case study extreme Thunderstorm in « Haute Loire » (France) for 17:15. IR10.8 enhanced image, RDT cell, radar reflectivities and lightning strokes

In the figure below the lightning jumps are illustrated for the cell during a 7 hours tracking time. A hail event has been reported at 17:30 associated to this cell, preceded by 5 lightning jumps: it illustrates the usefulness of this diagnosis as a hail precursor. Hail event is followed by jumps: it illustrates the usefulness of the diagnosis as a proxy for hail.

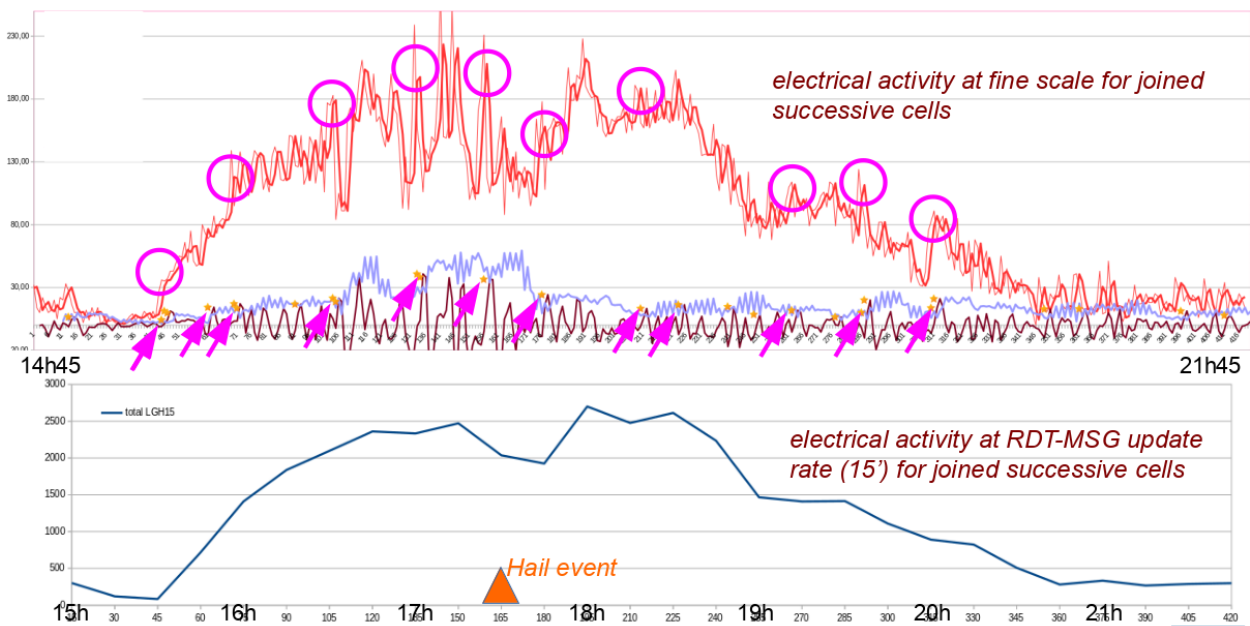


Figure 54: Top: Jumps calculated for the cell described in previous figure above. Time-series of lightning rate (red), standard deviation of lightning rate in the last 12 minutes (blue), lightning rate change (brown). Jumps are plot in magenta. Hail event has been reported after the fifth jump at 17:30. Bottom: time-series of 15min flash number of successive RDT-CW cell

3.6 FORECAST OF CLOUD SYSTEMS

RDT-CW software provides the user the possibility to forecast cloud cell position using the diagnosed movement speed of the cloud cell.

Extrapolated cloud cells positions are obtained through Lagrangian forecast, i.e. the whole object is moved according to direction/speed of the diagnosed movement.

Consequently, quality of this extrapolation relies highly on the quality of movement diagnosis. The use of a pre-initialized guess of movement field from blending NWP wind data and HRW, and a final-step coherence checking has allowed to filter erratic speed and/or direction due to split/merge or to threshold temperature changes. Thus, confidence in Lagrangian extrapolation has become much higher, as illustrated in figure below.

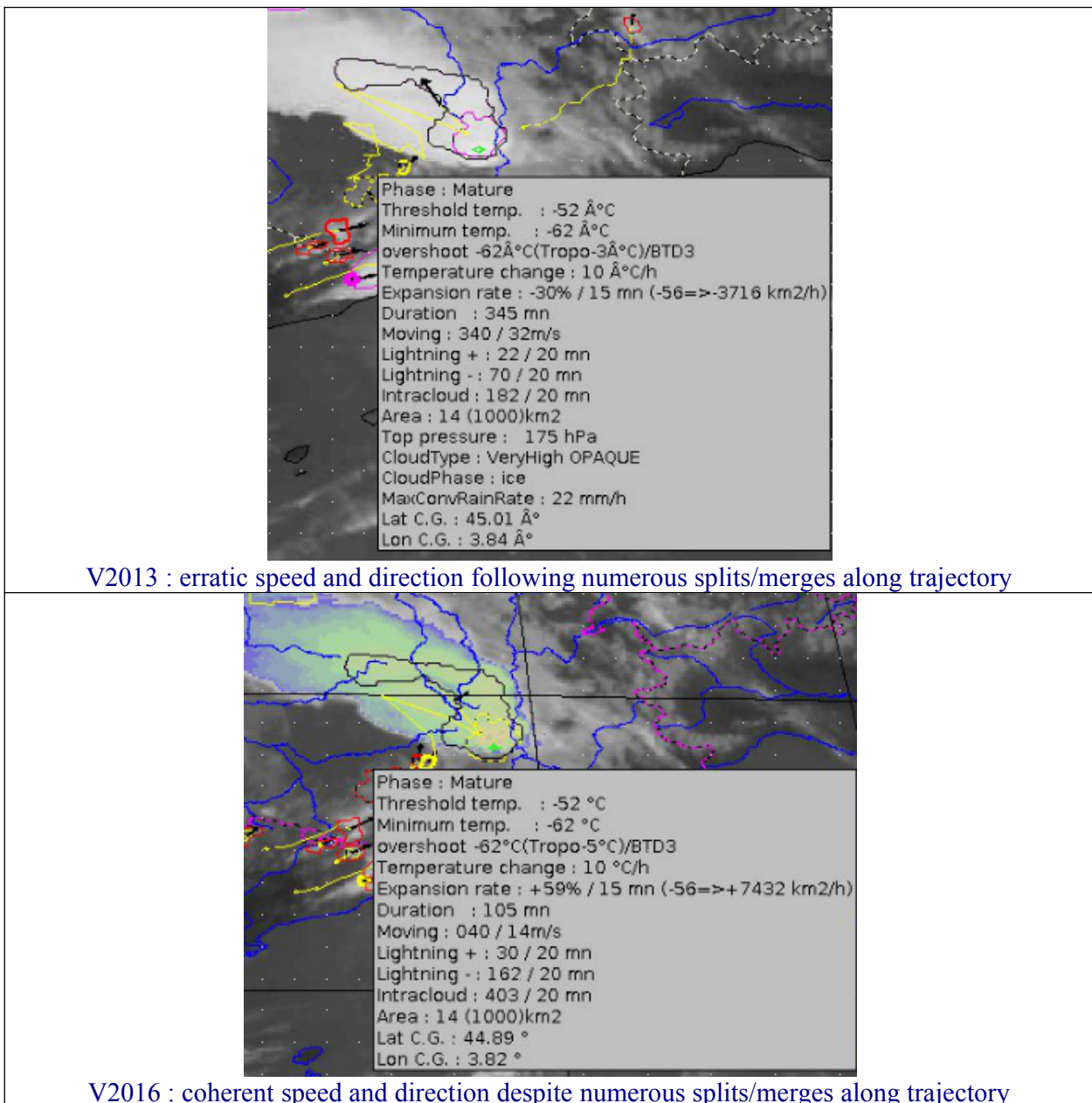


Figure 55: v2013 vs v2016 illustration of RDT motion vectors improvement

 	Validation report of the Convection Product Processors of the NWC/GEO	Code: NWC/CDOP3/GEO/MF-PI/SCI/VR Issue: 1.1 Date: 18th December 2019 File: NWC-CDOP3-GEO-MF-PI-SCI-VR-Convection_v1.1.odt Page: 62/67
---	--	---

Concerning forecast positions, it must be reminded that a cloud cell definition/contour corresponds to a given threshold temperature, and that this threshold changes dynamically/automatically from one slot to the other. *A forecast contour remains based on the same temperature threshold than the observed/analysed object.* It will consequently be very difficult to assess the position of a forecast contour when compared to the following corresponding observed contours, because it is likely that those contours will not correspond to the same threshold temperature. Moreover, the longer the forecast ranges, the less precise the localization of forecast convective object is.

Assessment of forecast products position should ideally take into account for each cloud cell the stage of development, the morphological evolution or the expansion rate. Forecast cloud cell position can consequently only subjectively be regarded.

The objective validation of the forecast part has been carried out in a scientific report in 2018 [RD.3.], some of results are available for v2018. Around 20% of cells are new at each slot of MSG (15' scan) over Europe. Since the forecast scheme doesn't see these new cells, it gives the ratio of misses at step +15'. The ratio of false detection is also around 20%. Concerning the error on gravity centre position, the error value of 50 km is reached after the forecast range of 60 minutes.

Trends attributes of observed cloud cells are used to give indication of possible values changes of some parameters in the first forecast ranges (trend's values used for 15min range, half values for 30min). Here again those values can only be regarded as estimation and not pure forecast:

- Temperature change of coldest part of the cell (up to tropopause temperature limit if this value is available thanks to NWP data) and severity
- Lighting trend for lightning activity and severity
- Top pressure trend for top pressure estimation
- Expansion rate for amplification or limitation of contour dilatation

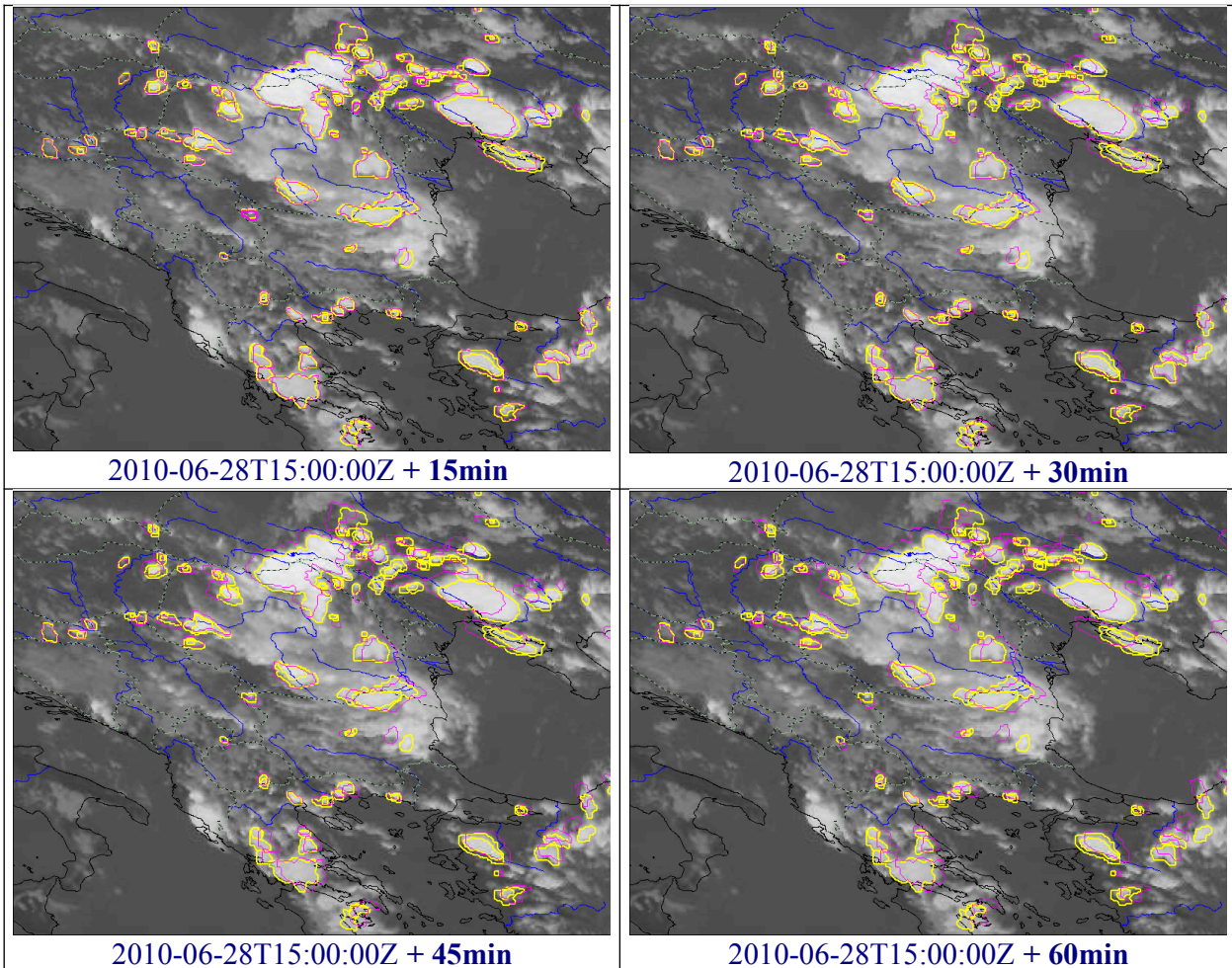


Figure 56: RDT-CW v2016 advection products (forecast contours in Magenta) from slot 2010-06-28T15:00:00Z (Observed contours in yellow).

Figure above displays forecast products (magenta contours) issued from a given slot 1500Z on the 28-06-2010. Yellow contours are observed at 1500Z. One can note very few overlap between forecast cells at various ranges, which assess a good spatial coherence of the movement speed of each cloud system.

The cyclonic movement field is very well taken into account with the forecast cloud systems.

This forecast set has been produced without smoothing neither dilation of the contours.

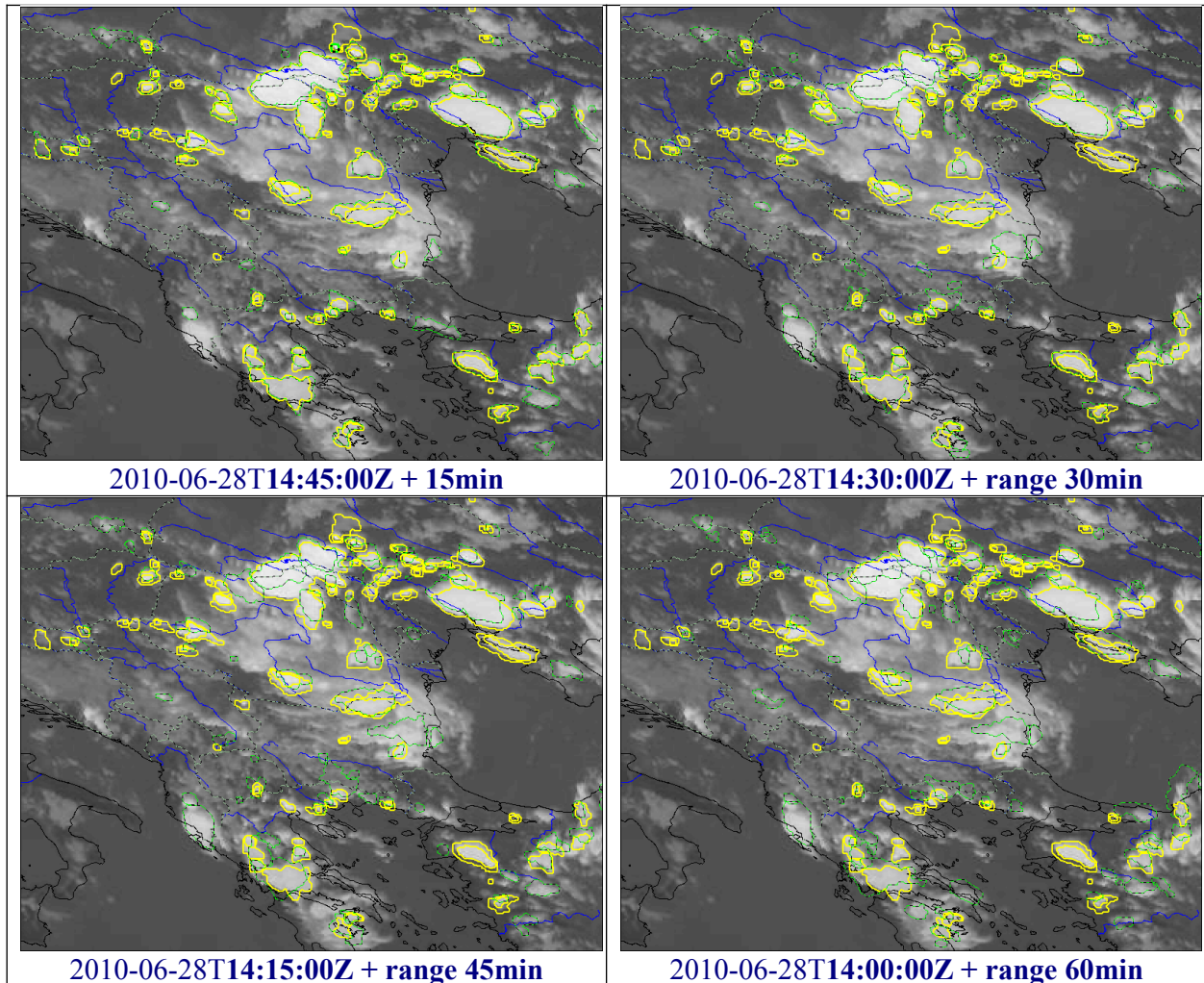


Figure 57: RDT-CW v2016 advection products (green forecast contours) from previous slots valid for slot 2010-06-28T15:00:00Z (yellow observed contours).

Figure above displays forecast products (green contours) valid for a same slot 1500Z on the 28-06-2010. Yellow contours are observed at 1500Z. The first ranges (15 and 30min) show a pretty good correspondence between previous forecast and current observation. For larger ranges, mainly large cloud systems, with longer duration, find a correspondence in the observed set.

One can note that some forecast green contours are no more valid in the analysed set, probably after declassification of the cloud system (no observed yellow contour).

On the other hand, some new cloud cells (yellow contours) appear only on the analysed set, and can not be anticipated from the previous slots.

3.7 END-USERS FEEDBACKS

RDT, a very satisfying product widely used for Research and Operations, by Météo-France and its partners.

The use of RDT concerns for example

- Forecasters of Météo-France, in France and overseas territories (La Réunion, Antilles, Polynésie, Wallis et Futuna, Nouvelle Calédonie). RDT provides a significant help for regions not covered by radars.

	Validation report of the Convection Product Processors of the NWC/GEO	Code: NWC/CDOP3/GEO/MF-PI/SCI/VR Issue: 1.1 Date: 18th December 2019 File: NWC-CDOP3-GEO-MF-PI-SCI-VR-Convection_v1.1.odt Page: 65/67
---	---	---

- HAIC project and successive experiments (2014 and 2016 Australia, 2015 French Guyana, 2016 Darwin/La Réunion)
- RDT provided to airlines through EFB (Electronic Flight Bag)
- Collaboration has previously concerned
- SESAR project and TOPMET/TOPLINK experiments
- Hymex project
- 2006 AMMA experiments (<http://aoc.amma-international.org/observation/mcstracking/>)
- European FlySafe Project with RDT software adapted to radar data
- NOAA for a RDT GOES (Operation + Research)
- From 2008, 2010 and 2015 Surveys distributed to SAF/NWC users, it appeared that RDT is mainly used for Research activities and operations for forecasting. The judgement of overall quality of RDT product is very satisfying (rate of 6.7/10 in 2015 survey).

RDT produced by Météo-France is downloaded by ACMAD and some African countries can visualize real-time RDT through ACMAD website (www.acmad.net).

RDT is operated by SAWS, hereafter two feedbacks

- De Coning, E., Strydom, J., Powell, C., Gijben, M., de Beer, A., 2016, Nowcasting for aviation purposes in South Africa – a case study: Part1 – Satellite and radar based tools, WSN16 Hong-Kong, 25-29/7/2016

“[the RDT] has provided good validation against lightning occurrence and radar reflectivities of more than 35 dBZ over South Africa”

- De Coning, E., Gijben, M., 2017, Using Satellite and Lightning Data to Track Rapidly Developing Thunderstorms in Data Sparse Regions, *Atmosphere* 2017, 8 (4), 67; doi:10.3390/atmos8040067

“The outcomes of this study are very encouraging for other countries in Africa where convection and severe convection often occur and sophisticated data sources are absent. Initial studies over East Africa indicate that the RDT product can benefit operational practices for the nowcasting of severe convection events.”

RDT produced by SAWS is now available on WMO RSMC (*Regional Specialised Meteorological Center*) of Pretoria. Sixteen African countries of SWDFP (*Severe Weather Forecasting Demonstration Project*) from southern part of African continent can visualize real-time RDT.

3.8 CONCLUSION AND COMPLIANCE REQUIREMENTS

From a subjective point of view, the use of NWP data with RDT has allowed an improving gap of the discrimination efficiency. False alarms are lowered thanks to a “NWP convective mask” used as a guidance for the diagnosis, and precocity is increased with early diagnosis in warmest categories, thanks to a new tuning with NWP data and mask. The objective validation of GEN scheme over a wide region thanks to EUCLID data detailed in this report has confirmed this first analysis. It has been undertaken through various approaches from time step cell to the full life cycle of a cloud system, and taking into account the limitations of the ground truth. With a moderate ground truth (defined by 5 flash impacts at least during a trajectory) and non convective trajectories defined by being away from flashes of more than about 35km, satisfying skills are reached for full-trajectory approach: POD of 74% together with 2% POFD, FAR 22% and a TS of 61%. Scores are even better when considering sections of trajectories or cloud cells individually. RDT keeps good performances

 	Validation report of the Convection Product Processors of the NWC/GEO	Code: NWC/CDOP3/GEO/MF-PI/SCI/VR Issue: 1.1 Date: 18th December 2019 File: NWC-CDOP3-GEO-MF-PI-SCI-VR-Convection_v1.1.odt Page: 66/67
---	--	---

when taking into account intermediate season period (Spring, Autumn). Of course RDT scores are better for summer. Moreover, the skills obtained with EUCLID data over Europe are better in all configurations and for all approaches than for the previous validation. This improvement does not appear so clearly concerning the precocity of RDT GEN discrimination. It is limited to systems which are able to be early discriminated, i.e. with isolated convective system depicted from low levels. **Finally, those results fulfil the target accuracy requirements (see 1.2) over a large domain and for an extended period, i.e. 70% of detection and 25% of convective systems diagnosed before lightning activity.**

We consider nevertheless that progress can still be made to lower the false alarm and the number of miss cases, and to still improve the precocity.

RDT provides an accurate depiction of convective phenomena, from triggering phase to mature stage. The RDT object allows pointing out some areas of interest of a satellite image. It provides relevant information on triggering and development clouds and on mature systems. Even if the precocity on the first lightning occurrence remains to be improved, the subjective evaluation confirmed the precocity usefulness on moderate lightning activity.

Thanks to these good results the status of RDT had been set up to “operational” by EUMETSAT (since v2011).

Subjective validation exhibits very good results of the algorithm concerning OTD. It is a major point to improve RDT by focusing on the areas of more severe and intense convection. Now, depending on cloud system morphology, RDT is able to present a kind of multidimensional description of convective systems, thanks to second level identification and overshooting top detection. It completes the data fusion approach with other products of NWCSAF. .

	Validation report of the Convection Product Processors of the NWC/GEO	Code: NWC/CDOP3/GEO/MF-PI/SCI/VR Issue: 1.1 Date: 18th December 2019 File: NWC-CDOP3-GEO-MF-PI-SCI-VR-Convection_v1.1.odt Page: 67/67
---	--	---

4 CONCLUSION

CI and RDT-CW help to follow convection in different stage. There are compliant with MSG, GOES-16 and Himawari-8 satellites.

CI v2018, as a continuation of CI v2016, offers various improvements of the product: more precise use of Cloud products (cloud type and cloud top micro-physics), stricter definition of the areas of pixels of interest, day-time and night-time tunings. . This improvement reflects on subjective and the objective validation exhibit scores at the boundary of the requirements. The use of CI in conjunction with RDT-CW offer to end-users reliable tools to assess various phases of convection.

RDT-CW v2018, as a continuation of RDT-CW v2016, is a mature product with several years of continuous development and improvement and several version operational. The calibrated discrimination scheme implemented in the v2018 delivery confirms the operational capability of RDT-CW to generate convection warning product from geostationary satellite data whatever the geographical region. Additionally the forecast scheme takes benefit from slight improvements in the movement estimation of cloud cells such that the nowcasting capabilities of the RDT-CW up to +1 hour can be made possible.